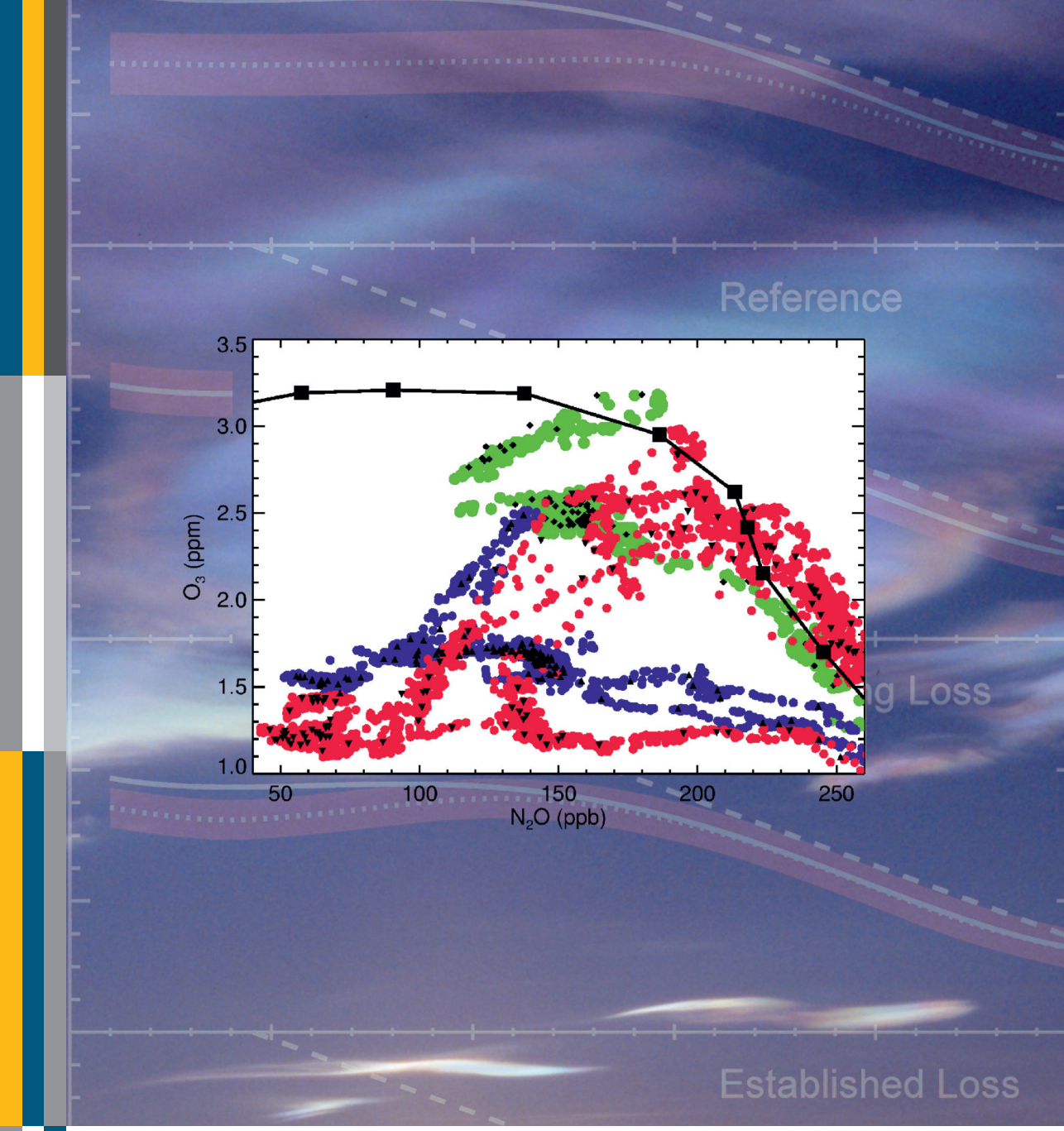

Tracer-tracer Relations as a Tool for Research on Polar Ozone Loss

Rolf Müller

Mitglied der Helmholtz-Gemeinschaft

JÜLICH
FORSCHUNGSZENTRUM

Schriften des Forschungszentrums Jülich
Reihe Energie & Umwelt / Energy & Environment Band / Volume 58

Forschungszentrum Jülich GmbH
Institute of Chemistry and Dynamics of the Geosphere (ICG)
Stratosphere (ICG-1)

Tracer-tracer Relations as a Tool for Research on Polar Ozone Loss

Rolf Müller

Schriften des Forschungszentrums Jülich
Reihe Energie & Umwelt / Energy & Environment Band / Volume 58

ISSN 1866-1793 ISBN 978-3-89336-614-9

Bibliographic information published by the Deutsche Nationalbibliothek.
The Deutsche Nationalbibliothek lists this publication in the Deutsche Nationalbibliografie; detailed bibliographic data are available in the Internet at http://dnb.d-nb.de.

Publisher and Distributor:	Forschungszentrum Jülich GmbH Zentralbibliothek, Verlag D-52425 Jülich phone:+49 2461 61-5368 · fax:+49 2461 61-6103 e-mail: zb-publikation@fz-juelich.de Internet: http://www.fz-juelich.de/zb
Cover Design:	Grafische Medien, Forschungszentrum Jülich GmbH
Printer:	Grafische Medien, Forschungszentrum Jülich GmbH
Copyright:	Forschungszentrum Jülich 2010

Schriften des Forschungszentrums Jülich
Reihe Energie & Umwelt / Energy & Environment Band / Volume 58

D 468 (Habil.-Schr., Wuppertal, Univ., 2010)

ISSN 1866-1793
ISBN: 978-3-89336-614-9

Table of Contents

1 Introduction

"...betrachte ich die Entdeckung des ozonisirten Sauerstoffs für eine der merkwürdigsten, die je gemacht wurden[1]."

Justus von Liebig, 1857
(Kahlbaum and Thon, 1900, p. 18)

"Recent attempts to consolidate assessments of the effect of human activities on stratospheric ozone (O_3) using one-dimensional models for 30°N have suggested that perturbations of total O_3 will remain small for at least the next decade. Results from such models are often accepted by default as global estimates. The inadequacy of this approach is here made evident by observations that the spring values of total O_3 in Antarctica have now fallen considerably."

Joseph C. Farman, Brian G. Gardiner, and Jonathan D. Shanklin, 1985
(Farman et al., 1985a)

"Future scientific questions that might be linked to the fate of the ozone hole include whether global warming will begin to affect ozone depletion, whether the Arctic stratosphere will change to be more like the Antarctic in coming centuries; and how possible changes in the atmospheric concentration of methane or nitrous oxide might affect ozone-hole chemistry."

Susan Solomon, 2004
(Solomon, 2004)

"...the generation of Jamie Paul and our future grandchildren, who will know so much more and who will celebrate the disappearance of the ozone hole."

Paul J. Crutzen, 1995
(Crutzen, 1995)

[1] ...I regard the discovery of ozonised oxygen as one of the most curious ever made

1.1 Ozone in the Atmosphere

1.1.1 Early Observations of Atmospheric Ozone

Ozone was discovered by Christian Friedrich Schönbein in 1839. Schönbein himself believed that ozone plays an important role in the Earth system and suggested (in 1853) that long-term ozone measurements in the atmosphere should be performed on an international scale: "Geneigt zu glauben, das atm. Ozon spiele im Haushalte der Erde eine wichtige Rolle, halte ich es für wünschenswerth, dass möglichst zahlreiche, sowohl grosse Zeiträume als bedeutende Länderstrecken umfassende, untereinander vergleichbare Beobachtungen über die Veränderungen des Ozongehaltes der Atmosphäre angestellt werden...[2]" (in a letter to Justus von Liebig, Kahlbaum and Thon, 1900, p. 10). Indeed numerous measurements were made during the second half of the 19th century using a method that Schönbein had developed (for a detailed discussion of the early measurements of atmospheric ozone see e.g., Crutzen, 1988; London and Liu, 1992; Sonnemann, 1992). This early interest in ozone was motivated to a large extent by the fact that ozone, at that time, was considered an indicator of clean, healthy air and that ozone-poor air was thought to promote sickness. Measurement series of ozone were performed in spas with the intention of demonstrating how beneficial to health a stay would be (Lender, 1872). This view persisted for many decades and was held by leading scientists in the field; as late as 1946 Regener stated "Anwesenheit von Ozon ist ein Indikator für gute Luft[3]". Today, of course, it is known that high concentrations of tropospheric ozone are detrimental to human health and similarly harmful to other living systems.

Since the early 1950s it has been understood that high ozone concentrations in the troposphere (referred to as "photochemical smog") are caused by pollution; ozone is chemically formed as a result of photochemical reactions involving NO_x and non-methane hydrocarbons from automobile exhausts and similar combustion processes (Haagen-Smit, 1952).

Another important aspect of ozone was also discovered in the 19th century, namely its importance as an absorber of light. In 1879 the French physicist Alfred Cornu recognised that solar radiation with a wavelength below 300 nm does not penetrate to the Earth's surface. Only three years later, Hartley (1881) suggested that ozone is responsible for this observation; the ozone absorption bands in this UV region are therefore today referred to as Hartley bands. The discovery of the spectroscopic properties of ozone opened up the possibility of making measurements of the total thickness of the atmospheric ozone (i.e., the total atmospheric column of ozone) including the ozone in the stratosphere. The first detailed measurements of the total atmospheric column of ozone were made by Fabry and Buisson (1921), who firmly established that ozone was responsible for the observed strong cut-off in solar UV spectra at about 300 nm towards shorter wavelengths. Fabry and Buisson (1921) speculated (correctly as we know today) that ozone was formed by solar UV radi-

[2] Inclined to believe that the atmospheric ozone plays an important role in the balance of the Earth, I consider it desirable that a great many observations of the changes of the ozone content of the atmosphere are conducted which are comparable amongst each other and cover both long time spans and considerable distances.

[3] The presence of ozone is an indication of good air.

ation. They also suggested that the ozone layer was situated at an altitude of about 50 km. And first measurements of the height of the ozone layer indeed confirmed an altitude of the ozone layer of 48-53 km (Cabannes and Dufay, 1925; Lambert et al., 1926).

In 1924, G. M. B. Dobson designed a spectrograph to measure the total ozone column that was more suitable for routine outdoor use and that was cheaper to construct than the Fabry and Buisson spectrograph. The aim was to develop an instrument that allowed regular measurements to be made over extended time periods. This development was very successful; today, the standard unit for the total atmospheric column of ozone bears Dobson's name: the Dobson unit[4] (DU). The first observations at Oxford in 1924-1925 showed a marked annual variation of ozone. Likewise, the data exhibited a strong day-to-day variability that was closely connected to meteorological conditions (Dobson and Harrison, 1926; Dobson, 1968). Between July 1926 and November 1927, seven instruments were constructed at Oxford and distributed throughout Europe covering the latitude range from 68°N to 47°N and one instrument was operated at 22°S in Chile (Dobson et al., 1929; Dobson, 1930). After the 1926-1927 observation period, the instruments were sent to Spitzbergen (via an Italian airship expedition), California, Egypt, S. India, and New Zealand (see Dobson, 1968; Farman, 1989; Brönnimann et al., 2003, for further details on the history of early total ozone measurements). In the former USSR, the first measurements of total ozone were made in 1933; later, in 1959, the M-83 ozonometer was developed which became the backbone of the USSR ozone station network (Gushchin, 1995). Even today, ground-based total ozone measurements are essential for long-term monitoring of the ozone content of the atmosphere (e.g., WMO, 1999, 2003, 2007). The longest records of continuous reliable measurements are available from stations equipped with Dobson spectrophotometers (e.g., Jones and Shanklin, 1995; Staehelin et al., 1998), whose design has remained essentially unchanged since 1930 (Dobson, 1968).

In the late twenties the ozone layer was still assumed to be located in the upper stratosphere. On the basis of their measurements, Götz and Dobson (1928) reported that the "...average height [of the ozone layer] seems to be between 30-40 km above sea-level". Bjerknes stated in 1929 that "...le fait qui parait aussi être bien établi, que la couche d'ozone se trouve à une altitude de 40-50 kilomètres" [5] (Bjerknes, 1929).

In ground-based measurements in Spitzbergen in 1929, Götz (1931) discovered the so called "Umkehreffekt" which allows a low-resolution vertical ozone profile to be deduced (e.g., Paetzold and Regener, 1957; Dütsch and Staehelin, 1992). He reported an average height of the ozone layer for the period 10 July to 28 August 1929 in Spitzbergen of 27.6 $\pm$ 8 km. At this time, Götz put forward these new ideas rather tentatively "...es fragt sich nun ob die geophysikalisch interessante tiefere Lage der Ozonschicht in der hohen Breite Spitzbergens, vor allem aber auch ihre Schwankung bis herunter zur minimalen Höhe des 26. August [11 km] als genügend gesichert angesehen werden dürfen" [6]. However, two

[4] Typical values for the total column ozone rage between 200-400 DU. See also Appendix A for a discussion on units of ozone abundance.

[5] ...the fact also seems to be well established that the ozone layer is located at an altitude of 40-50 kilometres.

[6] ...the question is now whether the geophysically interesting lower altitude of the ozone layer in the high latitude of Spitzbergen, in particular also its variation down to the minimum height on 26 August [11 km], can be considered as being sufficiently well established.

years later (Götz et al., 1933) the Spitzbergen measurements were confirmed by mid-latitude measurements and Götz et al. stated with much more confidence that "the average height [of the ozone in the atmosphere] at Arosa now appears to be about 20 km, which is much below the former estimates".

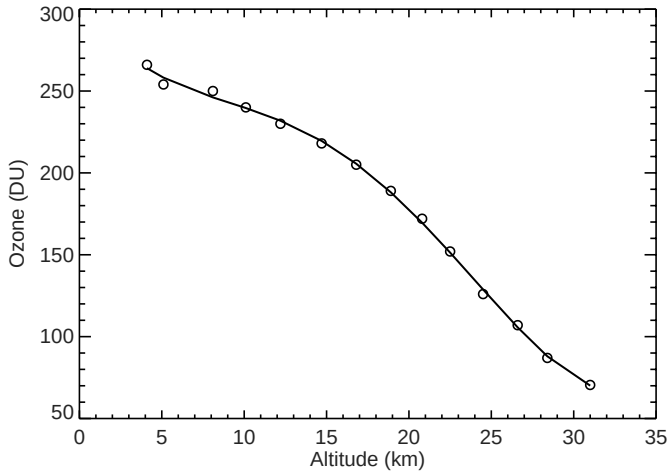

Figure 1.1: The first balloon-borne measurement of the vertical distribution of ozone in the atmosphere from Stuttgart (48.8°N) on 31 July 1934 (Regener and Regener, 1934). Here the original measurements of Regener and Regener are shown which are reported as column ozone above the balloon. Note that the absolute values reported by Regener and Regener (1934) were deduced from relative measurements assuming a value of 240 DU at 10 km. The altitude was deduced as a log-pressure height from the pressure recorded on the balloon payload.

Soon after, the first balloon-borne measurements of the solar UV spectrum in the stratosphere (Regener and Regener, 1934) and the ozone profiles deduced from these measurements independently confirmed the first Umkehr observations[7]. The payload for this balloon experiment weighted only 2.7 kg and was launched to an altitude of about 31 km using two standard meteorological balloons. Figure 1.1 shows the original values (ozone column above the balloon) for the ozone profile on 31 July 1934 from Stuttgart published by Regener and Regener (1934). In Figure 1.2, the vertical profile of the ozone mixing ratio[8] deduced from these early measurements is compared with a corresponding ozone climatology deduced from measurements of the Halogen Occultation Experiment (HALOE) on the Upper Atmosphere Research Satellite (UARS) in the years 1991-2002 (Russell et al., 1993;

[7]The first attempt to measure the vertical profile of the atmospheric ozone concentration was made by James Glaisher and Henry Tracey Coxwell; on 5 September 1862 they conducted a balloon ascent from Wolverhampton in the UK and measured ozone using Schönbein's method. Although the balloon reached an altitude of 11 km, the last ozone measurement was only performed at an altitude of 4.8 km because they lost consciousness at greater altitudes. This balloon flight was described by Lender (1873) and later in the New York Times, 27 June.

[8]See Appendix A for a discussion on units of trace gas abundance.

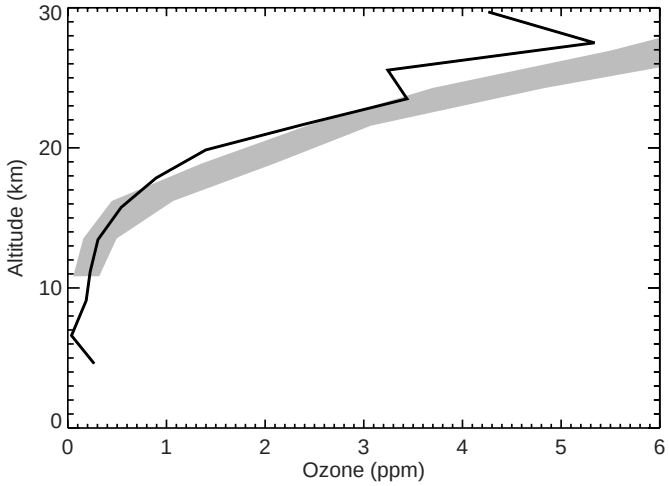

Figure 1.2: The balloon-borne measurement of the ozone profile from Figure 1.1 converted to molar mixing ratio. For comparison, as a grey scale, a modern ozone climatology is shown for July at 47.5°N equivalent latitude (plus/minus on standard deviation of a climatology based on HALOE measurements, Grooß and Russell, 2005). The column ozone above 10 km from the climatology is 293 DU and the Regener and Regener measurements have been scaled accordingly for a proper comparison.

Grooß and Russell, 2005) demonstrating a rather good agreement of the early measurements with a current climatology.

In 1937, Erich Regener was forced to resign from his chair at the University of Stuttgart by the Nazi regime. Nonetheless, he continued his scientific work; first, on 1 January 1938, he founded a private research institute, his "Forschungsstelle für Physik der Stratosphäre", which later than year was integrated into the "Kaiser-Wilhelm-Gesellschaft zur Förderung der Wissenschaften" (renamed "Max-Planck-Gesellschaft" in 1947). He developed the first scientific payload for a rocket to reach high altitudes; the A4 rocket carrying an assembly of instruments (Ordway III et al., 2007). This payload, referred to as the "Regener-Tonne" (Regener barrel) never flew but scientific payloads were launched on A4 rockets from New Mexico as early as 1946 (Ordway III et al., 2007).

1.1.2 The Chemistry of Stratospheric Ozone

When Dobson and Harrison first published their measurements of total ozone in 1926, the formation mechanism of stratospheric ozone was still unclear. They stated that is was uncertain "Whether the ozone is formed in the extreme upper atmosphere by ultraviolet radiation from the sun, or by electrical discharges in auroræ…". Today it is established that stratospheric ozone is produced by the photolysis of molecular oxygen (O_2) at ultraviolet

wavelengths below 242 nm,

$$\text{R1:} \qquad O_2 + h\nu \quad \longrightarrow \quad 2O,$$

where $h\nu$ denotes an ultraviolet photon.

The atomic oxygen (O) produced in reaction R1 reacts rapidly with molecular oxygen to form ozone (O_3)

$$\text{R2:} \qquad O + O_2 + M \quad \longrightarrow \quad O_3 + M,$$

where M denotes a collision partner (N_2 or O_2) that is not affected by the reaction. Ozone is photolysed rapidly

$$\text{R3:} \qquad O_3 + h\nu \quad \longrightarrow \quad O + O_2.$$

Through reactions R2 and R3, O_3 and O establish a rapid photochemical equilibrium. The sum of O_3 and O is therefore often considered and referred to as "odd oxygen", or as the "odd oxygen" family. This concept is useful because the sum of the family members is produced and destroyed much more slowly than the individual members. Throughout the stratosphere (up to about 50 km altitude) O_3 constitutes the vast majority of odd oxygen. Through the reaction

$$\text{R4:} \qquad O + O_3 \quad \longrightarrow \quad 2O_2.$$

an O atom and an O_3 molecule are lost. Because O and O_3 are in rapid photochemical equilibrium, the loss of one oxygen atom effectively implies the loss of an ozone molecule, so that R4 destroys two molecules of odd oxygen.

This set of reactions was originally proposed by Chapman (1930) as the first photochemical theory for the formation of ozone; these four reactions are therefore known as the Chapman reactions.

However, destruction by reaction R4 alone cannot explain the observed ozone abundances in the stratosphere. Today it is established that in the mid-latitudes and in the tropics the ozone production through reaction R1 is largely balanced by the destruction in catalytic cycles of the form

$$\begin{aligned} &\text{R5:} \qquad XO + O \quad \longrightarrow \quad X + O_2 \\ &\text{R6:} \qquad X + O_3 \quad \longrightarrow \quad XO + O_2 \end{aligned}$$

$$\text{C1:} \qquad \text{Net:} \quad O + O_3 \quad \longrightarrow \quad 2O_2$$

where the net reaction is identical to reaction R4. It is important that the catalyst X is not used up in the reaction cycle. The most important cycles of this type in the stratosphere involve reactive nitrogen (X = NO), originally proposed by Crutzen (1970), and hydrogen (X = H, OH) radicals, originally proposed by Bates and Nicolet (1950) with a mesospheric focus and by Hampson (1964) with a stratospheric focus. Moreover, the possibility of chlorine-catalysed ozone loss (via cycle C1 with X = Cl) was first introduced by Stolarski and Cicerone (1974). A more detailed discussion of the history of the discovery

of the various catalytic ozone loss cycles can be found elsewhere (Crutzen, 1996; Müller, 2009)

Interestingly, the possible importance of heterogeneous reactions in the stratosphere (albeit no heterogeneous reactions involving chlorine species) was already discussed in the mid-seventies by Cadle et al. (1975). Based on laboratory experiments, heterogeneous reactions were, however, for a long time thought to be unimportant. This situation only changed in 1986 when Solomon et al. suggested that heterogeneous chemistry could greatly enhance the ability of chlorine to destroy ozone in polar regions (see Section 1.3.3 below). The paper by Solomon et al. prompted numerous laboratory studies. Today, a large number of heterogeneous reactions are known which are important for stratospheric chemistry (e.g., Peter, 1997; Solomon, 1999). And recently Lefèvre et al. (2008) showed that heterogeneous chemistry on ice clouds also plays an important role on Mars in controlling the stability and composition of the atmosphere.

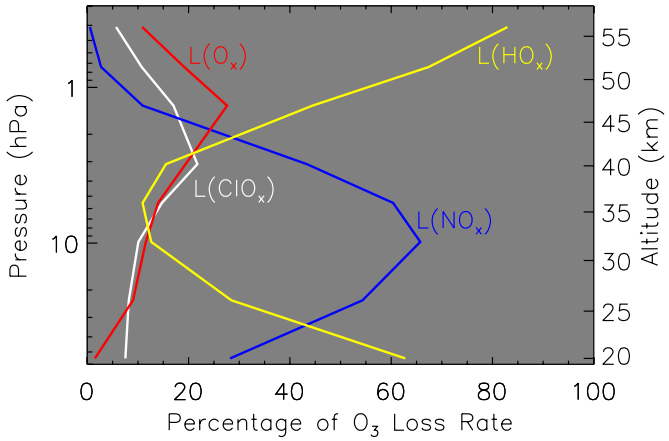

Figure 1.3: The vertical distribution of the relative importance of the individual contributions to ozone loss by the HO_x, ClO_x, and NO_x cycles as well as the Chapman loss cycle (R4). The calculations are based on HALOE (V19) satellite measurements and are for overhead sun (23°S, January) and for total inorganic chlorine (Cl_y) in the stratosphere corresponding to 1994 conditions. Reaction rate constants are based on DeMore et al. (1997). Courtesy of Jens-Uwe Grooß based on Grooß et al. (1999) and IPCC/TEAP (2005).

Because of the large increase of O with altitude, the rates of these cycles increase strongly between 25 and 40 km; the same is true for the rate of ozone production through reaction R1 (e.g., Crutzen et al., 1995; Grooß et al., 1999). Further, the relative importance of the cycles for ozone loss varies considerably with altitude. Between 25-40 km the NO_x cycle is the dominant ozone loss process, whereas above 45 km HO_x-catalysed ozone loss dominates (see Figure 1.3). The loss through the ClO_x cycle (which also depends on the stratospheric chlorine loading) peaks at 40 km. The reason that the HO_x cycle is the strongest ozone loss cycle below about 25 km (Figure 1.3) is the existence of a HO_x-catalysed cycle which only

involves O_3 and does not require O

$$\begin{aligned} &\text{R7:} && \mathrm{OH} + \mathrm{O_3} \longrightarrow \mathrm{HO_2} + \mathrm{O_2} \\ &\text{R8:} && \mathrm{HO_2} + \mathrm{O_3} \longrightarrow \mathrm{OH} + 2\,\mathrm{O_2} \end{aligned}$$

$$\text{C2:} \qquad \text{Net:} \quad \mathrm{O_3} + \mathrm{O_3} \longrightarrow 3\,\mathrm{O_2}$$

Because the concentration of O deceases strongly below about 25 km altitude, ozone loss below this altitude is dominated by cycle C2.

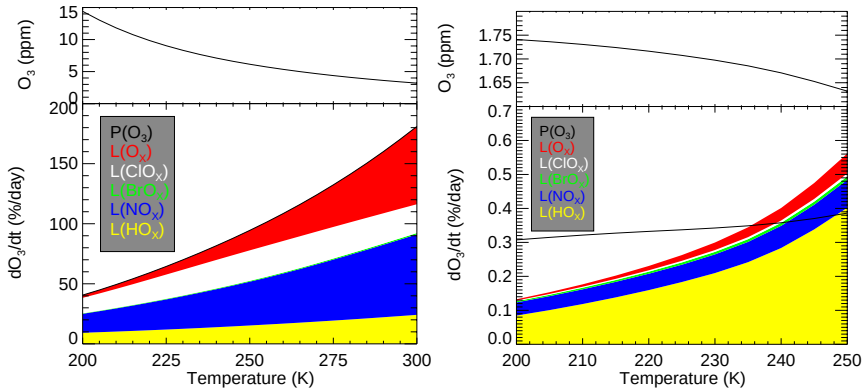

Figure 1.4: An estimate of the contribution of the various ozone loss cycles to the ozone loss rate, together with the rate of ozone production via reaction R1 P(O3), at 45°N for equinox conditions (end of March) as a function of temperature (bottom panels). The estimates were obtained from short (20-day) runs of a chemical box model, starting from climatological values of ozone; the ozone mixing ratios at the end of the run are shown in the top panels. Left-hand panels show conditions for 40 km altitude (2.5 hPa), where the climatological temperature is about 250 K; right-hand panels show conditions for 20 km (55 hPa), where the climatological temperature is about 215 K. Reaction rate constants were taken from Sander et al. (2003). The production and loss rates are for the simulated ozone value. Note that at 40 km ozone is in steady state (i.e., production equals the sum of all loss terms) and thus ozone is under photochemical control. At 20 km ozone production does not equal loss, implying that transport also has a strong influence on ozone concentrations. At 20 km the simulated ozone value after 20 days remains close to its initial climatological value of 1.70 ppm. (After IPCC/TEAP, 2005, courtesy of Jens-Uwe Grooß).

Two different chemical regimes can be identified for stratospheric ozone: the upper stratosphere and the lower stratosphere. In the upper stratosphere, the ozone distribution arises from a balance between production from the photolysis of molecular oxygen (R1) and destruction via the catalytic cycles involving hydrogen, nitrogen and halogen radical species discussed above (see Section 1.1.2). In the upper stratosphere, a reduction in temperature slows the destruction rate of ozone (see Figure 1.4). The rate of both ozone destruction

cycles and of ozone production via reaction R1 is substantially faster in the upper stratosphere than in the lower stratosphere; therefore, chemical equilibrium is reached rapidly in the upper stratosphere, which is not the case in the lower stratosphere (see Figure 1.4).

In the lower stratosphere, in addition, reactions on aerosol and cloud particles become important. The distribution of the radicals (and the partitioning of the nitrogen, hydrogen and halogen species between radicals and so-called reservoir species that do not destroy ozone) are affected by heterogeneous chemistry. In the mid-latitudes, reactions on aerosol surfaces convert active nitrogen to the less active HNO_3 reservoir, making mid-latitude ozone less vulnerable to active nitrogen (X = NO in cycle 1), but increasing the efficiency of chlorine-catalysed (X = Cl in cycle 1) ozone loss (Rodriguez et al., 1991; Fahey et al., 1993). Heterogeneous reaction at low temperatures are of particular importance in the chemical mechanisms causing polar ozone loss (Solomon et al., 1986, see Section 1.3.3 below).

1.1.3 The Distribution of Ozone in the Atmosphere

The distribution of ozone in the stratosphere is governed by three processes: photochemical production, photochemical destruction by catalytic cycles, and transport. Transport processes are typically divided into large-scale advection and mixing processes on smaller scales.

The large-scale circulation of the stratosphere, with rising motion at low latitudes followed by poleward motion and descent at high latitudes, systematically transports ozone poleward and downward (Figure 1.5). This circulation in the stratosphere is referred to as the 'Brewer-Dobson circulation' because such a circulation was originally suggested by Brewer (1949) based on water vapour measurements in the stratosphere and by Dobson et al. (1946) based on column ozone measurements. Because of the short photochemical lifetime of ozone in the upper stratosphere (see Section 1.1.2 above), this transport has little effect on the ozone distribution there (Figure 1.5). However, in the lower stratosphere, the photochemical lifetime of ozone is long (several months or longer, Sankey and Shepherd, 2003) so that transport processes dominate the distribution of ozone.

Maximum ozone mixing ratios occur in the tropics between ∼30-40 km (Figure 1.6). In this altitude region, ozone is very short-lived and is essentially in photochemical equilibrium; that is, rapid photochemical loss is balanced by rapid destruction (e.g., Crutzen et al., 1995; Grooß et al., 1999). Under these conditions, transport timescales are slow compared to chemical timescales. Therfore, the altitude region 30–40 km in the tropics cannot serve as a source region for the extratropical stratosphere. The region where the ozone mixing ratios that are exported to the extratropics are determined, is the transition region between the area of chemical control and the area where ozone is controlled by transport (Garcia and Solomon, 1985).

Transport of ozone from the high latitudes poleward is important in the extra-tropical lower stratosphere, where ozone can accumulate on the time scale of a season. Variations in the ozone concentration in this region, between the tropopause and ∼20-25 km altitude, control changes in total column ozone abundance (Figure 1.5). Below about ∼25 km, ozone mixing ratios in the extratropics are greater than in the high latitudes and column ozone is higher (Figure 1.6).

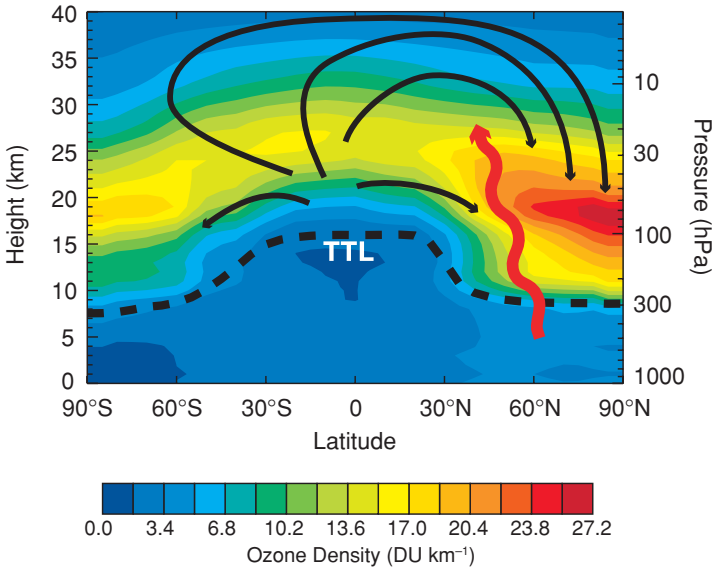

Figure 1.5: The meridional cross section of ozone density (in DU per km, see Appendix A) during northern hemisphere winter (January to March) based on the ozone climatology of Fortuin and Kelder (1998). The dashed line denotes the approximate location of the tropopause, and TTL stands for tropical tropopause layer. The black arrows indicate the Brewer-Dobson circulation in northern hemisphere winter, and the wiggly red arrow represents planetary waves that propagate from the troposphere into the stratosphere. (Figure reproduced from Box 1.2 in IPCC/TEAP, 2005).

Because the transport by the Brewer-Dobson circulation is strongest during winter and spring, ozone builds up in the extra-tropical lower stratosphere during that period (e.g., Tuck et al., 1992). It then decays photochemically during the summer when transport is weaker and strong NO_x-driven ozone loss occurs at the poles (e.g. Farman et al., 1985b; Fahey and Ravishankara, 1999). The development of total ozone over the year as a function of latitude (Figure 1.7) reflects the seasonality of the Brewer-Dobson circulation. Planetary wave activity is stronger in the northern hemisphere than in the southern hemisphere, because of the asymmetric distribution of the topography and land-sea thermal contrasts that force planetary waves. A stronger planetary wave activity causes the Brewer-Dobson circulation to be stronger during the northern hemisphere winter than during the southern hemisphere winter. As a consequence, the extra-tropical build-up of ozone during winter and spring is greater in the northern hemisphere than in the southern hemisphere winter. Therefore, climatological spring total ozone columns are greater in the northern than in the southern hemisphere (Figure 1.7).

Recently, interest has arisen in investigating not only seasonal cycles and other periodic signals in total ozone time series, but also long-range correlations employing detrended fluctuation analysis (DFA, Jánosi and Müller, 2005). Deducing correlation properties from

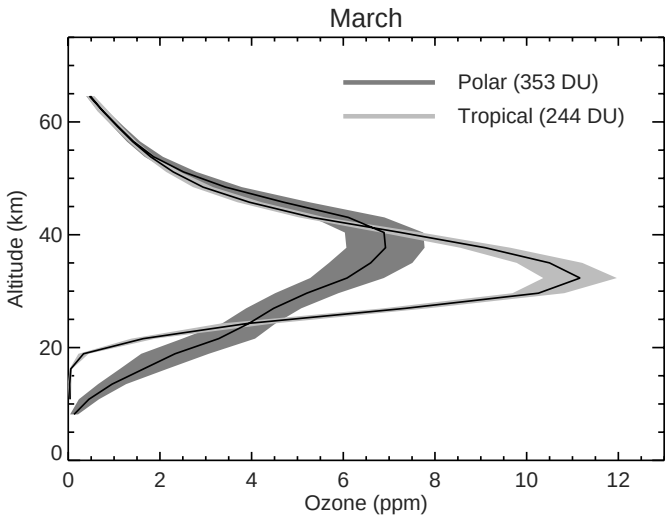

Figure 1.6: The vertical profile of ozone mixing ratio against altitude for polar (equivalent latitude 72.5°N) and tropical (equivalent latitude 2.5°N) conditions in March. The ozone data are from the climatology of Grooß and Russell (2005).

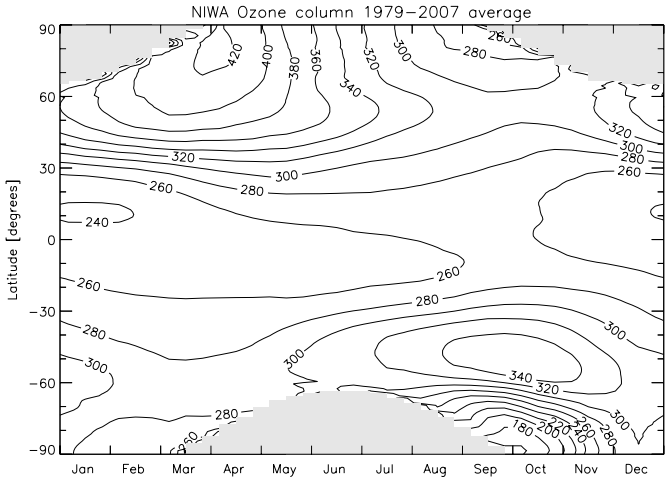

Figure 1.7: A climatology of total column ozone as a function of latitude and month. Data were taken from version 2.7 of the NIWA combined ozone database (courtesy of Greg Bodeker, Bodeker Scientific) which provides daily total column ozone fields from 1979 to 2007. (From Bodeker et al. (2005) and Müller et al. (2008); plot courtesy of Jens-Uwe Grooß).

ozone time series has important implications for ozone trend analysis (Vyushin et al., 2007; Kiss et al., 2007).

1.2 Anthropogenic Influence on the Ozone Layer

The first concern about an anthropogenic influence on the ozone layer was formulated in the late fifties due to the possible impact of nuclear weapons tests on the ozone layer. Later, in the early seventies, attention was focused on the effect a planned fleet of hundreds of supersonic aircraft might have on the stratospheric ozone layer (Johnston, 1971; Crutzen, 1971). Research programmes directed at assessing the impact of supersonic transport on stratospheric ozone greatly improved knowledge about stratospheric processes and paved the way for research on the question of the impact of anthropogenic halogen emissions on stratospheric ozone, the main focus of this section (see e.g. Tuck, 1978; Dotto and Schiff, 1978; Müller, 2009, for further discussion of the early research on anthropogenic influence on the ozone layer).

Human activities result in the emission of a variety of halogen source gases that contain chlorine and bromine atoms. Important examples of anthropogenic halogen source gases are chlorofluorocarbons (CFCs), once used in almost all refrigeration and air-conditioning systems, and halons, used as fire-extinguishing agents. Although production of practically all such substances has ceased because of the provisions of the Montreal Protocol and its amendments and adjustments, emissions continue because halogen source gases are still present in existing equipment, chemical stockpiles, foams etc.; halogen source gases not yet released to the atmosphere are referred to as 'banks'.

The most important chlorine source gas, where a substantial fraction of the emissions is due to natural production, is methyl chloride. Methyl chloride is present in the troposphere in globally averaged concentrations of about 550 ppt (Koppmann et al., 1993; WMO, 2007, Figure 1.8). At the end of the 21st century, when the abundance of anthropogenic chlorine source gases (e.g. CFCs) will have been greatly reduced as a consequence of the Montreal protocol, methylchloride is expected to account for a large fraction of the remaining stratospheric chlorine.

The emission of halogen source gases to the atmosphere ultimately leads to stratospheric ozone depletion. The first step is the photochemical breakdown of the source gases. Because of the great chemical stability of most source gases, this breakdown only occurs at appreciable rates in the upper stratosphere, where there is high-energy solar radiation. The chlorine atoms released in this way from the source gases are mostly converted to so-called 'reservoir species', the most important being HCl and $ClONO_2$. Together, these reservoir species are referred to as 'total inorganic chlorine'. The chemical symbol used for total inorganic chlorine is Cl_y. Reservoir species themselves do not cause ozone depletion, for ozone depletion to occur the chlorine has to be liberated from the reservoirs and converted into an 'active' form. This occurs through gas-phase processes in the upper stratosphere and through heterogeneous chemistry in the polar lower stratosphere in winter (Solomon, 1999, see also below).

An important measure of the potential for ozone depletion in the stratosphere due to the

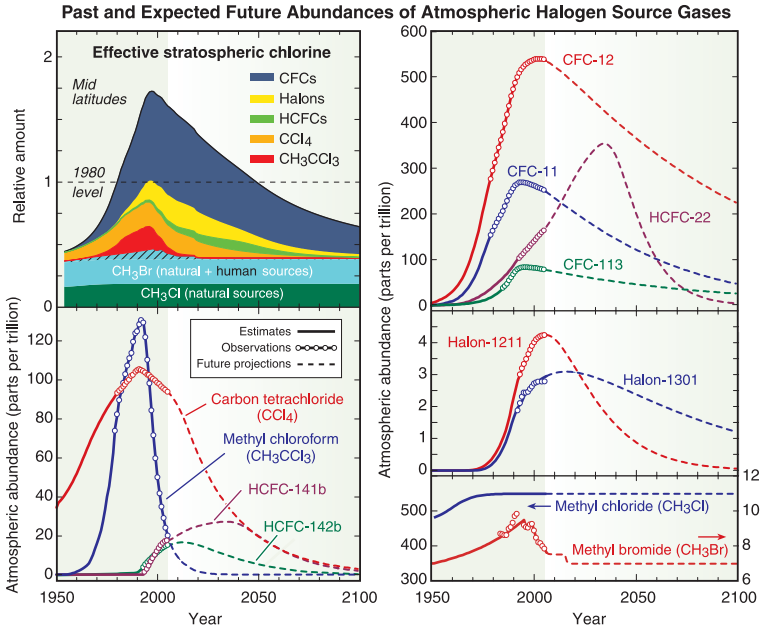

Figure 1.8: Halogen source gas changes. The rise in effective stratospheric chlorine values in the 20th century has slowed and reversed in the past decade (top left panel). Effective stratospheric chlorine values are a measure of the potential for ozone depletion in the stratosphere, obtained by summing over adjusted amounts of all chlorine and bromine gases. Effective stratospheric chlorine levels as shown here for mid-latitudes will return to 1980 values around 2050. The return to 1980 values will occur around 2065 in polar regions (Newman et al., 2007). In 1980, ozone was not significantly depleted by the chlorine and bromine then present in the stratosphere. A decrease in effective stratospheric chlorine abundance follows reductions in emissions of individual halogen source gases. Overall emissions and atmospheric concentrations have decreased and will continue to decrease given international compliance with the provisions of the Montreal Protocol. The changes in the atmospheric abundance of individual gases at the Earth's surface shown in the panels were obtained using a combination of direct atmospheric measurements, estimates of historical abundance, and future projections of abundance. The past increases of CFCs, along with those of carbon tetrachloride and methyl chloroform, have slowed significantly and most have reversed in the past decade. Amounts of HCFCs, which are used as CFC substitutes, will continue to increase in the coming decades. The abundances of some halon compounds will also continue to grow in the future while halons still present in existing equipment (so called "banks") are released to the atmosphere. Smaller relative decreases are expected for methyl bromide in response to production and use restrictions because it has substantial natural sources. Methyl chloride has large natural sources and is not regulated under the Montreal Protocol. (Figure from WMO, 2007).

presence of halogen-containing (ozone-depleting) source gases in the stratosphere is the so-called "effective stratospheric chlorine" (Daniel et al., 1996; WMO, 2007). Effective stratospheric chlorine values are calculated by summing over adjusted amounts of all chlorine and bromine gases. The adjustments are designed to account for the different rates of decomposition of the gases and the greater per-atom effectiveness of bromine in depleting ozone compared to chlorine (see Section 1.1.2).

In the latter half of the 20^{th} century up until the 1990s, effective stratospheric chlorine values increased steadily and rapidly (see Figure 1.8). Values are derived from individual halogen source gas abundances obtained from measurements, historical estimates of abundances, and projections of future abundances. As a result of the regulations of the Montreal Protocol, the long-term increase in effective stratospheric chlorine slowed, reached a peak, and began to decrease in the 1990s. With a delay of a few years, the stratospheric abundance of halogen source gases is expected to follow the changes observed in the troposphere. Although measurements in the stratosphere are much sparser, declining growth rates of CFC-12 in the stratosphere have been reported (Engel et al., 1998). The start of a reduction in effective stratospheric chlorine values means that, as a result of the Montreal Protocol, the potential for stratospheric ozone depletion has begun to decrease.

The possibility of chlorine-catalysed ozone loss was first related to the accumulation of anthropogenic CFCs in the atmosphere by Molina and Rowland (1974). Early model studies (Crutzen, 1974) predicted that enhanced levels of chlorine in the stratosphere would lead to a depletion of upper stratospheric ozone via cycle C1 with X = Cl. This notion was subsequently confirmed by a variety of model studies (WMO, 1986). The first policy measures were taken on the basis of these early warnings. The United States phased out the use of CFCs as a propellant in spray cans as of 1 January 1979. This action was soon followed by similar bans in Canada, Sweden, and Norway. However, it took until 1987 for the first international agreement to be signed, the "Montreal Protocol on substances that deplete the ozone layer".

The predictions of these early studies were remarkably far-sighted. It is stated that CFCs accumulate in the lower atmosphere, with photolysis in the middle and upper stratosphere being the major sink. It was already understood in 1974 that this constitutes a long-term problem, on the timescale of many decades. Most importantly, it was predicted that enhanced levels of stratospheric chlorine would lead to a decline of ozone in the upper stratosphere by a catalytic ozone loss cycle (cycle C1, with X = Cl).

Today, more than thirty years after the first scientific studies were published linking the danger of future stratospheric ozone loss with the accumulation of anthropogenic CFCs in the atmosphere (Molina and Rowland, 1974; Crutzen, 1974), ozone decline has been unequivocally detected in the altitude region between 30 and 50 km by a variety of ground-based and space-borne instruments (WMO, 1995; Harris et al., 1998; WMO, 2007). The observed altitude variation of loss of upper stratospheric ozone – peak percentage losses around 40 km – was correctly predicted by the first model studies (Crutzen, 1974, see also Figure 1.9, panel a). Overall, the understanding of upper stratospheric chemistry, as expressed in current models, is consistent with observations (WMO, 2007).

As early as in the late seventies, it was predicted that an important factor influencing upper stratospheric ozone is temperature so that increasing CO_2 in the stratosphere should have

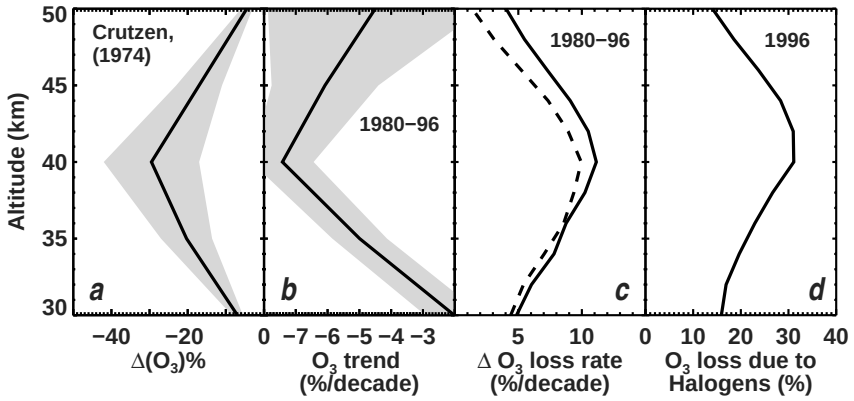

Figure 1.9: Upper stratospheric ozone trend and ozone loss rates caused by chlorine-catalysed reaction cycles for mid-latitudes of the northern hemisphere. Panel (a) shows the percentage reduction in ozone concentrations predicted to occur by Crutzen (1974) due to the build-up of CFCs. The calculation assumed a growth of Cl_y to a level of 5.3 ppb in the uppermost stratosphere. Panel (b) shows the observed reduction of upper stratospheric ozone for the latitude range 30° to 50°N, between 1980 and 1996, derived from SAGE, SBUV and Umkehr measurements (Harris et al., 1998; WMO, 1999). The shaded areas indicate the range of uncertainty. Panel (c) shows the change in the total odd oxygen loss rate for 35°N, September (solid line), calculated using the photochemical model described by Osterman et al. (1997), allowing for a change in Cl_y from 2.0 ppb (appropriate for 1980) to 3.6 ppb (appropriate for 1996). The model result represented by the dashed line allows for the observed decrease in temperature between 1980 and 1996 WMO (Chapter 5 in 1999) in addition to the increase in Cl_y. Changes in the total ozone loss rate are expressed in units of % per decade to be directly comparable to the observed change in ozone. Panel (d) shows the the fraction of the total odd oxygen loss rate due to the catalytic cycle limited by ClO + O (cycle C1 with X = Cl) for 35°N, September, 1996 (Cl_y = 3.6 ppb in the uppermost stratosphere) based on the model described by Osterman et al. (1997). (Figure from WMO, 1999).

an impact on ozone (Groves et al., 1978; Groves and Tuck, 1979; Haigh and Pyle, 1979). Because the rates of the gas-phase ozone destruction cycles decrease with lower temperature (Figure 1.4), a cooling of the stratosphere leads to an increase of ozone concentrations above about 25 km (IPCC/TEAP, 2005). Increases in CO_2 in the atmosphere are expected to cool the stratosphere and a cooling of the stratosphere, at a rate of 0.5-1.5 K/decade from 1979-2005, is indeed observed (Randel et al., 2009).

The relation of the observed decline of upper stratospheric ozone and the increase of the stratospheric chlorine loading is shown schematically in Figure 1.9. A significant reduction in the concentration of ozone was observed during the 1980s and 1990s, with the largest losses reaching 7.4 $\pm$ 1 %/decade at 40 km altitude (Harris et al., 1998, Figure 1.9, panel b). A similar pattern of the decline in upper stratospheric ozone due to the build-up of athropogenic chlorine was predicted by the first modelling studies (Figure 1.9, panel a). These calculations were based on a projected increase of Cl_y to a level of 5.3 ppb, a value never reached in the contemporary stratosphere (Figure 1.8).

Model calculations using a simple photochemical model (based on kinetic parameters from DeMore et al., 1997; Lipson et al., 1997) show that a substantial fraction of the loss of ozone in today's upper stratosphere occurs by the ClO + O cycle (C1), peaking at a value of $\sim 30\%$ of the overall ozone loss rate at an altitude of 40 km (Figures 1.9, panel d, and 1.5). In this model, allowing upper stratospheric Cl_y (at 55 km) to increase from a value of 2 ppb in 1980 to 3.6 ppb in 1996, and leaving everything else unchanged, leads to a calculated increase in the overall ozone loss rate very similar in shape and magnitude to the observed decline in ozone (Figure 1.9, panel c, solid line). Prescribing, in addition, a reduction in upper stratospheric temperature as observed during the past two decades (WMO, 2007; Randel et al., 2009) results in a slightly lower estimate for the increase in the overall ozone loss rate (Figure 1.9, panel c, dashed line) mainly because of the temperature dependence of the rate limiting reactions for ozone removal (Figure 1.4). The decline of upper stratospheric ozone, observed for 1980-1996, has slowed substantially over the last decade and there is evidence that this decline can be attributed to the decline of halogen source gases in the atmosphere (Newchurch et al., 2003; Steinbrecht et al., 2006; WMO, 2007).

1.3 Polar Stratospheric Ozone Loss

1.3.1 The Antarctic Ozone Hole

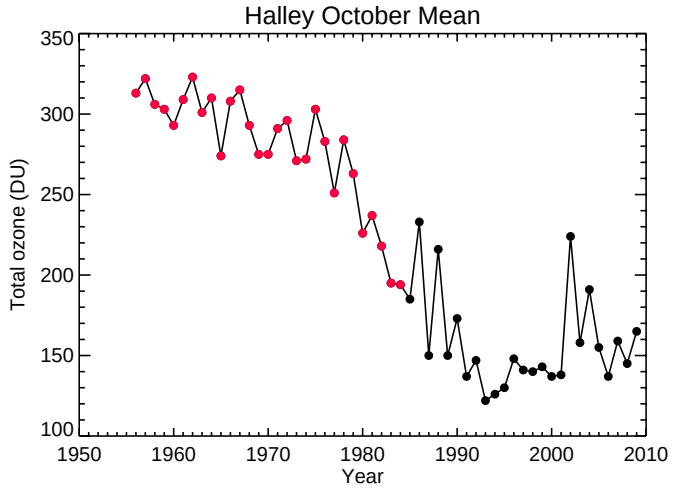

Figure 1.10: October mean total column ozone from Dobson spectrophotometer measurements at Halley, Antarctica (75.35°S, 26.34°W). Updated until the year 2009 from Jones and Shanklin (1995); the data originally published by Farman et al. (1985a) are shown in red. (Data courtesy of J. Shanklin, British Antarctic Survey).

In 1985, Farman, Gardiner, and Shanklin reported that in the Antarctic spring strongly reduced total ozone values occurred at the British Antarctic Survey station at Halley (Farman

et al., 1985a; Jones and Shanklin, 1995). The data from the original publication are shown in Figure 1.10. This phenomenon, soon referred to as the Antarctic "ozone hole", is one of the most striking examples of the direct impact of human activities on the atmosphere. The discovery by Farman et al., which was based on a time series of measurements by classical Dobson instruments started by Dobson himself in 1956 (Dobson, 1968), was soon confirmed by satellite measurements which showed that the ozone depletion extended over roughly the entire Antarctic continent (Stolarski et al., 1986). Independent methods for measuring total column ozone provided further support for the depletion of springtime ozone in Antarctica (e.g., Solomon, 1999).

The term 'ozone hole' for the phenomenon of low total ozone values in Antarctic spring was first used by Stolarski et al. (1986): "The deep minimum, or hole…". But of course, the Antarctic ozone hole is not a true hole. Some column ozone always remains; e.g., the October mean at Halley never dropped below 100 DU (Figure 1.10). Interestingly, Chapman (1934) had already asked the question "Can a hole be made in the ozone layer?". What he suggested was the artificial removal of most of the ozone in a column of air to allow astronomers to make better observations is the ultraviolet (see also Wells, 1997). Likewise Regener (1946) used the term "ein Loch in der Ozonschicht" ("a hole in the ozone layer") and pointed out that such a hole would be welcomed by astronomers.

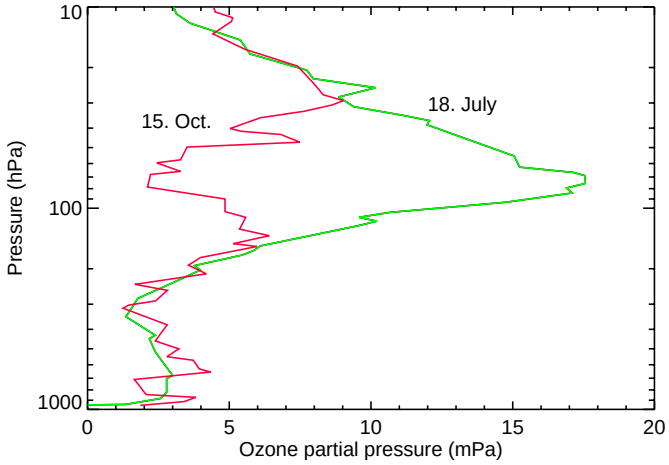

Figure 1.11: Vertical profiles of ozone partial pressure measured on 18 July and 15 October 1985 from Georg Forster Station (70.77°S, 11.85°E). The total ozone column on 15 October 1985 was 214 DU. (Data courtesy of Hartwig Gernandt, Alfred Wegener Institute).

The first measurement of a vertical ozone profile under ozone hole conditions was reported by Chubachi (1984). Measurements describing the development of the vertical structure of ozone in the Antarctic spring rapidly followed. A time series of 66 sondes flown between May and December 1985 from the Georg Forster Station (71°S) of the former German Democratic Republic was reported by Gernandt et al. (1987); Gernandt (1987), Iwasaka and Kondoh (1987) described the 1981-1984 ozone sonde measurements from Syowa Sta-

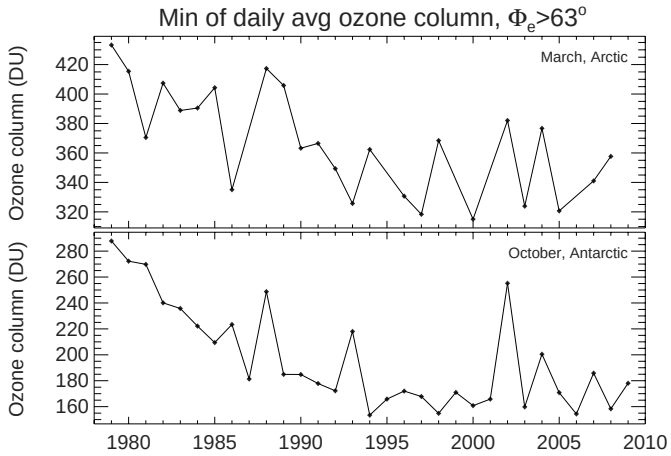

Figure 1.12: Time series of minimum of daily average column ozone poleward of 63° equivalent latitude for March in the Arctic (top panel) and October in the Antarctic (bottom panel). Winters in which the vortex broke up before March (1987, 1999, 2001, 2006, and 2009) are not shown for the Arctic time series. Data were taken from version 2.7 of the NIWA combined ozone database (courtesy of Greg Bodeker, Bodeker Scientific). (Figure adapted and updated from Müller et al., 2008).

tion (69°S) in detail, and Hofmann et al. (1987) described measurements during the period freom 25 August to 6 November 1986 from McMurdo Station (78°S). When ozone measurements in mid-winter and spring are compared (Figure 1.11), the signature of the ozone hole becomes obvious through substantially lower ozone partial pressures in October in the altitude range ($\sim$ 200-30 hPa) where the ozone maximum occurs during mid-winter. More recently, satellite measurements (e.g., Hoppel et al., 2003; Tilmes et al., 2006c) have provided additional, detailed information on the vertical ozone distribution and on chemical ozone loss in the ozone hole. Nonetheless, ozone sonde observations remain important as they provide unique information. Measurements of extremely low ozone mixing ratios (below 0.01 ppm) are not possible with satellite instruments but such observations could potentially provide insights into future ozone layer recovery (Solomon et al., 2005, 2007a).

1.3.2 Arctic Ozone Loss

In many respects, the Arctic wintertime stratosphere resembles its Antarctic counterpart; it exhibits a cold polar vortex separating the air enclosed in it from mid-latitude air. Strong diabatic descent throughout the winter transports air from the upper stratosphere and partly from the mesosphere to the lower stratosphere (e.g., Tuck, 1989). However, the Arctic polar vortex is warmer, smaller and more variable than the Antarctic vortex. The reason for this difference is a stronger planetary wave activity in the northern hemisphere that is caused by the different (less zonally symmetric) distribution of land masses in the northern hemisphere (e.g., Shepherd, 2003, see also Section1.1.3).

The stronger dynamical variability in the Arctic compared to the Antarctic leads to a stronger interannual variability in both chemical loss of ozone and in dynamical supply of ozone-rich air to high latitudes. Therefore, compared to the Antarctic, Arctic ozone abundances in the winter and spring are more variable (Figure 1.12). Nonetheless, in particularly cold winters and in winters with an enhanced burden of volcanic aerosol substantial chemical loss of ozone has been observed in the Arctic (e.g., Tilmes et al., 2004; Goutail et al., 2005; Rex et al., 2006; Tilmes et al., 2008b; WMO, 2007) and has led to Arctic column ozone losses of up to 30%. In dynamically active and therefore warm winters, however, the estimated chemical ozone loss has been very small.

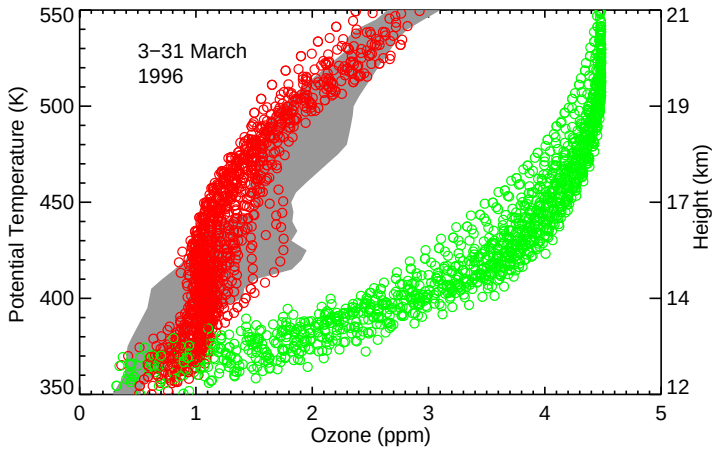

Figure 1.13: Vertical profiles of ozone mixing ratios (red symbols) measured by HALOE inside the polar vortex in March 1996. Potential temperature is used as the altitude scale; approximate geometric height is shown on the right axis. All HALOE observations clearly inside the vortex in March 1996 are shown. Also shown is the proxy ozone mixing ratio $\hat{O}_3$ expected if chemical processing had not occurred (green symbols) derived from the simultaneous methane measurement by HALOE. For comparison, the range of ozone mixing ratios measured in Antarctica in 1985 at the Georg Forster Station (70.77°S, 11.85°E) by ozone sondes (Gernandt, 1987) is shown for September (i.e. for the corresponding season). (Adapted from Müller et al., 1997).

Figure 1.13 shows the vertical profile of ozone mixing ratios (red symbols) measured by the the HALOE satellite experiment in the Arctic vortex in winter 1995/1996 (Müller et al., 1997). These ozone mixing ratios are compared with a proxy for the ozone mixing ratio that would be expected for the Arctic spring in the absence of chemical change (green symbols). This proxy is derived from ozone-tracer relations using chemically long-lived species measured concurrently with ozone (e.g. Müller et al., 1996; Tilmes et al., 2004; Müller et al., 2005). The difference between the measured ozone profile and the proxy ozone profile is a measure for the accumulated chemical loss over winter and early spring 1996/1996. In this very cold Arctic winter, the local ozone loss in the lower stratosphere exceeds 50% and the column loss exceeds 80 DU (Tilmes et al., 2004). Moreover, in Figure 1.13, the ozone profiles measured in austral spring 1985, at the Georg Forster Station (71°S) are shown

(Gernandt et al., 1987; Gernandt, 1987, see also Figure 1.11). The Antarctic profiles measured in 1985 are fairly close to the ozone profiles measured about ten years later in the Arctic.

Nonetheless, a comparison between Arctic and Antarctic ozone loss shows that the two polar regions display a fundamentally different character. Chemical ozone loss of the extent shown in Figure 1.13 is large by Arctic standards. Extreme anomalies associated with the springtime Antarctic ozone hole as observed in many records (frequent removal of more than 90% of the ozone at 70 hPa ($\sim$18 km) and sometimes more than 99%) and ozone mixing ratios of less than 0.1 ppm are not observed in any of the available long-term Arctic records (Solomon et al., 2007a). Therefore, the extreme depletion of ozone that characterises the Antarctic ozone hole is a unique feature on Earth.

1.3.3 Chemical Mechanisms of Polar Ozone Destruction

Farman et al. (1985a) had already tried to link their observations of Antarctic ozone loss with the increase of anthropogenic CFCs in the atmosphere. Alternative explanations were put forward (Tung et al., 1986; Mahlman et al., 1986; Callis and Natarajan, 1986), but these were eventually discarded in favour of a linkage with CFCs, albeit via a completely different chemical mechanism than that Farman et al. had proposed (Solomon, 1999). First signs of a strong perturbation of the Antarctic chlorine chemistry were already perceived during the National Ozone Expedition (NOZE) in 1986 through ground-based observations of strongly reduced column values of HCl (Farmer et al., 1987), strongly enhanced column values of OClO (Solomon et al., 1987), and high concentrations of ClO below 20 km (de Zafra et al., 1987). In 1987, as part of the Airborne Antarctic Ozone Experiment (AAOE, Tuck et al., 1989), aircraft measurements in the stratosphere provided even clearer evidence that the cause of the Antarctic ozone hole is indeed a strongly perturbed chlorine chemistry. These first measurements were subsequently confirmed by a great number of further measurements in the Antarctic from a variety of field campaigns and remote sensing instruments. Likewise, a perturbed chlorine chemistry was found in measurements in the Arctic stratosphere. In both polar regions in winter, strongly enhanced ClO mixing ratios (e.g., Anderson et al., 1991; Waters et al., 1993; Woyke et al., 1999; Vogel et al., 2003; von Hobe et al., 2006), enhanced OClO, (e.g., Schiller et al., 1990; Brandtjen et al., 1994; Kreher et al., 1996; Wagner et al., 2001), and strongly depleted HCl and $ClONO_2$, (e.g., Webster et al., 1993; Oelhaf et al., 1994; Müller et al., 1996; Tilmes et al., 2004; Santee et al., 2008) were detected from balloon, aircraft, and remote sensing experiments.

One year after the discovery of the ozone hole, Solomon et al. (1986) proposed that the reaction of HCl and $ClONO_2$ on the surfaces of polar stratospheric clouds (PSCs) constituted the key initiation step leading to the perturbed polar chlorine chemistry and the subsequent greatly accelerated ozone loss. Later in the same year, Toon et al. (1986) and Crutzen and Arnold (1986) suggested that PSCs were crystalline particles consisting of nitric acid trihydrate (NAT) rather than ice as was previously thought. NAT particles form in the polar region when temperatures drop below $\sim$195 K and thus at significantly higher temperatures than ice particles. Toon et al. (1986) further proposed (correctly as we know today) that sedimentation of PSC particles may remove active nitrogen species from the polar strato-

sphere and that this process contributes to bringing about a perturbed chlorine chemistry in the polar stratosphere.

The suggestion that NAT particles prevailed in the winter polar stratosphere was shown to be correct much later through balloon-borne mass spectrometer measurements in the Arctic (Voigt et al., 2000). The characteristic radii of type I PSCs were originally assumed to be 0.5–3.0 μm (e.g., Hofmann et al., 1989; WMO, 1990). However, from January to March 2000 large NAT particles with radii of 20–40 μm (often referred to as "NAT rocks") were detected by in situ measurements on high-flying aircraft (Fahey et al., 2001). This observation demonstrated that NAT particles can reach sedimentation velocities large enough to allow HNO_3 to be removed from the polar stratosphere thereby causing a "denitrification" of the polar stratosphere. There are also liquid PSC particles, super-cooled ternary solutions (STS) consisting of liquid $H_2O/HNO_3/H_2SO_4$ aerosol particles and, when temperatures drop several degrees Kelvin below the frost point, ice crystals may form (e.g., Carslaw et al., 1997; Peter, 1997; Solomon, 1999).

Both in the Arctic and Antarctic, temperatures reach minimum values in the lower stratosphere in winter. However, average minimum temperatures in the Antarctic are much lower (by about 10 K) than in the Arctic (e.g. WMO, 2007). Therefore, the PSC period is much longer (5 to 6 months) in the Antarctic than in the Arctic, where in warm winters practically no PSC formation occurs (e.g. Manney et al., 2005). Average minimum values over Antarctica are as low as $\sim$185 K in July and August, so that ice PSCs frequently form. In the Arctic, in contrast, ice PSC formation (and PSC formation in general) is often only possible when large amplitude temperature excursions occur caused by mountain waves (e.g. Peter et al., 1992; Carslaw et al., 1998; Fueglistaler et al., 2003).

Table 1.1: Key Heterogeneous Reactions

$HCl + ClONO_2$	$\longrightarrow$	$HNO_3 + Cl_2$
$N_2O_5 + H_2O$	$\longrightarrow$	$2 \times HNO_3$
$ClONO_2 + H_2O$	$\longrightarrow$	$HNO_3 + HOCl$
$HCl + HOCl$	$\longrightarrow$	$H_2O + Cl_2$
$BrONO_2 + H_2O$	$\longrightarrow$	$HNO_3 + HOBr$
$HCl + BrONO_2$	$\longrightarrow$	$HNO_3 + BrCl$
$HCl + HOBr$	$\longrightarrow$	$H_2O + BrCl$

Solomon et al. (1986) first proposed that HCl and $ClONO_2$ would react rapidly on the surfaces of PSCs

$$\text{R9:} \qquad HCl + ClONO_2 \longrightarrow Cl_2 + HNO_3,$$

thereby greatly perturbing gas phase chlorine partitioning in a manner that could strongly accelerate ozone loss in the Antarctic lower stratosphere. Later Prather (1992) and Crutzen et al. (1992) argued that the heterogeneous reaction

$$\text{R10:} \qquad HCl + HOCl \longrightarrow H_2O + Cl_2$$

is an important reaction channel for the activation of HCl and thus for a complete activation of the stratospheric chlorine reservoir.

Today, a variety of heterogeneous reactions of importance to stratospheric chemistry are known (e.g., Sander et al., 2006), the most important are listed in Table 1.1. Originally, it was thought that stratospheric heterogeneous reactions in the polar regions occur only on solid surfaces (e.g., Peter, 1997). Heterogeneous reactions on the ubiquitous stratospheric sulphate aerosol, which is non-crystalline, were known to be important for mid-latitude chemistry (e.g., Rodriguez et al., 1988; Hofmann and Solomon, 1989; Brasseur et al., 1990), but were not thought to be of great relevance for polar chlorine activation.

Due to laboratory measurements of heterogeneous reaction rates of chlorine compounds on stratospheric sulphate aerosol (Tolbert et al., 1988; Hanson and Ravishankara, 1991) and follow-up theoretical studies (Wolff and Mulvaney, 1991; Cox et al., 1994) it emerged that reactions on stratospheric sulphate aerosol, especially when the aerosol is enhanced after strong volcanic eruptions, are very effective for heterogeneous chlorine activation. Today, information from laboratory studies on the reaction probabilities of stratospheric species is available for a variety of solid and liquid aerosol particles. These reaction probabilities are frequently strongly temperature dependent (being relevant only at low temperatures), with the important exception of the reaction of N_2O_5 with H_2O (Table 1.1), which is important at all temperatures occurring in the stratosphere.

Hanson et al. (1994) developed a framework for applying rates of heterogeneous chemical reactions measured in the laboratory to stratospheric conditions and, for the first time, included HCl reactions in sulphuric acid in a photochemical model. Their findings indicated that chlorine activation may occur on background sulphuric acid aerosol at high latitudes. Recently, Katja Drdla revisited this issue in a presentation at the AGU fall meeting in San Francisco in 2005. Based on new laboratory measurements (Shi et al., 2001), she put forward the concept that PSCs are not necessary for polar chlorine activation, but that rather liquid binary H_2SO_4/H_2O sulphate aerosol particles dominate chlorine activation; this is an issue of current scientific research (see also Tilmes et al., 2007, 2008a; Feck et al., 2008). The importance of heterogeneous decomposition of CFCs on the surfaces of PSC particles by dissociative electron attachment as a "pathway to the ozone hole" was suggested by Lu and Sanche (2001a,b). This issue is discussed below in Section 2.2. Based on the evidence provided there, heterogeneous reactions of CFCs on PSCs cannot be of substantial importance to polar ozone chemistry.

The implementation of heterogeneous reactions in photochemical models of stratospheric chemistry is difficult. First, a heterogeneous reaction is a complex process involving adsorption of the reactants on the particle surface, diffusion into the particle and a complicated reaction scheme often involving ionic processes. Second, heterogeneous reactions are triggered when temperatures fall below a certain threshold and model results are rather sensitive to (uncertain) assumptions about these thresholds (e.g., Krämer et al., 2003; Santee et al., 2008).

The Cl_2 formed in the heterogeneous reactions R9 and R10 photolyses rapidly in sunlit air and forms ClO. Further, reactions R9, R10, and related heterogeneous reactions (Table 1.1) suppress the concentration of NO_2 by forming HNO_3. If NO_2 concentrations were not suppressed, the released ClO would readily reform the $ClONO_2$ reservoir (e.g., Müller et al.,

1994; Douglass et al., 1995). Thus, rapid chlorine-catalysed ozone loss requires both the heterogeneous release of chlorine from the HCl and $ClONO_2$ reservoirs ('activation') and the suppression of NO_2 in the gas phase so that chlorine can remain in an active form. The production of Cl_2 in this process implies that sunlight is required to release Cl and start the catalytic cycles.

In the polar regions, the conventional ozone loss cycles (C1) are not effective because of the lack of atomic oxygen (O). At the poles, two different catalytic cycles are responsible for the major fraction of chemical ozone loss; the efficiency of both cycles depends on the concentration of ClO. The most important cycle was proposed by Molina and Molina (1987):

$$\begin{aligned}
&\text{R11:} && \mathrm{ClO + ClO + M} \longrightarrow \mathrm{Cl_2O_2 + M} \\
&\text{R12:} && \mathrm{Cl_2O_2 + h\nu} \longrightarrow \mathrm{Cl + ClOO} \quad (\lambda \leq 400\,\mathrm{nm}) \\
&\text{R13:} && \mathrm{ClOO + M} \longrightarrow \mathrm{Cl + O_2 + M} \\
&\text{R14:} && 2 \times (\mathrm{Cl + O_3} \longrightarrow \mathrm{ClO + O_2})
\end{aligned}$$

$$\text{C3:} \qquad \text{Net:} \quad 2\mathrm{O_3} \longrightarrow 3\mathrm{O_2}$$

where $h\nu$ denotes a photon and M a collision partner (N_2 or O_2). The second cycle also depends on BrO concentrations and thus on the stratospheric bromine loading (Tung et al., 1986; McElroy et al., 1986):

$$\begin{aligned}
&\text{R15:} && \mathrm{ClO + BrO} \longrightarrow \mathrm{Cl + Br + O_2} \\
&\text{R14:} && \mathrm{Cl + O_3} \longrightarrow \mathrm{ClO + O_2} \\
&\text{R16:} && \mathrm{Br + O_3} \longrightarrow \mathrm{BrO + O_2}
\end{aligned}$$

$$\text{C4:} \qquad \text{Net:} \quad 2\mathrm{O_3} \longrightarrow 3\mathrm{O_2}$$

The net result of both cycle 3 and cycle 4 is the destruction of two ozone molecules. Like cycle C1, cycles C3 and C4 are catalytic: chlorine (Cl) and bromine (Br) are not lost in the reaction cycle. In the stratosphere, chlorine is much more abundant than bromine (160 times). Nonetheless, cycle C4 is important as bromine atoms are about 60 times more efficient than chlorine atoms in chemically destroying ozone (Chipperfield and Pyle, 1998; WMO, 2007).

Sunlight is necessary to maintain a large ClO abundance through the photolysis of Cl_2O_2. However, in contrast to the rather shortwave radiation required to produce atomic oxygen, the species that is essential for cycle C1, the photolysis of Cl_2O_2 proceeds at rather long wavelengths and thus under the conditions of low sun found at the poles in spring[9]. Cycles

[9] A recent laboratory study (Pope et al., 2007) questions whether Cl_2O_2 is efficiently photolysed under these

C3 and C4 account for the majority of the ozone loss observed in late winter/early spring in the polar stratosphere. Under cold polar vortex condition, with high ClO abundances, the rate of ozone destruction can reach substantial values, up to 2-3% per day (e.g., McKenna et al., 1990; Salawitch et al., 1990; Rex et al., 1997; Becker et al., 1998, 2000). Outside the polar regions both cycles are of minor importance; C3 is negligible because it is only effective at the low polar temperatures in winter and spring, and C4 is of minor significance because of the much lower ClO concentrations. In summary, large ozone loss rates can only occur when air is both sufficiently cold as well as sunlit, i.e. conditions which largely prevail in spring when ozone depletion is indeed observed.

1.4 The Future of the Stratospheric Ozone Layer

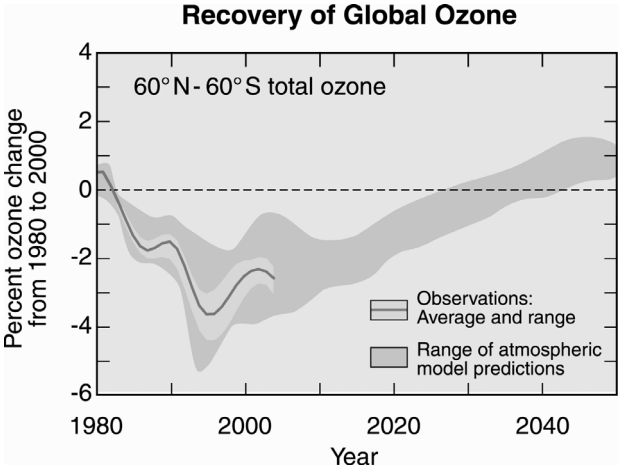

Figure 1.14: Prediction of global ozone recovery. Observed values of mid-latitude total ozone have decreased beginning in the early 1980s. As halogen source gas concentrations decrease in the 21st century, ozone values are expected to recover by increasing towards pre-1980 values. Results from atmospheric computer models that account for changes in halogen gases and other atmospheric parameters show that full recovery is expected in mid-latitudes by 2050, or perhaps earlier. The range of model projections is due to the use of several different models of the future atmosphere. (Figure adapted from WMO, 2007).

Substantial recovery of the ozone layer is expected near the middle of the 21st century. Recovery will occur as halogen source gases that cause ozone depletion decrease in the coming decades under the provisions of the Montreal Protocol and its adjustments and amendments (Figure 1.8). However, the atmosphere will not return to pre-1980 conditions; the influence

conditions; this is a matter of current scientific debate (e.g., von Hobe et al., 2007; von Hobe, 2007; von Hobe et al., 2009).

of climate change and changes in other atmospheric parameters could accelerate or delay ozone recovery (IPCC/TEAP, 2005; WMO, 2007).

Numerical models are used to assess past changes in the global ozone distribution and to project future changes (e.g., Eyring et al., 2006, 2007). Quantities are commonly employed as measures of chemical ozone depletion that rely solely on total column ozone data (e.g., Huck et al., 2007; Müller et al., 2008). For global ozone loss, mostly total ozone averaged between 60°N and 60°S latitude is considered. This measure shows ongoing ozone depletion that began in the 1980s (see Figure 1.14). The model projections indicate that for 60°N-60°S total ozone, the first two stages of ozone recovery (a slowing of the decline and a turnaround WMO, 2007) will be reached before 2020. Full recovery, with ozone reaching or exceeding pre-1980 values, is expected to occur by the middle of the 21st century.

Models predict that over the Antarctic column ozone will increase in spring of around 5 to 10% between 2000 and 2020 (WMO, 2007). The general characteristics of the ozone recovery are similar among the various models (Figure 1.15), namely, the peak depletion occurs around 2000 within a broad minimum, followed by a slow increase in ozone values. Note that in the Antarctic ozone loss is saturated, which means all the ozone in the lower stratosphere is chemically destroyed (e.g., Tilmes et al., 2006a). Under such conditions, ozone loss is expected to remain constant for some time even when stratospheric halogen levels decline. Moreover, the decline in halogen levels will occur later over the Antarctic than at lower latitudes because air in the Antarctic stratosphere is older than air found at lower latitudes (Newman et al., 2007). As a result, reductions in halogen loading to pre-1980 values will occur 10-15 years later in the Antarctic stratosphere than in the mid-latitude stratosphere.

For the Arctic, most models currently predict that springtime column ozone in 2020 will be 0 to 10% above 2000 levels and that ozone turnaround in the Arctic will occur before 2020 (WMO, 2007). For Arctic conditions, there is a large interannual variability in the model projections that does not allow a year to be identified when the ozone turnaround due to a decreasing halogen burden will occur. Model predictions show Arctic ozone increasing to pre-1980 values before 2050. Further, in these predictions, Arctic ozone increases to 1980 values before Antarctic ozone does. However, the strong natural year-to-year variability in the Arctic makes it difficult to obtain accurate model simulations for this region, in particular for polar temperatures and transport barriers (Sankey and Shepherd, 2003; Tilmes et al., 2007).

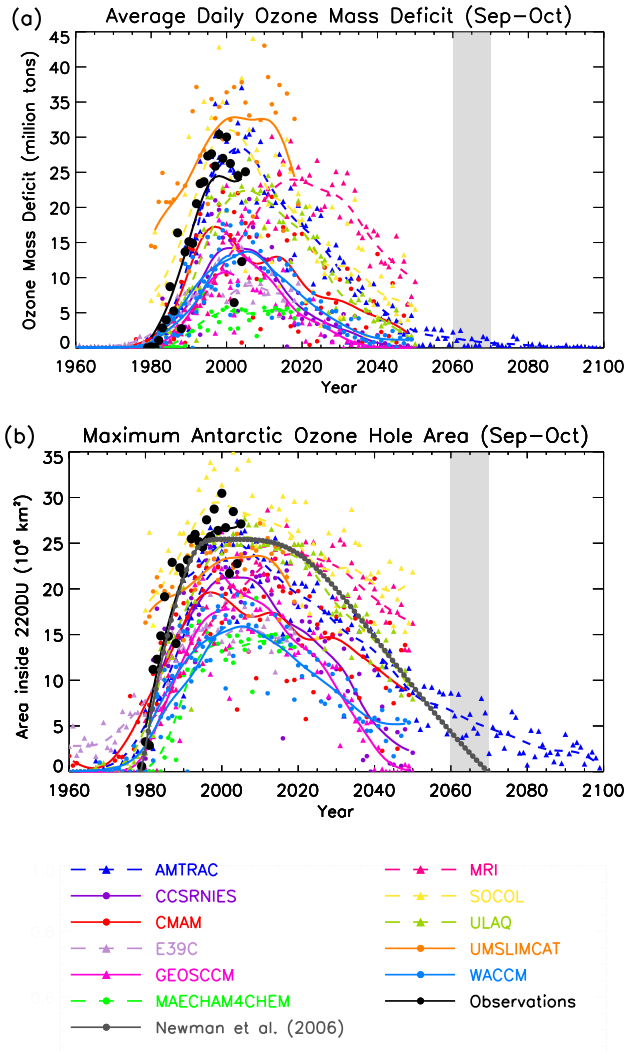

Figure 1.15: The Antarctic September to October average daily ozone mass deficit for each year (top panel) and the maximum Antarctic ozone hole area between September and October (bottom panel) calculated by a variety of chemical climate models (WMO, 2007). Model results are compared with observations calculated using the National Institute of Water and Atmospheric Research (NIWA) combined total column ozone database (Bodeker et al., 2005). Solid and dashed curves show smoothed data derived by applying a 1:2:1 filter iteratively 30 times. Grey circles show the projection from Newman et al. (2006). The light grey shading between 2060 and 2070 shows the period when effective stratospheric chlorine is expected to return to 1980 values. (Figure from WMO, 2007).

1.5 Aims of this Study

Ozone–tracer relations have been used to determine chemical ozone loss in the polar vortices in a large number of studies (e.g., Müller et al., 1996; Richard et al., 2001; Rex et al., 2002; Salawitch et al., 2002; Ulanovskii et al., 2004; Tilmes et al., 2004, 2006c; Lemmen et al., 2006a; Müller et al., 2007) following the pioneering work by Proffitt et al. (1989, 1990, 1992).

However, Plumb et al. (2000) argued that reliable estimates of chemical ozone loss cannot be deduced from ozone-tracer relationships in the polar vortex because the impact of mixing on these relationships cannot be eliminated. Similarly, Muscari et al. (2007), on the basis of an analysis of ground-based measurements of O_3 and N_2O by millimetre-wave spectroscopy, report evidence that mixing within the Arctic vortex in winter 2001/2002 likely mimicked local ozone loss. These arguments were recently summarised by Plumb (2007) as follows:

> In principle, anomalies in these plots [tracer-tracer relations] identify anomalous behavior in at least one of the two tracers, and observation of such anomalies has been used to quantify ozone loss [e.g., Proffitt et al., 1990; Müller et al., 1996] and denitrification [Fahey et al., 1990] in the polar vortices. However, since it has become clear that distinct relationships develop within the vortices because of mixing through the winter, shielded at least in part from the midlatitude relationships by the transport barrier at the vortex edge, it is difficult if not impossible to separate chemical or microphysical processes from the effects of transport.

The aim of this study is to demonstrate the validity of the two main hypotheses that the ozone-tracer correlation method for deducing ozone loss hinges on, first, that a compact ozone-tracer relation is established in the 'early' polar vortex and, second, that any change of the ozone-tracer relation in a sufficiently isolated polar vortex over the course of winter is caused predominantly by chemical ozone loss. The discussion of mixing processes will encompass mixing of polar vortex air with mid-latitude air across the vortex edge (Tuck, 1989; Plumb et al., 2000), of mixing within the vortex caused by differential diabatic descent (Ray et al., 2002; Müller et al., 2005), and of mixing of stratospheric air with air masses intruding from the mesosphere (Engel et al., 2006).

The representation of ozone-tracer relations in models is considered in Section 3.3.1; in particular it is demonstrated which model assumptions in the conceptual model of Plumb et al. (2000) limit the applicability of the model results to the stratospheric polar vortex. Further, cases will be discussed where measurements of ozone-tracer relations are misinterpreted in such a way that mixing in the established polar vortex was assumed to produce substantial changes in ozone tracer relations (Michelsen et al., 1998, see Section 3.3.1) or could "mimic" chemical ozone loss (Muscari et al., 2007, see Section 3.3.3).

A comparison of ozone loss estimated on the basis of ozone-tracer correlations with ozone loss deduced by other methods is discussed in detail elsewhere (Harris et al., 2002b; Tilmes et al., 2004; WMO, 2007). Likewise, a comprehensive discussion of chemical polar ozone

loss based on ozone-tracer relations for the time period 1991-2005 is reported by Tilmes et al. (2004, 2006a). Here, ozone loss estimates are reported for Arctic winter 2002/2003 combining data from two satellite experiments (Section 3.5).

This study was originally submitted as a "Habilitationsschrift" to the Bergische Universität Wuppertal in June 2008. This book constitutes a revised version of the submitted thesis. The thesis was based on five papers, either published in or submitted to peer-reviewed journals. All of these papers have appeared in the meantime and are listed below. The last paper in the list below grew out of the historical material presented in the introduction of this book, but additionally contains a great deal of material not shown here.

- *R. Müller: Impact of cosmic rays on stratospheric chlorine chemistry and ozone depletion,* Phys. Rev. Lett.*,* 91*, 058502, 2003.*

- *R. Müller, S. Tilmes, P. Konopka, J.-U. Grooß, and H.-J. Jost: Impact of mixing and chemical change on ozone-tracer relations in the polar vortex,* Atmos. Chem. Phys.*,* 5*, 3139–3151, 2005.*

- *R. Müller, S. Tilmes, J.-U. Grooß, A. Engel, H. Oelhaf, G. Wetzel, N. Huret, M. Pirre, V. Catoire, G. Toon, and H. Nakajima: Impact of mesospheric intrusions on ozone–tracer relations in the stratospheric polar vortex,* J. Geophys. Res.*,* 112*, D23307, doi: 10.1029/2006JD008315.*, 2007.

- *R. Müller and S. Tilmes: Comment on "Middle atmospheric O_3, CO, N_2O, HNO_3, and temperature profiles during the warm Arctic winter 2001–2002." by Giovanni Muscari et al.,* J. Geophys. Res.*,* 113*, D18303, doi: 10.1029/2007JD009709, 2008.*

- *R. Müller: Comment on: "Resonant dissociative electron transfer of the presolvated electron to CCl_4 in liquid: Direct observation and lifetime of the $CCl_4^{\star-}$ transition state" [JCP 128, 041102 (2008)],* J. Chem. Phys.*,* 129*, 027101, 2008.*

- *R. Müller: A brief history of stratospheric ozone research,* Meteorol. Z.*,* 18*, 3–24, doi: 10.1127/0941-2948/2009/353, 2009.*

2 Tracer-Tracer Relations in the Stratosphere

2.1 Tracer-Tracer Relations as a Tool in Atmospheric Research

Since summer 1958, over a period of several years, the Canberra aircraft of the Meteorological Research Flight of the United Kingdom collected data on temperature, wind, ozone, and water vapour up to an altitude of 15 km. Based on these data, the first plot of a tracer-tracer relation was produced [1]. Roach (1962) published a scatter diagram of ozone and water vapour measurements (Figure 2.1) that he had produced to structure a set of observations which otherwise appeared disordered: "If, however, all individual observations of q [the water vapour mixing ratio] made during the period are plotted against the simultaneous observations of ozone concentration [...], the observations made above the tropopause are seen to fall into two definite groups..." (Roach, 1962). Later, Allam et al. (1981) analysed the ozone-water vapour relations simulated by a numerical model. Ehhalt et al. (1983) suggested a related methodology to reduce the relative variance in stratospheric observations of long-lived trace gases. They found that when the local mean standard deviation of vertical tracer profiles was normalised by the local vertical gradient (a measure that they refer to as 'equivalent displacement height'), this relative variance was greatly reduced.

After these earlier observations, Kelly et al. (1989), considering the methane-nitrous oxide correlation derived from high-altitude aircraft measurements, argued that two lower stratospheric tracers have a compact relationship and that this is because they are both remote from their sources and sinks and are subject to common mixing processes.

Today, these concepts play an important role in research on the tropopause functioning as a transport barrier, both in the tropics and in the extratropics. Hoor et al. (2002) used correlations between CO and ozone (i.e., a tropospheric and a stratospheric tracer) to identify a mixing layer in the lowermost stratosphere and to investigate its seasonal variability. Pan et al. (2006) showed that the mixing between stratospheric and tropospheric air masses deduced from observed CO-ozone relations can be reproduced by transport models. Considering O_3-H_2O and O_3-CH_4 relations from aircraft measurements, Richard et al. (2006) investigated the recirculation between the lower stratosphere and the upper tropical troposphere. Satellite data were also employed for such studies. Park et al. (2008) used chemical constituents obtained from the Atmospheric Chemistry Experiment Fourier Transform

[1] More than forty years later (Tuck et al., 2003) combined the Roach data with more recent high-altitude aircraft (ER-2) measurements to demonstrate the role of the subtropical jet as a mixing and exchange zone.

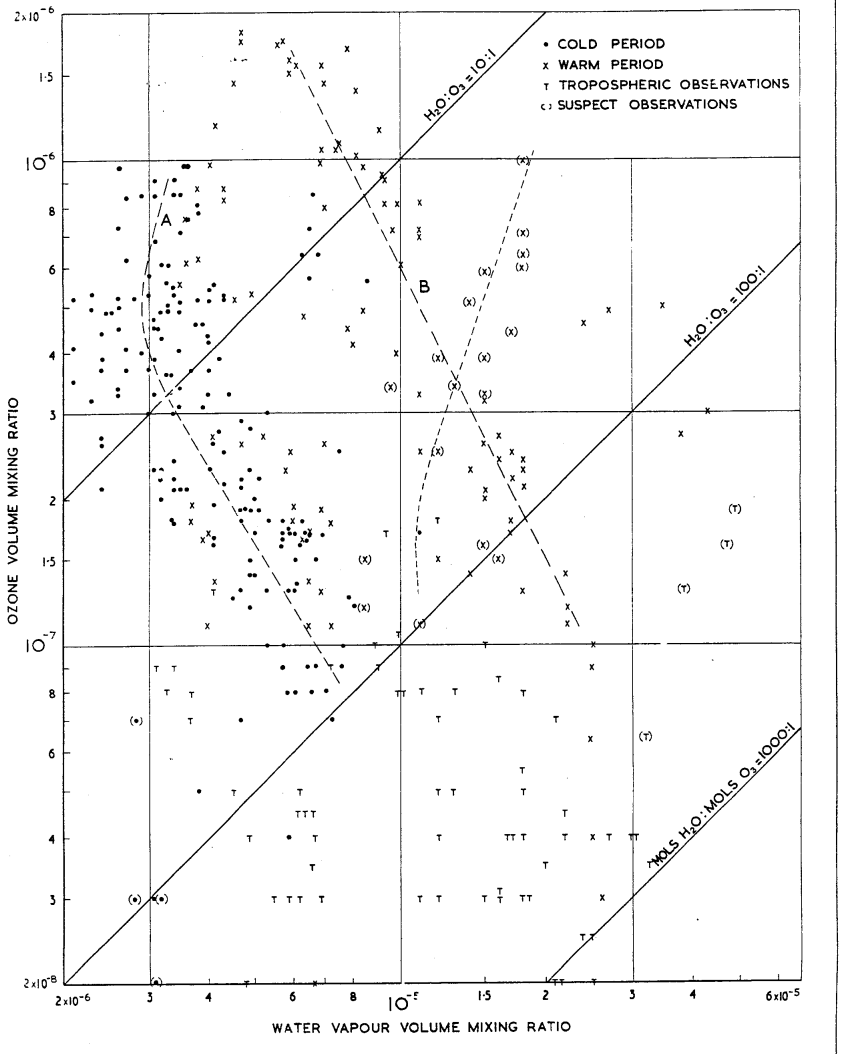

Figure 2.1: The first published tracer-tracer relation (from Roach, 1962). The figure shows measurements taken by the Canberra aircraft of the Meteorological Research Flight of the United Kingdom between 9 January and 14 February 1962 between 52°N and 68°N near the Greenwich meridian.

Spectrometer (ACE-FTS) instrument during summer to provide evidence of chemical isolation in the Asian monsoon anticyclone. Further, they deduced the relative chemical lifetimes of species in the anticyclone with common sources (Ehhalt et al., 1998) from the slope of tracer-tracer relations.

Proffitt et al. (1989) extended the idea of studying relations of two passive (i.e., chemically long-lived for the timescales in question) tracers by considering the relation between a long-lived tracer (nitrous oxide) and a tracer that is subject to chemical change (ozone). In this way they were able to diagnose chemical ozone loss. Soon after, Proffitt et al. (1990, 1993) applied this concept to chemical ozone loss in the Arctic region and Fahey et al. (1990) expanded it to include the analysis of denitrification (removal of total active nitrogen NO_y) of the polar stratosphere by sedimenting PSC particles. Later correlations of long-lived tracers with aerosol number, surface and volume (Borrmann et al., 1993) and hydrochloric acid (HCl) mixing ratios (Müller et al., 1996) were considered to compare aerosol mixing ratios before and after the eruption of Mt Pinatubo and to analyse heterogeneous chlorine activation.

Today, tracer-tracer correlations have been used for many years to quantify chemical ozone loss both in the Arctic and the Antarctic [2]. Measurements from aircraft (Richard et al., 2001; Ross et al., 2004; Ulanovskii et al., 2004), from different satellite experiments (Müller et al., 1996; Tilmes et al., 2003b, 2004, 2006c), balloons (Müller et al., 2001; Salawitch et al., 2002; Vogel et al., 2003; Robinson et al., 2005), and from the space shuttle (Michelsen et al., 1998) were used for such analyses.

Recently, Lemmen et al. (2006b) showed that ozone–tracer relations may also be used to deduce the chemical ozone loss as simulated in chemistry climate models (CCMs) where mixing across the vortex edge is very likely stronger than in the real atmosphere. Using this technique, Lemmen et al. (2006a) demonstrated that chemical ozone loss in the Antarctic vortex is underestimated in the ECHAM4.DLR(L39)/CHEM model (Dameris et al., 2005). Tilmes et al. (2007) analysed results of the Whole Atmosphere Community Climate Model (WACCM3) (Garcia et al., 2007) using ozone–tracer relations and found that chemical ozone loss can be reproduced in the core of the Antarctic vortex, but that it is underestimated in the outer vortex and, even more severely, in the Arctic vortex.

A related, but somewhat different, method to the one described above for using ozone-tracer correlations was put forward by Proffitt et al. (2003). This method involves seasonally averaged ozone and N_2O data partitioned in equal bins of altitude or potential temperature, resulting in separated families of ozone-N_2O curves. In this way, variability in ozone due to recent latitudinal transport is reduced compared to a direct analysis of the ozone measurements. Using measurements from the ILAS and ILAS-II experiments aboard the ADEOS and ADEOS-II satellites (Nakajima et al., 2006), Khosrawi et al. (2004b, 2006) extended the analysis up to altitudes of 1000 K and to the southern hemisphere. Such data sets constitute tools that may be applied for testing atmospheric photochemical models.

[2] In several recent publications (e.g., Tilmes et al., 2004; Müller et al., 2005; Lemmen et al., 2006b), the abbreviation 'TRAC' has been introduced for the tracer-tracer correlation technique to deduce chemical polar ozone loss. Because this abbreviation has not become widely accepted in the scientific literature it is not used here.

2.1.1 Climatology of Ozone–Tracer Relations in the Middle Atmosphere

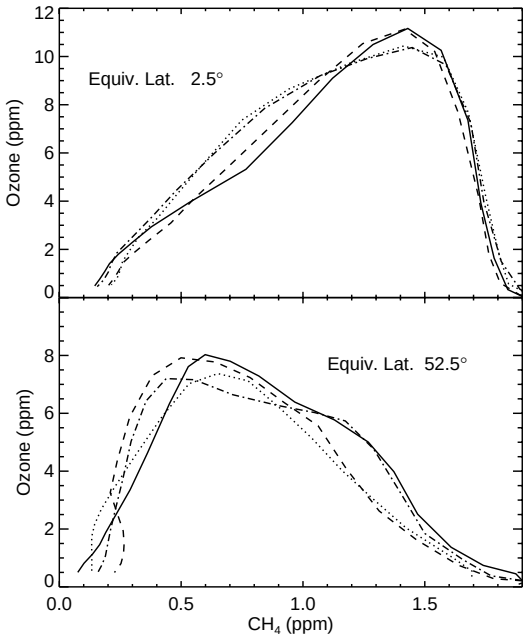

Figure 2.2: The methane–ozone relation at 2.5°N (top panel) and 52.5°N (bottom panel) from a climatology based on HALOE measurements (Grooß and Russell, 2005). Solid lines show data for March, dotted lines for June, dashed lines for September, and dash-dotted lines for December. (From Müller et al., 2007).

The general pattern of ozone–tracer relations above the tropopause is governed by the photochemical sources and sinks of the two species. Ozone mixing ratios are low right above the tropopause, increase with altitude in the stratosphere to reach a maximum above which, due to the HO_x-driven ozone loss cycles increasing in efficiency, mixing ratios decline again (see Section 1.1.2 and Figures 1.3 and 1.5). Long-lived stratospheric tracers with a purely tropospheric source (e.g., CH_4, N_2O, or CFCs) monotonically decline with altitude above the troposphere. (Stratospheric tracers with no tropospheric source that are produced in the stratosphere, e.g. HF, show the opposite behaviour).

Therefore, ozone and long-lived tracers with a tropospheric source are correlated in mesospheric air whereas they are anti-correlated in the lower stratosphere. In the tropics and the mid-latitudes, a 'mountain-shaped' ozone–methane relation thus develops (Figure 2.2). In the tropics, the maximum ozone mixing ratios are greater than at mid-latitudes (Figure 1.6) and the maximum ozone corresponds to higher mixing ratios of methane. This is so because in the tropics substantial ozone production via the photolysis of molecular oxygen begins

at altitudes ($\sim$ 30 hPa) where the stratospheric air is rather young so that methane mixing ratios are still large and thus close to tropospheric mixing ratios. In the mid-latitudes, the stratospheric air is older and thus methane mixing ratios are lower than in the tropics at the altitudes where the maximum ozone occurs (Figure 2.2).

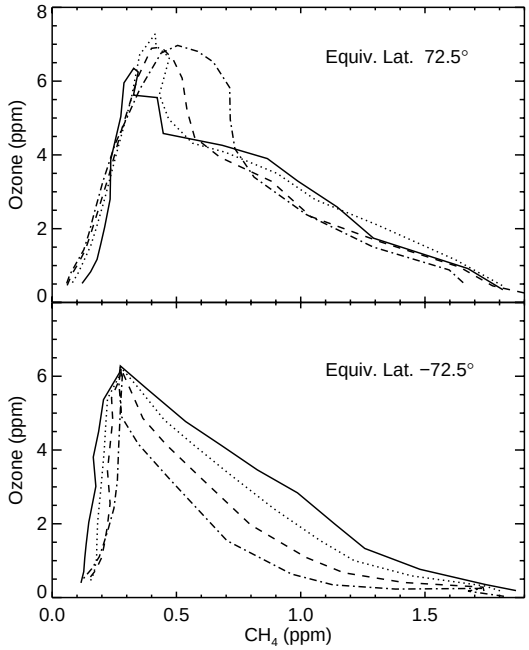

Figure 2.3: Similar to Figure 2.2, but for the polar regions in winter and spring. Top panel shows the methane–ozone relation at 72.5°N and the bottom panel at −72.5°N. In the top panel, the solid line shows data for January, the dotted line for February, dashed line for March, and dash-dotted line for April. In the bottom panel, the solid line shows data for June, the dotted line for July, dashed lines for August, and dash-dotted line for September. (From Müller et al., 2007).

In the polar regions, the ozone–tracer relations are more complex. In late November or early December, a distinct 'early vortex' ozone-tracer relation develops in the Arctic vortex (e.g., Müller et al., 1996; Tilmes et al., 2003b, 2004). The 'early vortex' ozone-tracer relation develops when the transport barrier at the vortex edge becomes strong enough to inhibit in-mixing of mid-latitude air masses. Mixing within the vortex compactifies the relations. The resulting relations are similar to the climatological January relation (Figure 2.3, top panel), but differ from winter to winter (Figure 2.4).

In late winter and early spring, the vortex breaks down starting from the top (e.g., Harvey et al., 2002; Manney et al., 2005), which means that in the vortex in the upper stratosphere and lower mesosphere both ozone and methane increase as air rich in ozone and methane is mixed in from lower latitudes. A mixing zone develops at the interface between the mesospheric air with a positive ozone–methane correlation and the stratospheric vortex air

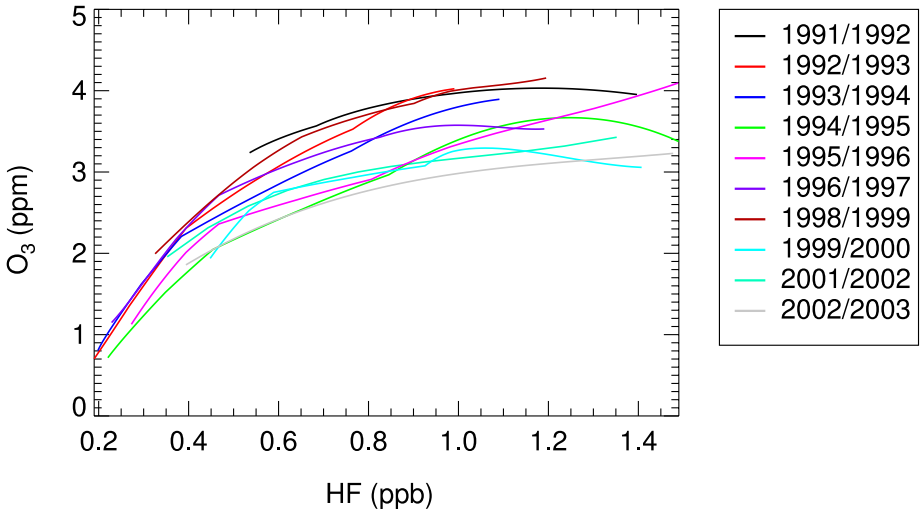

Figure 2.4: Early winter reference relations for ten years from 1991/1992 to 2002/2003 (coloured lines). HF is used here as the chemically long-lived tracer. HF mixing ratios are corrected for the growth rate of HF derived from the HALOE CH_4-HF relationship for each year. Note that because HF increases with altitude in the stratosphere in contrast to CH_4, the ozone–HF relation looks like a 'mirror image' of the ozone-CH_4 relation. (Adapted from Tilmes et al., 2004, Figure 5).

(which shows relatively low ozone mixing ratios) with a negative ozone–methane correlation. In this way, a 'thumb-shaped' ozone–tracer relation (Figure 2.3) develops (see also Plumb et al., 2000, their plate 1).

In the Arctic, the vortex in the upper stratosphere is perturbed owing to the occurrence of midwinter wave events (Waugh and Randel, 1999; Steinhorst et al., 2005). Therefore, this 'thumb-shaped' ozone–tracer relation prevails in the Arctic between February and April and becomes more and more pronounced (Figure 2.3, top panel). By June (not shown), the vortex and thus the signature of ozone-poor vortex air has disappeared and a 'mountain-shaped' ozone–tracer relation is re-established.

In the Antarctic, in contrast, the vortex has a longer life span than in the Arctic and the vortex breaks down more than a month later than its Arctic counterpart (Waugh and Randel, 1999). This difference in the dynamics of the Arctic and Antarctic polar vortex is the reason for the observed differences in the ozone–methane relations. The Antarctic ozone–methane relation in the vortex through winter and early spring (from June to September) is fairly stable (Figure 2.3, bottom panel). Only continously decreasing ozone mixing ratios (due to chemical ozone loss) within the polar vortex are obvious. The effect of the polar vortex breakdown from the top, resulting in the 'thumb-shaped' ozone–tracer relation (not shown) occurs later in the season, in November/December (corresponding to May/June in the northern hemisphere). For the Antarctic, the 'mountain-shaped' ozone–tracer relation is only re-established by January (not shown).

When interpreting Figures 2.2 and 2.3, it must be taken into account that ozone and methane can no longer be considered tracers in the mesosphere (e.g., at 70 km the lifetime of methane and N_2O is about one month, and the lifetime of ozone is about an hour). Therefore, the tracer relations in Figures 2.2 and 2.3 at mesospheric altitudes are only valid in a climatological sense, and specific measurements will not show compact relations.

2.2 Impact of Cosmic-Ray-Induced Heterogeneous Chemistry on Polar Ozone

2.2.1 Relation between Chlorofluorocarbons and Nitrous Oxide: Implications for Chlorofluorocarbon Degradation in the Stratosphere

The importance of heterogeneous reactions for stratospheric chemistry was first discussed by Cadle et al. (1975). Solomon et al. (1986) first suggested the relevance of heterogeneous activation of HCl and $ClONO_2$ for the formation of the ozone hole. Today it is well established that these reactions play an important role in the chemistry of polar ozone depletion (Section 1.3.3). Further, it has been established that cosmic-ray-induced ionisation causes the production of radicals (NO and OH) and that these radicals play a role in the stratospheric polar ozone chemistry (Crutzen and Arnold, 1986; Müller and Crutzen, 1993). However, in a series of papers, Lu and Madey (1999), Lu and Sanche (2001a,b, 2002a,b), and Lu (2009, 2010) go beyond these accepted mechanisms and suggest that the action of cosmic rays on polar stratospheric clouds (PSCs) causes rapid destruction of CFC and that this process "may play a significant role in causing the ozone hole". They suggest that the chemical basis of this process is dissociative electron attachment (DEA) to CFCs on the surface of PSC particles, due to cosmic ray radiation that causes CFC-11 and CFC-12 to be rapidly destroyed in the winter polar stratosphere at altitudes below 20 km. Indeed, DEA to CFCs has been investigated in several laboratory studies (e.g., Kiendler et al., 1996; Lu and Madey, 1999; Nakayama et al., 2004).

The view that DEA-induced CFC destruction on the surfaces of PSC is an important process for stratospheric polar ozone loss has been criticised on the basis of the argument that no significant correlation exits between polar column ozone levels and cosmic ray intensity (Patra and Santhanam, 2002; Müller, 2003) and that both observed CFC distributions and observed CFC/N_2O correlations in the polar stratosphere are inconsistent with a destruction of CFCs on PSC surfaces by DEA (Patra and Santhanam, 2002; Harris et al., 2002a; Müller, 2003; Müller and Grooß, 2009). Further, (Harris et al., 2002a) pointed out that DEA-induced degradation of CFCs would reduce the atmospheric lifetime of CFCs so that it is not obvious what the impact of this process is on estimates of the recovery of the ozone hole.

Nonetheless, until very recently (Lu, 2009, 2010), the Lu and Sanche mechanism has been put forward as of "high relevance to the formation of the ozone hole in earth's atmosphere" (Lu et al., 2004), it is stated that it "plays a crucial role in [...] ozone-depleting reactions in the stratosphere" (Wang et al., 2008), or that there is "strong evidence of the physical mechanism that the CR-driven electron-induced reaction of halogenated molecules plays the dominant role in causing the ozone hole" (Lu, 2009). Ryu et al. (2006) argue more carefully that it "still remains a subject of debate as to its actual role in polar ozone depletion". Below, earlier arguments (Patra and Santhanam, 2002; Harris et al., 2002a; Müller, 2003) regarding the question of a relation between PSC occurrence, cosmic ray flux, CFC degradation, and stratospheric polar ozone depletion are revisited. It is argued that, while some further study

of these questions might be warranted, the Lu and Sanche (2001a,b) mechanism should by no means be considered a new pathway to the ozone hole.

Lu and Sanche (2001a) conjecture that the depletion of CFCs in the stratosphere is related to the combined effect of cosmic ray radiation and the presence of PSCs, but not to solar radiation. This would imply that CFCs are solely depleted by the action of cosmic rays within PSCs, that is solely and extremely rapidly with a lifetime in the order of hours within the polar regions in winter. Such a view contrasts with observations of both substantially reduced CFC mixing ratios (compared to tropospheric mixing ratios) in the tropical upper stratosphere (where PSCs do not occur) and low, but non-zero, mixing ratios of CFCs in the polar vortex in air masses that have experienced PSC processing over at least a few days (Schmidt et al., 1994; Riese et al., 1999; Müller et al., 2001; Hoffmann et al., 2008).

The observed stratospheric CFC patterns (Roche et al., 1998; Riese et al., 1999; Lu and Sanche, 2002a; Khosrawi et al., 2004a; Hoffmann et al., 2008) are, however, in accordance with the conventional picture of being due to the combined effect of large-scale transport and degradation of CFC by photolysis (Harris et al., 2002a; Patra and Santhanam, 2002). The large-scale circulation in the stratosphere, the so-called Brewer-Dobson circulation (see Section 1.1.3), is characterised by slow upward motion in the tropics, poleward and downward motion in mid-latitudes and by descent in the high latitudes (e.g., Holton et al., 1995).

Long-lived trace gases with a tropospheric source (such as CFCs) are destroyed photochemically in the stratosphere during upward transport in the tropics, so that mixing ratios decrease with altitude. In case of the CFCs, the destruction occurs by photolysis. Further, air masses at greater altitudes, characterised by low tracer mixing ratios, are transported poleward, followed by downward transport due to diabatic descent into the winter polar region. This interplay berween the impact of transport and of chemistry on long-lived trace gases such as N_2O, CH_4, and CFCs has been being investigated for decades (e.g., Holton, 1981; Tung, 1982; Solomon and Garcia, 1984). Thus, by far the largest fraction of the CFCs in the air within the polar winter stratosphere has already been chemically converted so that if any additional CFC processing were to occur, it would have only a moderate impact on the lifetimes of CFCs. Disagreement between observed mixing ratios of CFC-12 and simulations with two-dimensional photochemical models (Lu and Sanche, 2002a) should not be taken as an indication of missing chemical processes, but are rather caused by the limitations of the representation of transport in two-dimensional models (WMO, 1999). Indeed, Eyring et al. (2006) demonstrate that problems representing the stratospheric transport accurately persist in modern three-dimensional models; problems that cause uncertainties in the simulated distributions of long-lived tracers and Cl_y.

Stratospheric tracers for which quasi-horizontal mixing along isentropes is fast compared to their local chemical lifetimes show compact relations in scatter diagrams of the mixing ratios of two such trace gases plotted against each other (Plumb and Ko, 1992). Deviation from such compact relations are used for the identification of physiochemical change in the presence of trace gas variations due to transport (e.g., Müller et al., 1997; Tilmes et al., 2004; Müller et al., 2005, see also Section 2.1). Figure 2.5 shows an example of the compact relation of CFC-11 and CFC-12 inside the polar vortex plotted against the chemically long-lived (and thus quasi-inert over the time scales in question) tracer of stratospheric motion N_2O. Both relations are rather compact irrespective of when and where the contributing

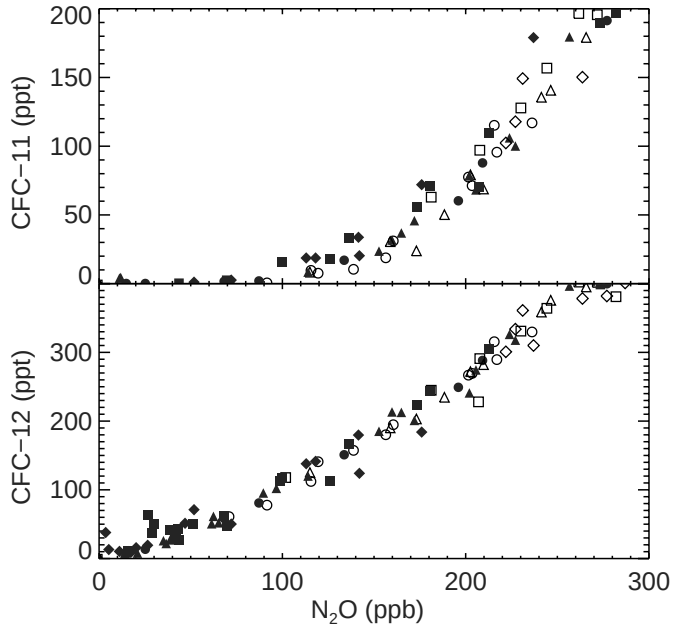

Figure 2.5: Scatter diagrams of the observed mixing ratios of N_2O and CFC-11 ($CFCl_3$) and N_2O and CFC-12 (CF_2Cl_2), top and bottom panels, respectively, in winter 1991-1992. Shown are measurements inside (solid symbols) and outside (open symbols) the polar vortex. Measurements were made in December (circles), January (triangles), February (diamonds), and March (squares). (See Schmidt et al., 1994; Müller et al., 2001, for detailed information on the measurements). Figure adapted from Müller (2003).

measurements were taken. Such a pattern is incompatible with the view that the lifetime of both CFC-11 and CFC-12 is in the order of hours in the presence of PSCs. DEA-induced heterogeneous loss of CFCs should have led to extremely low concentrations of CFC-11 and CFC-12 inside the Arctic vortex during January 1992, a period that was characterised by temperatures low enough to promote strong PSC activity (Farman et al., 1994).

2.2.2 Model Calculations of the Potential Impact of Cosmic-Ray-Initiated Heterogeneous Reactions on Stratospheric Chemistry

The DEA-induced destruction of CFC-11, CFC-12, and HCl on PSC has been implemented in a numerical model of stratospheric chemistry (McKenna et al., 2002a); it is assumed that CFC-11, CFC-12, and HCl are decomposed on the surfaces of PSC particles with lifetimes taken from Lu and Sanche (2001a,b) (Table 2.1). These lifetimes were calculated on the basis of the assumption that CFC-11, CFC-12, and HCl are adsorbed on the surface of the

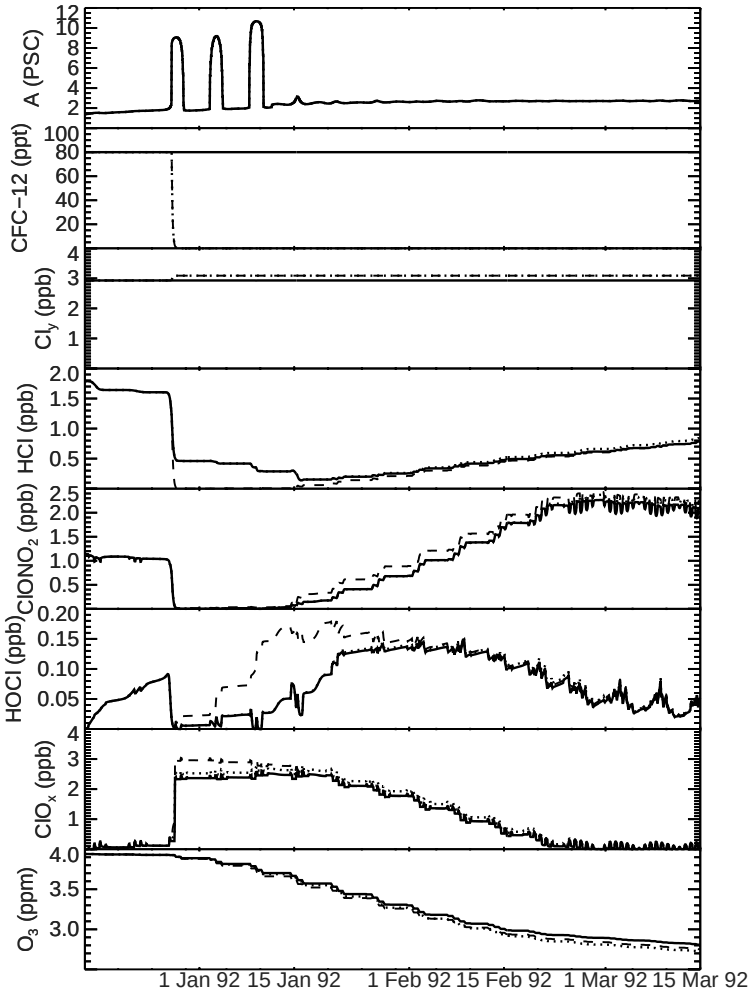

Figure 2.6: Results of model simulations of an air mass representative of the Arctic polar vortex in 1991-1992. Three cases are shown: dashed line, a simulation including DEA-induced heterogeneous destruction of CFC-11, CFC-12, and HCl (case a), dotted line, a simulation with DEA-induced destruction only of CFC-11 and CFC-12 (case b), and, solid line, a simulation without any DEA-induced heterogeneous chemistry (case c). The top panel shows the total simulated PSC surface area density (in $\mu m^2/cm^3$), and the panels below the volume mixing ratios of key chemical species (where the active chlorine ClO_x is defined as ClO + 2 $\times$ Cl_2O_2 and total inorganic chlorine Cl_y as HCl + $ClONO_2$ + HOCl + ClO_x). Figure taken from Müller (2003).

Table 2.1: Lifetimes of CFC-11, CFC-12, and HCl due to DEA on PSC Surfaces

Species	σ_{DEA} (cm^{-2})	R (s^{-1})	τ (s)	τ (h)
CFC-11	$1.1 \cdot 10^{-13}$ [a]	$3.6 \cdot 10^{-4}$ [a]	$2.8 \cdot 10^{3}$	0.8
CFC-12	$1.3 \cdot 10^{-14}$ [a]	$4.3 \cdot 10^{-5}$ [a]	$2.3 \cdot 10^{4}$	6.5
HCl	$4.0 \cdot 10^{-15}$ [b]	$1.3 \cdot 10^{-5}$	$7.7 \cdot 10^{4}$	21

The lifetimes of CFC-11, CFC-12, and HCl assumed in the model calculations for DEA on PSC surfaces
[a] Taken from Lu and Sanche (2001a)
[b] Taken from Lu and Sanche (2001b)

PSC. Without adsorption, DEA-induced destruction on PSCs cannot occur (Harris et al., 2002a). On the other hand, because there are no reaction channels competing with DEA-induced loss of CFC, the results of the model calculations are not sensitive to the precise value of the assumed loss rates. The air mass considered is representative of the polar vortex in the Arctic in winter 1991-1992 (Becker et al., 1998). The calculation is initialised for 15 December 1991; initial mixing ratios are taken from Becker et al. (1998), except for CFC-11 (4 ppt) and CFC-12 (80 ppt), corresponding to N_2O = 80 ppb (Figure 2.5). The calculation is carried through until 15 March 1992; the vortex air descends from ∼21 km to ∼17 km over that time period (Becker et al., 1998). Three cases were considered (Figure 2.6): a) a calculation including DEA-induced heterogeneous destruction of CFC-11, CFC-12, and HCl, b) a simulation with DEA-induced destruction of only CFC-11 and CFC-12, and c), the standard case, a simulation without any DEA-induced heterogeneous chemistry.

Compared to the standard case c), considering DEA-induced destruction of only CFC-11 and CFC-12 (case b) results in somewhat greater mixing ratios of active chlorine (ClO + $2 \times Cl_2O_2$), due to the activation of the chlorine contained in CFC-11 and CFC-12, and, consequently, a somewhat greater degree of ozone destruction (by ∼8%). However, the air in the polar vortex has been in the stratosphere long enough (typically several years) for the major fraction of CFC-11 and CFC-12 to be chemically converted to other compounds (mainly HCl and $ClONO_2$) at the time when PSCs form. Therefore, at that time the chlorine contained in CFC-11 and CFC-12 constitutes only a minor fraction of the atmospheric chlorine so that any additional processing can have only a minor effect on the levels of total inorganic chlorine (Cl_y) and thus on the levels of active chlorine (ClO_x).

A somewhat greater impact on the model results is given by the assumption of DEA-induced HCl destruction that leads to a practically complete activation of the HCl reservoir in case a) compared to b) (Figure 2.6). While this does not impact Cl_y, it results in initially greater active chlorine mixing ratios. However, the extremely low HCl mixing ratios allow a more rapid increase of $ClONO_2$, i.e., a more rapid deactivation of chlorine starting after the last simulated PSC activity around mid-January that eventually leads to slightly lower ozone loss in case a) compared to b).

The major result of the model simulations is that the temporal development of the key

chemical species, and in particular the ozone loss, does not drastically alter depending on whether loss of CFC-11, CFC-12, and HCl on PSCs due to DEA is included in the model or not. The only exceptions are the concentrations of CFC-11 (not shown) and CFC-12 (Figure 2.6) that take on mixing ratios of practically zero within hours after the first PSC event if destruction due to DEA is included in the model. Otherwise, CFC-11 and CFC-12 are practically chemically inert in the polar winter stratosphere (Figure 2.6). In the case of HCl, DEA-induced destruction on PSC competes with the likewise very rapid heterogeneous reaction of HCl with $ClONO_2$ and HOCl on PSC surfaces (Peter, 1997). Consequently, the simulated HCl concentrations with and without DEA-induced HCl degradation do not differ substantially; only in the former case do HCl concentrations reach extremely low levels within hours after the first occurrence of PSC, a process that is otherwise halted by the titration of the heterogeneous reaction partners ($ClONO_2$ and HOCl) of HCl (Figure 2.6). The loss rate of ozone is little affected by assumptions about the occurrence of DEA-induced reactions on PSCs; about 5% more ozone is chemically destroyed in the model when DEA-induced loss of CFC-11, CFC-12, and HCl is taken into account. The rather small changes predicted for the mixing ratios of key species due to DEA-induced reactions are unlikely to be detectable by satellite measurements. However, high precision in situ measurements of CFC-11, CFC-12, and HCl in an air mass shortly after the first occurrence of PSC might allow the effect of DEA-induced reactions to be identified in the atmosphere.

2.2.3 Correlation between Polar Ozone Levels and Cosmic Ray Intensity

In support of their proposed mechanism, Lu and Sanche (2001a) further argue that the annual average ozone for latitudes 0°-65°S over the period 1979-1992 exhibits a variation in inverse phase with cosmic ray activity. Indeed, it is well established that long-term total ozone variations in the tropics and mid-latitudes possess a component that is in phase with the 11-year solar cycle (and thus in inverse phase with cosmic ray activity) (Chandra and McPeters, 1994) and that upper stratospheric ozone concentrations vary with an amplitude of a few percent over a solar cycle (Chandra and McPeters, 1994; Miller et al., 1997). However, the Lu and Sanche (2001a) mechanism requires the presence of PSCs that only occur in the polar regions in the lower stratosphere and only during winter (Solomon, 1999; Peter, 1997).

Therefore, Müller (2003) compared cosmic ray intensity with the average total ozone value for the northern and southern hemisphere polar regions in March and October, respectively (Newman et al., 1997) and found that there is no apparent correlation between cosmic ray intensity and polar ozone. Similarly Patra and Santhanam (2002), considering total ozone time series from the two longest-serving stations in the northern (Arosa; 46.8°N, 9.68°E) and the southern (Halley; 75.35°S, 26.34°W) hemisphere, argued that the correlation between cosmic ray intensity and ozone depletion claimed by Lu and Sanche (2001a) has not been clearly established.

However, the arguments by Patra and Santhanam (2002) and Müller (2003) that no significant correlations exits between polar ozone and cosmic ray intensity have been based

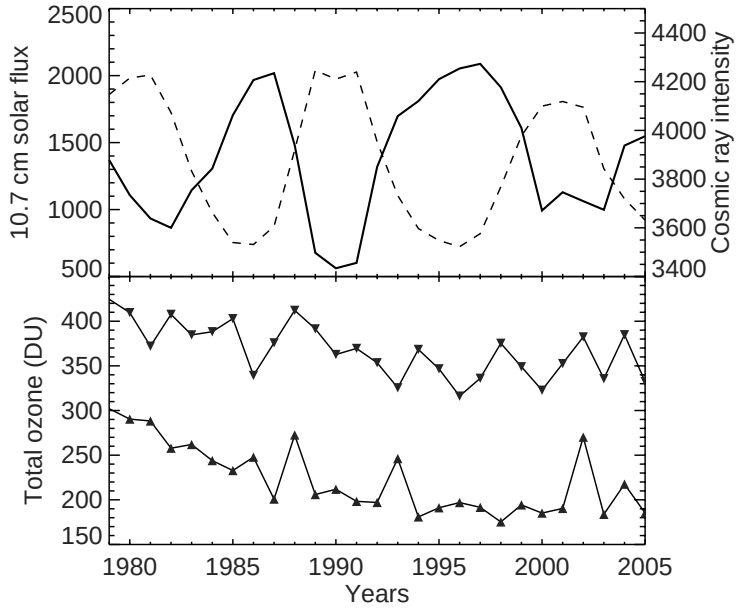

Figure 2.7: The variation over the time period 1979-2005 of cosmic ray intensity (solid line, top panel), solar intensity (dashed line, top panel), and minimum of daily average column ozone in the polar region (bottom panel). Column ozone is given in Dobson units (DU). The pressure-corrected neutron count (counts per minute) at Climax, Colorado, USA, is shown as a measure of cosmic ray intensity and the 10.7 cm (2800 MHz) solar flux adjusted to 1 A.U. in units of 10^{-21} W m^{-2} Hz^{-1} as a measure of solar intensity. The minimum values of daily average column ozone poleward of 60° equivalent latitude for March in the Arctic and October in the Antarctic were taken from Müller et al. (2008). Winters in which the vortex broke up before March (1987, 1999, and 2001) are not shown for the Arctic ozone time series. (Taken from Müller, 2008).

so far on rather simple measures of polar chemical ozone loss. Recently, it has been proposed that the minimum of daily average total ozone poleward of a given equivalent latitude would be a more useful measure of polar ozone loss (Müller et al., 2008). Figure 2.7 shows a comparison of cosmic ray intensity with this measure of polar ozone loss over the time period 1979-2005. This comparison corroborates the findings of earlier studies (Patra and Santhanam, 2002; Müller, 2003) indicating that there is no significant correlation between cosmic ray intensity and polar ozone.

But even the minimum of daily average total ozone over the pole is only an approximate measure of chemical ozone loss (Müller et al., 2008). As will be discussed in detail in Chapter 3 below, when sufficient information is available, it is always preferable to employ sophisticated measures of chemical polar ozone loss that allow the signal of *chemical* ozone change to be isolated from ozone changes caused by transport. Such measures of chemical ozone loss show a very close correlation with the potential for heterogeneous chlorine activation on PSCs (Rex et al., 2004; Tilmes et al., 2006a, 2008b,a). Chemical ozone loss

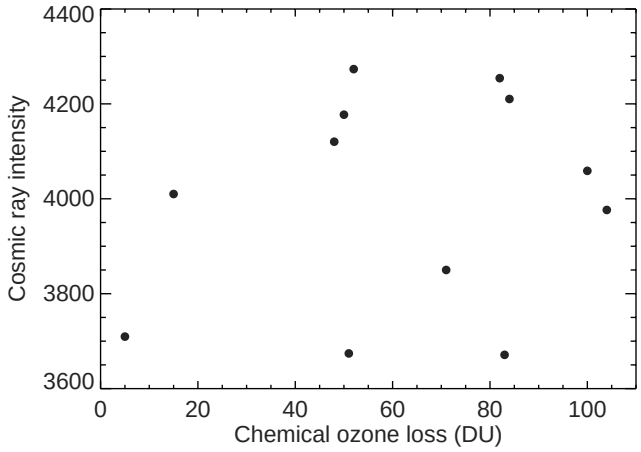

Figure 2.8: Scatter plot of chemical ozone loss in the core of the Arctic vortex in the lower stratosphere for the time period 1992 to 2005 (no data are available for 2001 and 2004) deduced from ozone-tracer relations (Tilmes et al., 2004; von Hobe et al., 2006; Tilmes et al., 2008b) plotted against cosmic ray activity. As in Figure 2.7, the neutron count (counts per minute) at Climax is taken as a measure of cosmic ray intensity. (Taken from Müller, 2008).

estimates are available for the time period 1992 to 2005 from satellite measurements of ozone-tracer relations (Tilmes et al., 2004; von Hobe et al., 2006; Tilmes et al., 2008b, see also Section 3.5 below). In Figure 2.8, these chemical ozone loss estimates are plotted against cosmic ray activity. Clearly there is no significant correlation, the correlation coefficient is 0.21.

2.2.4 Conclusions on the Impact of Cosmic-Ray-Induced Chemistry on Stratospheric Chemistry

The ozone loss mechanism proposed originally by Lu and Sanche (2001a,b) cannot be of relevance outside the polar regions in winter where PSCs do not occur (e.g., Peter, 1997; Solomon, 1999; WMO, 2007). In the polar regions, there is neither a significant correlation between cosmic ray activity and column ozone levels (Figure 2.7, see also Müller and Grooß, 2009) nor between cosmic ray activity and chemical ozone loss estimates (Figure 2.8). Further, both the observed spatial distributions of CFC-11 and CFC-12 in the stratosphere and the development of CFC-11/N_2O and CFC-12/N_2O tracer relations in polar winter are inconsistent with the notion that these compounds are exclusively, and very rapidly, destroyed by DEA on PSC particles (Figure 2.5, see also Müller and Grooß, 2009). Moreover, model simulations indicate that stratospheric polar ozone chemistry – most notably chemical ozone destruction – is not substantially altered if DEA-induced processes on PSCs are taken into account (Figure 2.6). However, DEA-induced destruction of HCl on PSCs could have some influence on stratospheric chlorine chemistry. At the present time,

it seems to be an open question whether or not the latter process occurs in the atmosphere. Therefore, the role of the Lu and Sanche (2001a,b) mechanism as a key mechanism for the formation of the ozone hole should be presented as an issue debated in the scientific literature rather than as an established scientific fact. In any case, the potential impact of DEA processes on polar ozone recovery is expected to be small because of their limited influence on both CFC lifetimes and on chemical ozone loss.

3 Quantifying Polar Ozone Loss from Ozone-Tracer Relations

3.1 Principles of the Tracer-Tracer Correlation Technique

Based on model calculations and theoretical considerations, Plumb and Ko (1992) argued that throughout the stratosphere compact relationships are expected between tracers for which quasi-horizontal mixing along isentropes is fast compared to their local chemical lifetimes. The relationship, furthermore, should be linear if the local chemical lifetimes of the two tracers in question is long against the timescale of vertical advection (Plumb and Ko, 1992). Compact and over the course of the winter constant relationships of long-lived tracers are also expected for the special case of the air mass inside a polar vortex that is, to a large extent, isolated from its surroundings. Plumb and Ko (1992) expressed this fact as: "... we expect these relationships for long-lived species to remain valid inside the polar vortex, [...]. Since the vortex is in place only for a few months during winter, the correlations will be maintained through the winter, though the mixing ratio isopleths may become severely distorted at the vortex edge...". Such behaviour, for example, is found in HALOE observations in the Arctic vortex in 1995/1996 where the relation of the long-lived compounds HF and CH_4 was conserved over the course of the winter (Müller et al., 1999). Another example is the conservation of the relation between CFC-11 and CFC-12 and N_2O during winter 1991/1992 shown in Figure 2.5. It is important to note that distinct curves develop in the polar vortex, the mid-latitude "surf zones", and in the tropics (e.g., Proffitt et al., 1992, 1993; Müller et al., 1996; Plumb, 2007).

If one of the tracers for which the tracer-tracer relation in the polar vortex is considered is subject to chemical change on the timescale of weeks or even faster, this chemical change will lead to a breakdown of the conservation of the tracer-tracer relation. The tracer-tracer correlation technique makes use of this effect by considering relations between chemically long-lived (passive) tracers and tracers which could be subject to chemical or physical change; such changes are identified as changes in the tracer relations.

The tracer-tracer correlation technique has been applied almost exclusively to polar vortex studies so far, typically for seasonal studies like those of polar ozone loss, chlorine activation or denitrification in polar winter, where CH_4, N_2O, or HF were used as long-lived tracers. Physicochemically active species considered are ozone, $ClONO_2$, HCl, or NO_y (e.g., Fahey et al., 1990; Proffitt et al., 1990; Salawitch et al., 2002; Tilmes et al., 2004; Müller et al., 2007; Tilmes et al., 2008b).

First, we will focus on ozone-tracer relations for deducing chemical ozone loss in the

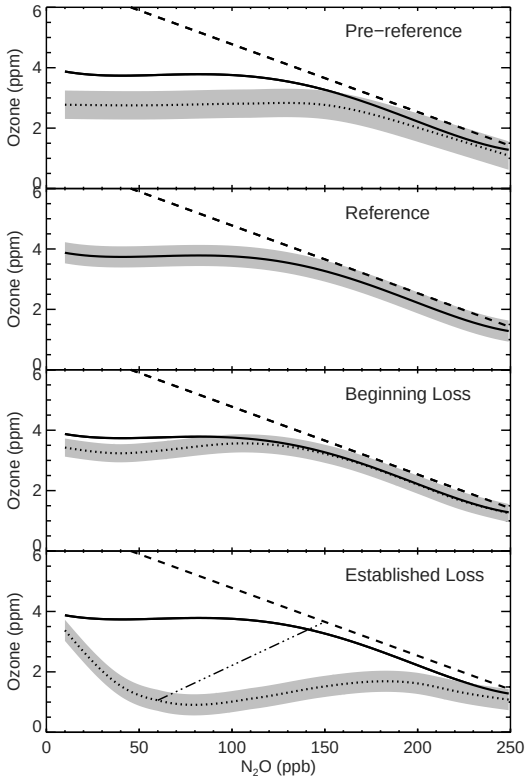

Figure 3.1: Schematic view of the of the development of ozone-tracer relations over the course of the winter inside the polar vortex. In all panels, the thick solid line indicates the reference relations for 'early vortex' conditions and the thick dashed line an average mid-latitude relation. The dotted line in the top panel indicates the ozone-tracer relation in the incipient vortex before a strong transport barrier is established at the vortex edge. The panel below shows the reference relation for an established vortex and one further panel below the ozone tracer relation for beginning chemical ozone loss. The bottom panel shows the conditions for established ozone loss, the dash-dotted line indicates a possible mixing line between vortex and out-of-vortex air. (Figure taken from Müller et al., 2005).

Arctic and Antarctic polar vortex. The polar vortex starts forming in late autumn (November in the northern hemisphere and May in the southern hemisphere). In this incipient vortex (Figure 3.1, top panel) the vortex air mass is characterised by low ozone mixing ratios; the remainders of polar ozone destruction due to NO_x-driven chemical cycles in summer (e.g., Farman et al., 1985b; Crutzen and Brühl, 2001) and autumn (Kawa et al., 2002; Tilmes et al., 2006b). Although the vortex air mass is separated to a certain extent from ozone-rich, mid-latitude air, the vortex is not yet completely isolated. Thus, through mixing, ozone values in the vortex increase during this period (Tilmes et al., 2003b, 2006b).

When the vortex is well established, the transport barrier at the vortex edge effectively separates the vortex air from mid-latitude air. Mixing within the vortex air mass produces a compact ozone-tracer relation in the vortex (Figure 3.1). At this point in time, a reference relation for the ozone-tracer relation, referred to as the "early winter reference function", should be derived. Ideally, the relation is determined at a time before chlorine is activated by heterogeneous reactions on PSCs and before ozone has changed chemically. This reference relation is empirically determined as a polynomial fit through the available ozone-tracer data in the early vortex that describes ozone as a function of the measured tracer (e.g., Müller et al., 1996; Tilmes et al., 2004); this is the first step in deriving chemical loss.

In cold Arctic winters, a beginning chemical ozone loss first becomes noticeable at greater altitudes (∼500 K), as a deviation of the ozone-tracer relation from the reference, typically in late January/early February in the Arctic (Tilmes et al., 2003b; Müller et al., 2005). Towards late winter, with solar illumination strongly increasing, the ozone loss accelerates. Thus, in early spring, the signal of accumulated ozone loss is very pronounced in the ozone-tracer relation (Figure 3.1, bottom panel).

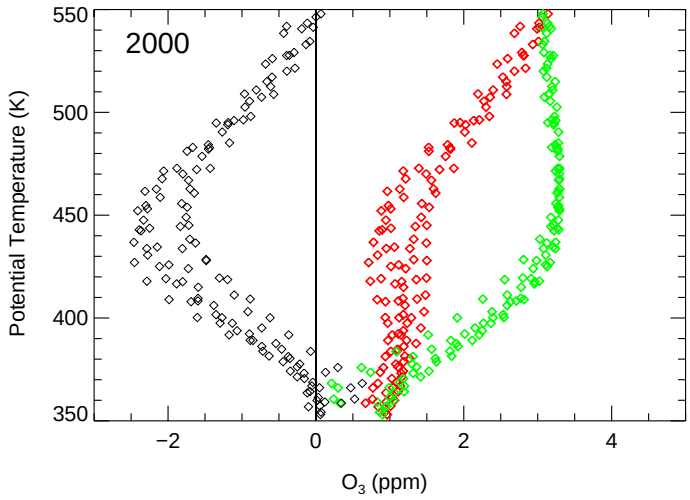

Figure 3.2: Vertical profile in the vortex core of measured ozone for the period 11–14 March 2000 (red symbols), proxy ozone $\hat{O}_3$ calculated from an early winter reference function (green symbols), and of chemical ozone loss (black symbols). Chemical ozone loss is calculated as the difference between proxy ozone $\hat{O}_3$ and measured ozone. (Figure adapted from Müller et al., 2002; Tilmes, 2004).

To quantify chemical ozone loss from ozone-tracer relations, a proxy for the ozone mixing ratio under chemically unperturbed conditions ($\hat{O}_3$, green symbols in Figure 3.2) is computed by combining the tracer measurements in March with the reference relationship. Thus, $\hat{O}_3$ describes the ozone mixing ratio that would be expected in the vortex in early spring in the absence of chemical change (e.g., Müller et al., 1996; Tilmes et al., 2004).

The vertical profile of this proxy is compared with the measured vertical distribution

of ozone mixing ratios (red symbols in Figure 3.2) in the vortex in spring, the difference between the proxy ozone and the measured ozone is the chemical ozone loss (black symbols in Figure 3.2). Integrating in the vertical over the ozone loss profile yields the chemical loss in column ozone (see Appendix B for details).

3.2 Reference Ozone-Tracer Relations in the 'Early' Polar Vortex

3.2.1 Reference Relations Constructed from Mixing Lines

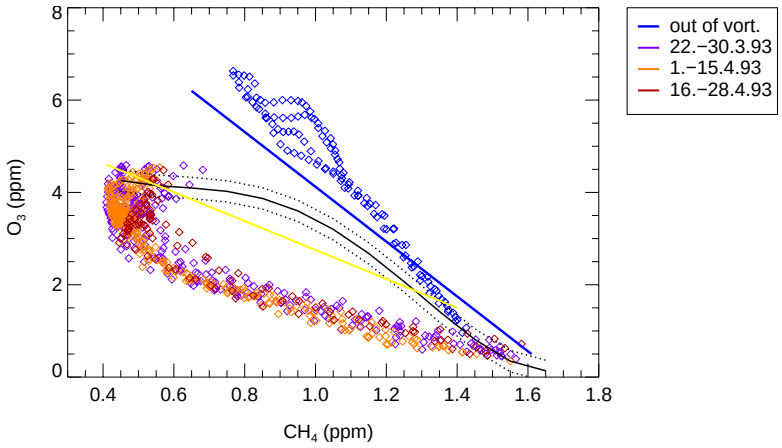

Figure 3.3: Reference relations for the ozone-methane relation in the early vortex in winter 1992/1993 from HALOE (Russell et al., 1993) and ATMOS (Michelsen et al., 1998). The black line shows the reference relation deduced from HALOE measurements in November 1992 in the early vortex, the dotted lines give the range of uncertainty (Tilmes et al., 2004). The yellow line shows the 'mixing line' reference estimated by Michelsen et al. (1998) based on ATMOS measurements, and the solid blue line shows the out-of-vortex, high latitude (63°N-69°N), reference based on ATMOS measurements from 8-16 April 1993 (Michelsen et al., 1998). The ATMOS relations were converted from a N_2O-O_3 relation to a CH_4-O_3 relation using the reported ATMOS CH_4-N_2O relation (Michelsen et al., 1998). Further shown are HALOE measurements inside the vortex in late March (purple diamonds), early April (orange diamonds), and late April 1993 (red diamonds). The blue diamonds indicate HALOE measurements in April 1993 in high latitudes outside the vortex. (Figure adapted from Müller et al., 2005).

Michelsen et al. (1998) analysed observations of ozone and N_2O made by the space shuttle experiment ATMOS (Atmospheric Trace Molecule Spectroscopy) in the Arctic in March/April 1993. By considering the O_3-N_2O relationship they found that, on the same N_2O level, much lower (∼50-60%) ozone mixing ratios are observed inside compared to outside the polar vortex. Michelsen et al. (1998) interpret this difference between the out-of-vortex reference (blue line in Figure 3.3) and the measurements inside the vortex as a signature of chemical ozone loss, but emphasise that chemical effects are unlikely to account for the entire difference. They also construct an alternative reference (the yellow line in their Plate 4a, see also Figure 3.3) for the O_3-N_2O relation by deducing mixing through considering the N_2O-CH_4 tracer space. This line is constructed as a mixing line for a single

mixing event (e.g., Plumb, 2007). However, it is unlikely that mixing of air between the two end-points of the mixing line separated by $\sim$25 km in altitude for an out-of-vortex profile (Michelsen et al., 1998, Plate 3) actually occurred in reality. Thus, this line should only be seen as an approximation to a reference relation that would develop by continuous mixing.

Comparing this reference with the March/April 1993 vortex observations from ATMOS, Michelsen et al. (1998) deduced only half of the ozone deficit that they deduced from an out-of-vortex reference. This finding is sometimes erroneously generalised to cases (e.g., Müller et al., 1996; Salawitch et al., 2002; Tilmes et al., 2004; Müller et al., 2007) where ozone-tracer relationships in the late vortex are compared with an *early vortex* reference (that is, a reference derived from observations made inside the vortex at a time before chemical ozone loss occurs) to deduce chemical ozone loss. Out-of-vortex ozone-tracer relations are characterised by greater ozone mixing ratios for a given tracer value than vortex relations (Proffitt et al., 1993; Müller et al., 2001; Tilmes et al., 2004). Therefore, it is incorrect to interpret the findings of Michelsen et al. (1998) to mean that "mixing could produce about half the changes in the O_3-N_2O relation" as it is stated, for example, by Plumb et al. (2000).

In Figure 3.3, we compare the out-of-vortex measurements from ATMOS in April 1993 (blue line), the Michelsen et al. (1998) 'mixing reference' (the yellow line in their Plate4a shown here again as a yellow line) and the early vortex reference derived from HALOE early vortex measurements in 1992 (Tilmes et al., 2004, black line). Obviously, the latter reference and the best reference (yellow line) suggested by Michelsen et al. (1998) are in reasonable agreement. Certainly, they are closer to each other than any of them to the out-of-vortex ATMOS measurements. Therefore, ozone loss estimates deduced from these two references will be rather similar. Using the early vortex reference from Tilmes et al. (2004) yields an ozone loss of 117 ± 17 DU for April 1993 in the altitude range 380-550 K (corresponding to 1.4 ppm $< CH_4 <$ 0.5 ppm) whereas employing the 'mixing line reference' from Michelsen et al. (1998) yields an ozone loss of 98 DU: that is, only 16% less ozone loss than that obtained from the Tilmes et al. (2004) reference. Nonetheless, long-range (in tracer space) mixing lines can only yield an approximation to the atmospheric conditions. Therefore, if used as reference relations for ozone loss estimates, mixing line references will be associated with a greater uncertainty than an early vortex reference deduced from measurements.

Note that the HALOE measurements between late March and late April 1993 in the polar vortex (Figure 3.3) show a compact relation, clearly distinct from any of the reference relations. These HALOE measurements are rather similar to the ATMOS vortex observations in April 1993 (Plumb et al., 2000). The out-of-vortex HALOE observations at 71°N (blue diamonds in Figure 3.3) in April 1993 are comparable to the ATMOS out-of-vortex data.

3.2.2 Representation of Ozone-Tracer Reference Relations in Models

While classical two-dimensional models have been used in the past to study tracer-tracer relations (Plumb and Ko, 1992; Proffitt et al., 1992), today three-dimensional models are available for the simulation of transport and chemistry in the stratosphere. A particular

advantage of three-dimensional models is that transport barriers in the stratosphere can be better represented than in two-dimensional models. The most important stratospheric transport barriers, the polar vortex edge and the subtropical barrier, are essential for the formation of different compact tracer-tracer relations in the stratosphere (e.g., Michelsen et al., 1998; Plumb, 2002; Proffitt et al., 2003).

Nevertheless, even state-of-the-art three-dimensional models will misrepresent transport, and thus tracer-tracer relations, in some way. Depending on the numerical advection scheme employed, transport errors are introduced through numerical diffusion and dispersion (e.g., Rood, 1987; Müller, 1992). Dispersion errors that arise particularly strongly in centred difference and in spectral schemes may lead to spurious scatter in simulations of nonlinear tracer-tracer relationships (Thuburn and McIntyre, 1997).

Three-dimensional Eulerian models

Sankey and Shepherd (2003) presented a thorough investigation of tracer relations in the stratosphere using the Canadian Middle Atmosphere Model version 7 (CMAM); they applied a number of observed tracer-tracer relations to validate the model results. The model utilises a (T32) spectral transport scheme with 50 layers in the vertical and a ~ 3 km vertical resolution in the middle atmosphere. The vertical diffusion coefficient K_{zz} is set to $1\,\mathrm{m^2 s^{-1}}$. In the model simulations, distinct tracer-tracer relations develop in the tropics, the mid-latitude surf zone, and in the Antarctic winter vortex in accordance with observations (e.g., Michelsen et al., 1998; Ray et al., 2002; Proffitt et al., 2003) and with the theoretical arguments of Plumb (2002, 2007).

However, the model is incapable of producing a strong polar vortex in the Arctic; "there is virtually no barrier at all in the CMAM Arctic vortex" (Sankey and Shepherd, 2003). A transport barrier at the Arctic vortex edge (together with rapid mixing within the vortex) is the reason why compact tracer-tracer relations develop inside the polar vortex that are distinct from the tracer-tracer relations outside the vortex (e.g., Plumb, 2002, 2007). The segregation between compact tracer-tracer relationships inside and outside the vortex has been observed on many occasions (e.g., Proffitt et al., 1993; Michelsen et al., 1998; Müller et al., 1999; Ray et al., 2002; Tilmes et al., 2003b, 2006c).

The existence of such a segregation and of a transport barrier at the edge of the Arctic vortex is the central assumption for applying ozone-tracer relations for deducing chemical ozone loss inside the vortex (e.g., Müller et al., 1996; Tilmes, 2004; Müller et al., 2005). Thus, the fact that based on CMAM data using this methodology it would be impossible to deduce chemical ozone loss in the Arctic vortex (Sankey and Shepherd, 2003) is due to the lack of a transport barrier at the edge of the Arctic vortex in CMAM. Indeed, in the CMAM Antarctic vortex, for which a transport barrier is simulated, a compact ozone-tracer relation develops in the model. In CMAM it takes months for the compact correlation to develop; a truly compact correlation is established in August. A recent analysis of ILAS II measurements in Antarctic winter 2003 indicates that a compact relation had developed by the end of June (Tilmes et al., 2006b,c). Moreover, the fact that the simulated ozone-tracer relation in the Antarctic vortex in CMAM does not resemble measurements by HALOE, ATMOS, and ILAS II (Müller et al., 1996; Michelsen et al., 1998; Tilmes et al., 2006c) is

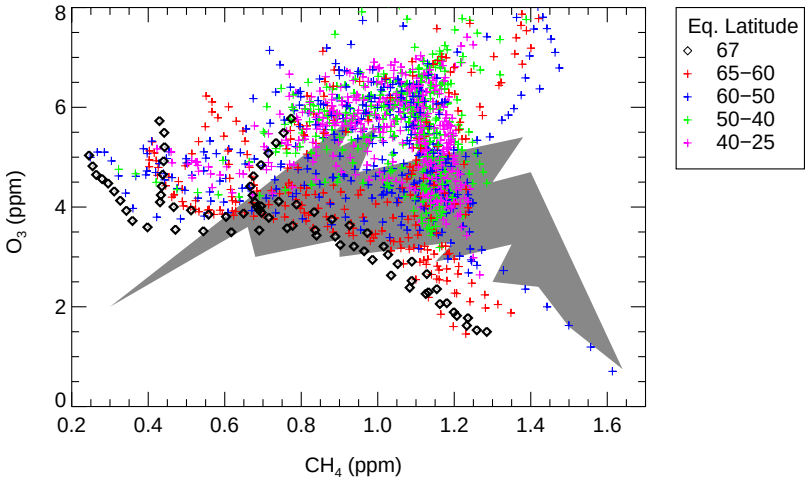

Figure 3.4: The ozone-methane relation in the northern hemisphere in January 1992. Shown are HALOE observations for the altitude range 10-100 hPa for the period 10 to 14 January 1992. The observations were made at equivalent latitudes of 25°–40°N (purple symbols), 40°–50°N (green symbols), 50°–60°N (blue symbols), 60°–65°N (red symbols). The black diamonds are observations inside the polar vortex according to the potential vorticity criterion of Tilmes (2004). The grey shaded area shows the range of CMAM model results for the vortex in a simulated January (Sankey and Shepherd, 2003). (The vortex is defined for the model results as potential vorticity greater than 400 PVU at 10 hPa) (Figure adapted from Müller et al., 2005).

most likely caused by an underestimate of halogen-catalysed ozone depletion in the CMAM Antarctic vortex.

Sankey and Shepherd (2003) raised the question of whether, given limited observations at a particular latitude, one could be under the false impression that a compact ozone-tracer relation exists, when in reality this is not the case. To illustrate their point, they consider (their Figure 19) CMAM data for the O_3-CH_4 relation inside the polar vortex for 1 January. (The vortex being defined as a column of air with potential vorticity greater than 400 PVU at 10 hPa, D. Sankey, pers. comm.). The CMAM model vortex is then sampled at the actual locations of HALOE measurements in January 1992. Due to the HALOE measurement geometry, these measurement locations intercept the CMAM vortex only very rarely. The CMAM O_3-CH_4 values at the HALOE measurement locations form a compact relation for CH_4 lower than ~ 1.3 ppm; for CH_4 greater than ~ 1.3 ppm, the CMAM O_3 values at the HALOE measurement locations show some scatter, albeit less scatter than all the CMAM vortex model points (Sankey and Shepherd, 2003). That is, if the real atmosphere were as simulated by CMAM, and had HALOE observed that model atmosphere during January 1992 the apparent correlation would have been the result of insufficient sampling. This thought experiment indicates the possible existence of a problem (Sankey and Shepherd, 2003).

To address the question whether such a problem might exist for conditions in the early polar vortex in the Arctic, we consider the actual HALOE measurements in mid January 1992 (Figure 3.4) colour-coded according to equivalent latitude. Based on the selection criteria of Tilmes et al. (2004), three HALOE measurements (black symbols in Figure 3.4) are located in the polar vortex in January 1992. These profiles show a rather compact O_3-CH_4 relation, clearly more compact than the CMAM relation at the location of the HALOE measurements. An exception is the measurements at top altitudes that show characteristics of outside vortex air. The O_3-CH_4 relation for outside vortex, mid-latitude air shows considerable scatter, but always greater ozone values than the vortex air.

Further, measurements of the ILAS instrument (Sasano et al., 1999), which provides a very good coverage of the polar area in winter 1996-97, demonstrate that a compact ozone-tracer relation develops in the Arctic vortex which is clearly separated from the out-of-vortex relation (Tilmes et al., 2003b). The ILAS Arctic vortex measurements show no indication of a variability of the ozone-tracer relation resembling that in the CMAM model vortex. Also, HALOE measurements of the early spring vortex in years when HALOE provides a good coverage of the polar area (e.g., early April 1992, 1995, 1996) show compact relations of both HCl and ozone with long-lived tracers (Müller et al., 1996; Tilmes et al., 2004).

In summary, the lack of a compact O_3-CH_4 relationship in the CMAM is caused by a model deficiency in the CMAM version 7, namely a too leaky (and too warm) vortex. This deficiency has been rectified in the the most recent CMAM version 8 by reducing the critical inverse Froude number used to define wave breaking in the orographic gravity wave drag parameterisation (Hegglin and Shepherd, 2007). This problem of the model simulating the transport barrier at the Arctic vortex edge could lead to the conclusion that compact correlations in the vortex may be erroneous due to insufficient sampling of the vortex air-mass when in reality no compact relation exits (Sankey and Shepherd, 2003). However, there is no evidence from measurements in the polar regions that such a problem occurs in reality.

Three-dimensional Lagrangian models

In the Chemical Lagrangian Model of the Stratosphere (CLaMS, McKenna et al., 2002b,a) advection and mixing are represented in a way that is very different from the transport schemes employed in Eulerian models. The mixing intensity in CLaMS can be controlled and is anisotropic in space and time (McKenna et al., 2002b; Konopka et al., 2004, 2005b, 2007b). Owing to these features, transport barriers can be represented particularly well in CLaMS.

For Arctic winter 2002/2003, a CLaMS calculation was performed describing the development over the course of the winter of passive ozone (O_3^{pass}) and CH_4, both treated as pure transport quantities. The probability distribution function (PDF) for O_3^{pass} and CH_4 on 11 January 2003 shows that a clear separation between mid-latitude and vortex air masses develops in the model (Figure 3.5); shown are all CLaMS model points poleward of an equivalent latitude of 40°N between the 350 K and 700 K isentropes.

These CLaMS results suggest that in early January a transport barrier has formed in the model at the edge of the polar vortex leading to a separation between inside and outside

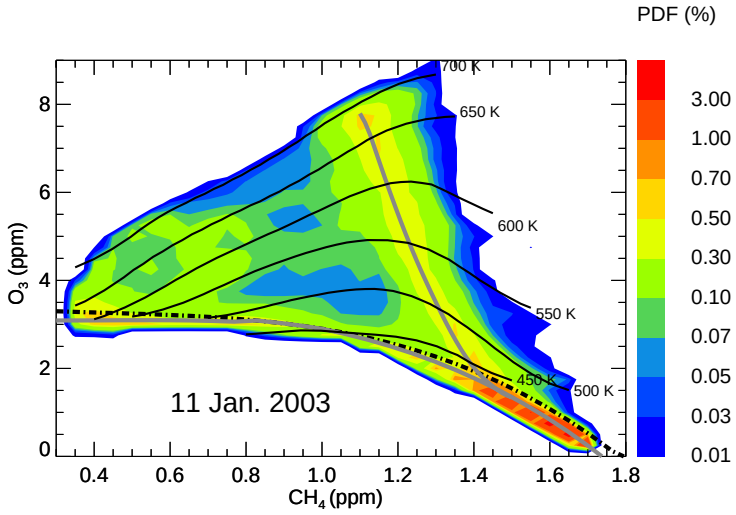

Figure 3.5: The relation of passive ozone (O_3^{pass}) and CH_4 on 11 January 2003 from model simulations of the Chemical Lagrangian Model of the Stratosphere (CLaMS). Shown are all CLaMS model points poleward of an equivalent latitude of 40°N between the 350 K and 700 K isentropes. The colour scale shows the probability distribution function (PDF) of O_3^{pass} and CH_4; reference relations for vortex air and mid-latitude air are shown as thick grey lines. For comparison, an early vortex reference relation (Tilmes et al., 2003a) deduced from MkIV measurements on 16 December 2002 is also shown (black dashed-dotted line). Also shown are approximate isolines of selected potential temperature levels. PDFs and potential temperature isolines were calculated for O_3^{pass} and CH_4 bin sizes of 0.05 ppm and 0.25 ppm, respectively. (Figure adapted from Müller et al., 2005).

tracer relations. Further, by that time, mixing within the vortex has homogenised the vortex air mass resulting in a compact ozone-tracer relation in the vortex.

3.3 Impact of Mixing on Ozone-Tracer Relations in the Polar Vortex

3.3.1 Impact of Cross Vortex Edge Mixing on Ozone-Tracer Relations in the Vortex

Mixing across the vortex edge is usually non-local in tracer-tracer space and thus has the potential to alter tracer-tracer relations. The ozone-tracer relation shows greater ozone mixing ratios outside the vortex than inside (e.g., Proffitt et al., 1993; Müller et al., 2001; Rex et al., 2002; Jost et al., 2002; Tilmes et al., 2004; Plumb, 2007), and mixing lines connecting inside and outside vortex air masses are thus expected to lie *between* the inside and the outside vortex ozone-tracer relation (Müller et al., 2001, 2005)

Observations of mixing across the vortex edge

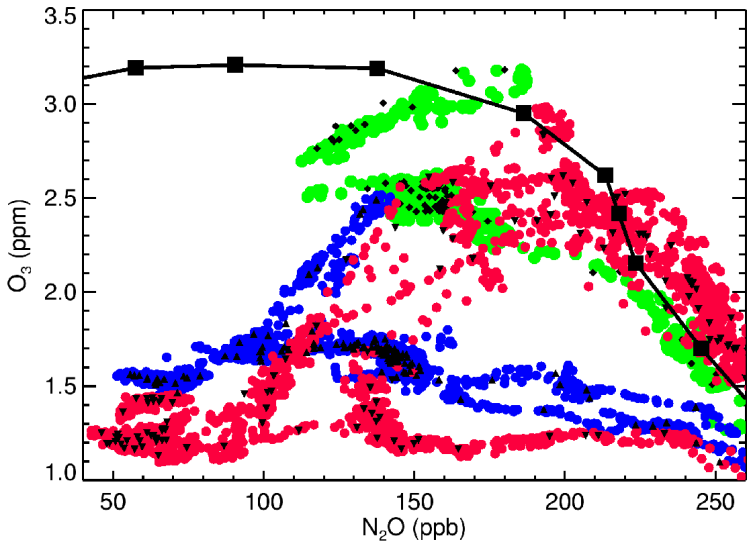

Figure 3.6: The O_3/N_2O relation from measurements during winter 1999/2000. The black symbols show measurements by the MkIV instrument (Toon et al., 1999) on 3 December 1999. The coloured symbols show measurements from the NASA-ER2 aircraft on 23 January 2000 (green), 7 March 2000 (blue), and 11 March 2000 (red). Ozone measurements were made with a UV-photometer (Proffitt and McLaughlin, 1983), the N_2O measurements by an in situ gas chromatograph (Elkins et al., 1996) (small black symbols) or from the ALIAS (Webster et al., 1994, 23. 1.) and Argus (Loewenstein et al., 2002, 3. and 11. 3.) instruments (Figure taken from Müller et al., 2005).

Based on high altitude aircraft measurements in the Arctic in early 2000, Rex et al. (2002) and Jost et al. (2002) demonstrated that mixing across the vortex edge leads to an increase in

the mixing ratio of ozone for a given value of N_2O. Moreover, Rex et al. (2002) and Ray et al. (2002) emphasise that although in this winter mixing lines were observed, entrainment of extra-vortex air did not significantly alter the composition of the vortex air between January and March 2000. Figure 3.6 shows an example of measurements of such mixing lines between vortex air, depleted in ozone, and outside-vortex air. The vortex air is characterised on 23 January 2000 by ozone mixing ratios up to about 2.5 ppm (green symbols), on 7 March 2000 by ozone mixing ratios up to about 1.7 ppm (blue symbols), and on 11 March 2000 by ozone mixing ratios of about 1.2 ppm. Clearly noticeable are the mixing lines towards air with greater ozone and greater N_2O mixing ratios, that is air of mid-latitude characteristics. Clearly, there is no evidence of measurements being located on the concave, 'low ozone' side of the reference curve.

Under conditions arising when the transport barrier at the edge of the vortex is weak, mixing is expected to noticeably influence the ozone-tracer relation inside the vortex. According to the arguments above, ozone would be expected to increase for a given tracer mixing ratio. This effect was indeed observed by the ILAS instrument in winter 1996-1997 (Tilmes et al., 2003b). In this winter, the vortex was perturbed by a stratospheric warming in early winter and therefore the vortex edge was permeable until late December. ILAS provided good coverage of the Arctic polar region in winter 1996-1997 covering a latitude range between 55°-77°N and measuring about fourteen profiles per day. These measurements show (see Figure 7 in Tilmes et al., 2003b) that inside the vortex ozone increased at a given N_2O level in December (when the vortex was still relatively weak) and that a compact O_3/N_2O relation was established by early January (when a strong vortex had formed).

Mixing across the vortex edge is likewise important for establishing the ozone tracer relation in the very early, incipient vortex. The air in high latitudes in autumn, from which the polar vortex forms, is characterised by low ozone mixing ratios, a remainder of summertime ozone loss. Because the transport barrier of the incipient vortex, while being established, is still somewhat permeable, ozone-rich, mid-latitude air is mixed into the vortex. In this way, the ozone-tracer relation in the vortex recovers from summertime ozone loss. This process was first noted by Proffitt et al. (1992) and analysed in detail based on ILAS II measurements in the high latitudes of both hemispheres by Tilmes et al. (2006b).

Cross vortex edge mixing in conceptual models

Plumb et al. (2000) presented a conceptual model a simple advective diffusive model in cylindrical geometry to describe the impact of mixing on tracer-tracer relations. In their model, they simulate the effect of mixing on the relationship of two artificial tracers χ_1 and χ_2 that are designed to resemble N_2O and NO_y. The relation of χ_1 and χ_2 is the same on both sides of a transport barrier that represents the vortex edge in the model. The typical time scale T for the model is the lifetime of the vortex, say four months or $\sim 10^7$ s, and the typical horizontal length scale L is from the pole to the subtropical transport barrier, say $\sim 7 \cdot 10^6$ m. The dimensionless diffusivity in the vortex edge region is chosen to be $K = 0.05$ by Plumb et al. (2000). If this dimensionless diffusivity is converted to a dimensioned diffusivity D, where $D = (K \cdot L^2)/T$, one obtains $D \sim 3 \cdot 10^5$ m^2 s^{-1}. This value may be compared with effective atmospheric diffusivities deduced from aircraft measurements

$D_{\text{eff}} = 5 \cdot 10^3$ m^2 s^{-1} (Waugh et al., 1997) or diffusivities ($D = 1.1 \cdot 10^3$ m^2 s^{-1}) employed in the chemical transport model CLaMS for reproducing observed filamentary tracer structures at the polar vortex edge (Konopka et al., 2003). That means the cross vortex edge diffusivity is likely to be substantially greater in the Plumb et al. (2000) conceptual model than in the stratosphere. Therefore, conclusions based on the results of this conceptual model cannot be directly transferred to stratospheric conditions.

A further caveat for the application of conclusions from this conceptual model to the behaviour of ozone-tracer relations in the stratospheric polar vortex is that Plumb et al. (2000) assume the same tracer-tracer relation inside and outside the vortex; an assumption that is not valid for the ozone-tracer relation in the polar region (e.g., Proffitt et al., 1992; Müller et al., 1996; Plumb, 2007, see also discussion below).

Cross vortex mixing in Lagrangian chemical transport models

Konopka et al. (2004, 2005a,b) have shown that in the Lagrangian model CLaMS rather little exchange occurs across the polar vortex edge as long as a stable vortex exists. If exchange occurs, air masses will mix approximately along isentropic surfaces leading to an increase of ozone mixing ratios with respect to the vortex reference relation (Figure 3.5). However, the lower the potential temperature level at which the mixing occurs, the smaller is the deviation of the isentropic surfaces from the vortex reference relation in ozone-tracer space (Figure 3.5). That means the lower down in the vortex mixing occurs, the smaller the impact of mixing events is on the ozone tracer relation.

3.3.2 Impact of Differential Descent in the Vortex on Tracer Relations

Differential descent of air masses within an otherwise isolated polar vortex may impact non-linear tracer-tracer relations for the vortex (Ray et al., 2002; Salawitch et al., 2002). Potentially, this mechanism could have an influence on ozone loss estimates deduced using ozone-tracer correlations.

Here, a rather simple calculation is conducted to assess the impact of differential descent on ozone-tracer relationships in the polar vortex. We consider idealised conditions: the vortex is described by a single column of air; the vertical coordinate being potential temperature θ. In a given time step Δt the main vortex air mass descends by $\Delta\theta$, with a fraction α of the vortex air mass assumed to be descending (unmixed) by $\delta\Delta\theta$ with $\delta > 1$. The vortex air mass is then assumed to be immediately homogenised by horizontal mixing. This procedure is repeated n times with the intention of approximately describing the development of the vortex over a winter season.

For the vortex air mass, typical vertical profiles of ozone and N_2O are prescribed as initial conditions, resulting in an initial O_3/N_2O relation in the polar vortex (solid black line in Figure 3.7). The change of this initial O_3/N_2O relation due to the action of differential descent and subsequent mixing in the vortex can then be followed. In Figure 3.7, this change is shown for a rather extreme case, where $\Delta\theta = 5$ K, $\alpha = 0.33$, $\delta = 2$ (that is, one third of the vortex air mass descends twice as far as the remaining two thirds) and the number of

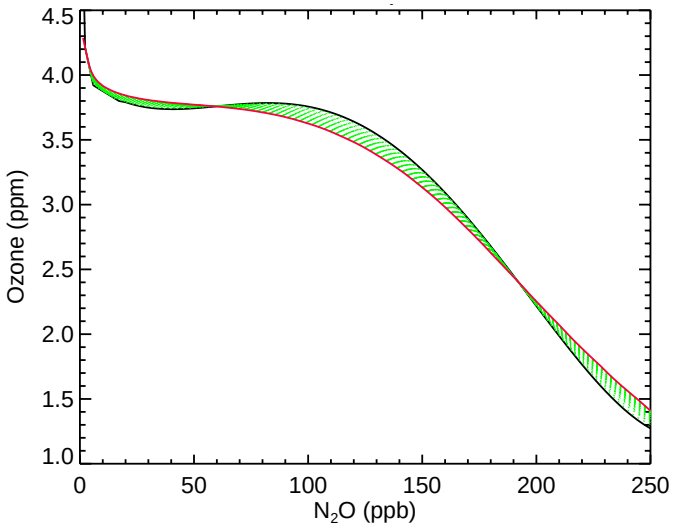

Figure 3.7: The impact of differential descent on the O_3/N_2O relation in the vortex from an idealised calculation. The solid black line shows the initial O_3/N_2O relation, the red line the O_3/N_2O relation after 20 iterations of differential descent. It is assumed that one third of the vortex air mass descends twice as far as the rest of the vortex air mass, followed by instantaneous horizontal mixing (see text for details). The dotted green lines show the gradual change of the O_3/N_2O relation with each time step. (Figure taken from Müller et al., 2005).

time steps $n = 20$. Obviously, even for such conditions, the O_3/N_2O relation is rather little affected by the effect of differential descent.

Ozone-tracer relations were used to calculate a proxy ozone profile from a tracer profile in late winter early spring. If the two relations shown in Figure 3.7 are used to deduce proxy ozone profiles from a late winter vortex tracer profile characterised by vertical descent, the column ozone corresponding to these profiles differs by only ~ 2.5 DU. In a scenario that is perhaps slightly more realistic, where $\Delta\theta = 2$ K, $\alpha = 0.33$, $\delta = 1.5$ and the number of time steps $n = 50$, the corresponding difference in column ozone is less than 1 DU; the maximum change of ozone for a given tracer value due to differential descent and subsequent mixing under these conditions is ~ 50 ppb.

This means that the contribution of the effect of differential descent to the overall uncertainty in the deduced chemical loss will be small. Given the magnitude of other sources of uncertainty, the contribution from differential descent is very likely to be insignificant. This finding corroborates the conclusions of Ray et al. (2002) and Salawitch et al. (2002) who report, based on balloon measurements in winter 1999-2000, that the effect of differential descent increased the uncertainty of column ozone loss estimates by $\sim$3-4%.

3.3.3 Can Mixing in the Arctic Vortex 'Mimic' Chemical Ozone Loss?

In a recent paper, Muscari et al. (2007) present measurements of stratospheric constituents in Arctic winter 2001/2002 from mid-January to early March that were obtained by the ground-based millimetre-wave spectrometer (GBMS) and a Lidar system working concurrently at Thule, Greenland (76.5°N, 68.7°W). Among the recent Arctic winters, winter 2001/2002 is one of the warmest on record (e.g., Tilmes et al., 2004; Manney et al., 2005; Rex et al., 2006). Using the GBMS stratospheric O_3, CO, N_2O, and HNO_3 measurements together with Lidar temperature observations, Muscari et al. (2007) characterise the polar stratosphere over Thule in the altitude range between ∼17-45 km.

Here statements by Muscari et al. (2007) are discussed that focus on the lower stratosphere: "... using correlations between GBMS O_3 and N_2O mixing ratios, in early February a large ozone deficiency owing to local ozone loss is noted inside the vortex. GBMS O_3-N_2O correlations suggest that isentropic transport brought a O_3 deficit also to regions near the vortex edge, where transport most likely mimicked local ozone loss".

Firstly, possible uncertainties are discussed in the way the chemical ozone loss is derived by Muscari et al. (2007) due to the selection criteria used to sort GBMS profiles into different vortex regions. Secondly, assuming the deduced ozone loss values to be correct, it is shown that they are difficult to reconcile with the current understanding of chemical ozone depletion in the polar stratosphere in winter and spring (Solomon, 1999; WMO, 2007).

To distinguish between data points inside, outside, and at the edge of the polar vortex, Muscari et al. (2007) use GBMS N_2O measurements instead of considering meteorological fields such as potential vorticity gradients and horizontal wind speed (e.g., Nash et al., 1996; Bodeker et al., 2001; Tilmes et al., 2006b; Manney et al., 2007). The authors state that they "trust the GBMS N_2O observations (O_3 and N_2O measurements were carried out within a total of 4 to 5 hours) more than the temporally and spatially coarser Potential Vorticity data analysis". Indeed, Greenblatt et al. (2002) developed a technique to accurately determine the edge of the polar vortex from in situ (aircraft and balloon) measurements of a long-lived trace gas like N_2O. They find that for high-resolution aircraft data, a potential vorticity analysis may misidentify the inner edge by more than 400 km. However, the GBMS measurements have a much coarser spatial and temporal resolution than the in situ data employed by Greenblatt et al. (2002). Although the width of the instantaneous field of view of the GBMS is ∼10 km in the lower stratosphere, the integration time of the measurements (∼ 1.5 hours for O_3, ∼ 3 hours for N_2O) means that the GBMS samples an air mass of a certain horizontal extent. Assuming wind speeds of 20-40 km/h at 10 hPa, Muscari et al. (2007) estimate an effective horizontal resolution of 90-180 km. Considering typical wind speeds for the lower polar stratosphere at approximately 480 K (e.g., Chan et al., 1990) to be between 40 km/h (vortex core) and 180 km/h (towards the vortex edge) results in a conservative estimate for the horizontal resolution ranging between 180 km and 810 km, a range that includes earlier estimates for GBMS measurements of a single species (about 200-300 km, Muscari et al., 2002). The vertical resolution of the GBMS is about 7 km in the Arctic lower stratosphere (Muscari et al., 2007). Current meteorological analyses reach higher spatial resolution, for example in 2000 the European Centre for Medium-Range Weather Forecasts

(ECMWF) introduced a T511/L60 system with a horizontal resolution of about 40×40 km and a vertical resolution of about 1 km in the upper troposphere and lower stratosphere (e.g., Jung and Leutbecher, 2007).

An appropriate criterion for determining whether profiles are measured inside or outside the vortex is essential for applying ozone-tracer relations to calculate polar ozone loss because the characteristics of air outside the vortex are very different from vortex air (Chapter 3). A criterion that leads to using a mixture of profiles measured inside and outside the vortex could cause the chemical ozone loss in the vortex to be underestimated (Tilmes et al., 2004).

Next, the chemical ozone loss in Arctic winter 2001/2002 is discussed. Based on correlations between GBMS O_3 and N_2O mixing ratios, Muscari et al. (2007) report large chemical ozone loss values for early February in the polar vortex. The ozone deficiency reported is $\sim$1.5 ppm at 480 K (40 ppb N_2O) for the vortex core. A chemical ozone loss of this magnitude differs from the ozone loss values deduced from ozone tracer (HF) relations in this winter measured by HALOE. Tilmes et al. (2004) report for March 2002 a *maximum* local loss of 0.5 ± 0.2 ppm, a vortex average column ozone loss of 12 ± 10 DU, and very little (5 ± 10 DU) ozone loss in the vortex core. Goutail et al. (2005), based on SAOZ (Système d'Analyse par Observation Zénithale) measurements, report an Arctic column ozone deficit of 10% for the end of March 2002, but the ozone deficit in mid-January is only about 5%. There are observations (e.g., Tilmes et al., 2004; Rex et al., 2004) of an accumulated chemical ozone loss in the lower stratosphere reaching and exceeding 1.5 ppm, but only for late winter (that is for "established ozone loss" conditions) and only for much colder winters than 2001/2002 (e.g., 1995/1996 or 1999/2000). For comparison, the accumulated column ozone loss reported by Goutail et al. (2005) is 30% for 1995–1996 and 23% for 1999-2000.

Because in winter 2001/2002 the last polar stratospheric clouds were observed in mid-January and no enhancement of ClO was detected by Odin/SMR after 8 January, Muscari et al. (2007) concluded that the ozone deficiency deduced from the GBMS measurements in early February ($\sim$ 1.5 ppm) was caused by chemical loss in the first half of January. They state that "because of the long lifetime of ozone in the lower stratosphere, the deficiency could have persisted at least until the beginning of February…". Indeed, the rate of photochemical ozone production in the polar lower stratosphere in spring is slow (and zero in complete darkness). Therefore, it is highly likely that the chemical ozone loss occurring in early January is still clearly detectable a few weeks later. Nevertheless, mixing between air masses which have been subject to chemical loss and surrounding air masses which are richer in ozone would reduce the signature of ozone loss to a certain extent.

However, an accumulated chemical ozone loss of about 1.5 ppm in the lower stratosphere between mid-December and mid-January 2002 means that ozone loss rates of $\sim$ 50 ppb per day were sustained for a month (and during a period of very low solar elevation in the Arctic). For comparison, ozone loss rates of 50 ppb per day have been observed only on one occasion to date, namely for about two weeks at the end of January 1992 (von der Gathen et al., 1995; Rex et al., 1998). Loss rates of this magnitude are greater than can be currently explained by model simulations (Becker et al., 1998; Rex et al., 2003).

Moreover, for the vortex edge region at 480 K (at 120 ppb N_2O), Muscari et al. (2007) find a significant O_3 deficit of about 1.2 ppm in late January to mid-February 2002. They offer

as an explanation that air masses subject to strong ozone loss in the vortex core were mixed with air masses in the vortex edge region, where chemical ozone loss is considered to be unlikely. Muscari et al. (2007) state that "transport brought a O_3 deficit also to regions near the vortex edge, where transport most likely mimicked local ozone loss". It is important to note that through the mixing of vortex core and vortex edge air masses, the apparent ozone loss in the vortex core air is *reduced* at the same time when the signature of chemical ozone loss is exported from the core to the vortex edge. (See also Lemmen et al., 2006b, for a detailed discussion of the impact of different mixing scenarios on an ozone-tracer relation in the vortex showing significant ozone loss). Further, because the polar isentropic tracer gradient between the vortex core and the vortex edge is rather small up to a few degrees from the vortex edge (e.g., Loewenstein et al., 1990; Manney et al., 1999; Riese et al., 2002; Manney et al., 2006; Tilmes et al., 2006b), mixing between core and edge air masses will occur for roughly constant tracer values. Therefore, relative to the 'early vortex reference', the mixed air parcel will show approximately the same ozone loss as the mean of the two original air parcels. Thus, the vortex average chemical ozone loss is not changed significantly by mixing between vortex core and vortex edge air masses. This process, therefore, cannot lead to an overestimation of chemical ozone loss. A clearer, more appropriate description of such conditions would be to say that ozone loss is *homogenised in the vortex*.

A homogenisation of the ozone loss signal in the vortex was observed in winter 1996–1997. In March 1997, ozone loss in the vortex was strongly inhomogeneous, as was noticeable both in observations and simulations (Schulz et al., 2000; McKenna et al., 2002a; Tilmes et al., 2003b). The ozone-tracer relation in March was not compact for a chemical reason, namely stronger chemical ozone loss in the vortex core than at the edge of the vortex (McKenna et al., 2002a; Tilmes et al., 2003b). In early May 1997, compact ozone-tracer relations were observed again in the remaining vortex indicating that mixing in the vortex had, by that time, again homogenised the vortex air mass and thus the ozone loss signal.

Muscari et al. (2007) emphasise that chemical ozone loss in Arctic winter 2001/2002 must have taken place in a limited region of the vortex. However, none of the six vortex observations or the four vortex edge observations by the GBMS instrument (with a horizontal resolution ranging between 180 km and 810 km) in early 2002 sampled air masses that were not affected by chemical loss.

In summary, the magnitude of Arctic ozone loss and the implied ozone loss rates reported by Muscari et al. (2007) are very difficult to reconcile with the current understanding of polar ozone chemistry (e.g., Solomon, 1999; WMO, 2007). This point was also made in a comment (Müller and Tilmes, 2008) on the paper by Muscari et al. (2007). In a reply to this comment, Muscari and de Zafra reported on reanalysed data that result in lower ozone loss estimates, which even become negligible in some cases (Muscari and de Zafra, 2008).

However, the conclusion by Muscari et al. (2007) is supported to the extent that *if* noticeable chemical ozone loss occurred in the polar vortex in 2001/2002, it can only have occurred locally in restricted areas of the vortex. Therefore, their findings do not cast doubt upon the notion that the average chemical ozone loss in the Arctic vortex shows a very close relation to temperature conditions and thus to the potential for chlorine activation in the Arctic vortex (e.g., Rex et al., 2004, 2006; Tilmes et al., 2006a, 2008b; WMO, 2007).

3.4 Impact of Mesospheric Intrusions on Ozone–Tracer Relations in the Stratospheric Polar Vortex

The question of the extent to which mixing across the vortex edge (Michelsen et al., 1998; Plumb et al., 2000) or differential descent with subsequent mixing within the vortex (Salawitch et al., 2002) may impact ozone–tracer relations in the vortex was discussed in detail in Section 3.3.

Another potential problem of the ozone-tracer relation method was raised by Engel et al. (2006), namely the question of whether the presence of a substantial amount of mesospheric air in the polar vortex may impact the uncertainty of estimates of chemical polar ozone loss based on ozone–tracer relations. Because ozone mixing ratios in the mesosphere (typically less than $\sim$2 ppm, see Figures 2.2 and 2.3) are lower than those in the stratosphere, mixing of mesospheric and lower stratospheric air could in principle impact ozone tracer relations in a way that would lead to an overestimation of chemical ozone loss deduced from tracer relations. Assuming that an intrusion of mesospheric air occurs in mid-winter

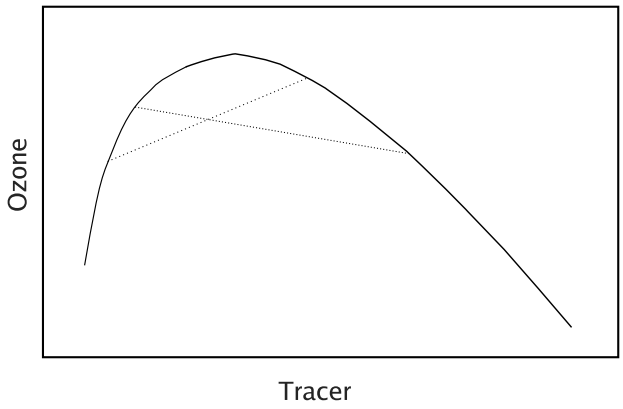

Figure 3.8: Schematic view of the impact of mixing between air of mesospheric origin (the mesospheric intrusion) and stratospheric air on ozone–tracer relations in the stratosphere for the hypothetical (and unrealistic) case of downward transport of mesospheric ozone without chemical change. The solid line indicates the ozone–tracer relation throughout the stratosphere and mesosphere for a tracer with a tropospheric source (such as CH_4 or N_2O). The dotted lines indicate possible mixing lines between stratospheric and mesospheric air masses at different altitudes. (Figure taken from Müller et al., 2007).

down to lower stratospheric altitudes and considering the hypothetical (and unrealistic) case that mesospheric air mixes with air in the polar lower stratosphere without any chemical change of the mesospheric ozone mixing ratio, the ozone–tracer relationship would be altered; examples of the resulting mixing lines are shown (dotted lines) in the schematic view in Figure 3.8. Mixing points deduced for this hypothetical case of downward transport of

mesospheric ozone without chemical change lie below the stratospheric ozone–tracer relation; therefore, in principle, mixing between stratospheric and mesospheric air could impact ozone loss estimates based on ozone–tracer relations.

It has been known for a long time that in the mesosphere much higher mixing ratios of CO prevail than in the stratosphere because at mesospheric heights CO_2 is dissociated (Hays and Olivero, 1970). The photochemical lifetime of CO in the mesosphere is sufficiently long so that this species can be considered as an indicator of mesospheric air; it provides a good tracer for testing mesospheric transport processes (e.g., Allen et al., 1981; Solomon et al., 1985). In the polar region in winter, diabatic cooling occurs as sunlight recedes from the polar region. This cooling results in strong diabatic descent in the polar region which draws air from a large range of altitudes, including the entire depth of the mesosphere, down into the polar stratosphere (e.g., Fisher et al., 1993). Particularly deep intrusions of mesospheric air into the polar stratosphere have been observed on various occasions (e.g., Kouker et al., 1995; Rinsland et al., 1999; Ray et al., 2002; Curtius et al., 2005; Engel et al., 2006; Randall et al., 2006).

Here, following Müller et al. (2007), the impact of intrusions of mesospheric air on the ozone-tracer relation method is revisited considering ozone–tracer relations in the Arctic winter 2002/2003, when an intrusion of mesospheric air into the stratosphere was observed (Engel et al., 2006; Huret et al., 2006). During this winter, the polar vortex split twice into two separate parts, from 19 to 21 January and again later between 16 and 21 February 2003 and, in both cases, was re-unified within a few days after the split. The vortex remained compact during March and the first part of April, before it broke down in late April. Details of the meteorological situation of this winter are described elsewhere (e.g., Tilmes et al., 2003a; Grooß et al., 2005; Streibel et al., 2006; Günther et al., 2008).

An intrusion of mesospheric air was clearly identified in early 2003 in the Arctic vortex by strongly enhanced CO mixing ratios that were observed in a layer descending from $\sim$30 km in late January to $\sim$25 km by early March (Engel et al., 2006; Huret et al., 2006). This mesospheric air was sampled again in the vortex in late March (Engel et al., 2006; Wetzel et al., 2006). Strongly enhanced values of CO of mesospheric origin down to 30 km were also observed in mid January 2003 by a ground-based millimetre-wave spectrometer (de Zafra and Muscari, 2004). These observations are further consistent with CO measurements from the MIPAS-Envisat instrument with a vertical resolution of $\sim$8 km (Funke et al., 2006) that show enhanced CO down to about 600 K in March 2003 (Konopka et al., 2007a). The penetration of mesospheric air to lower altitudes in the Arctic in 2003, however, did not lead to a noticeable enhancement of CO column densities (Velazco et al., 2007).

The impact of the mesospheric intrusion on stratospheric tracer-tracer relations in general will be investigated below focusing on the question of whether mesospheric intrusions may alter ozone-tracer relations in a way that might lead to an overestimate of chemical ozone loss (Plumb et al., 2000; Engel et al., 2006).

3.4.1 Balloon-Borne Measurements in Arctic Winter 2002/2003

In Arctic winter 2002/2003, four balloon-borne measurements of the ozone–tracer relation were made in the lower stratosphere (Tilmes et al., 2003a; Engel et al., 2006; Huret et al.,

2006; Wetzel et al., 2006). Here this set of measurements is analysed focusing on the identification of air masses of mesospheric origin. This mesospheric air has 'intruded' into the stratosphere meaning that the air above and below the layer of mesospheric air is 'younger' than the mesospheric air. However, mesospheric does not reach the stratosphere unmixed and chemical change occurs during descent.

Mixing Patterns and Mesospheric Air in the SPIRALE Measurements on 21 January 2003

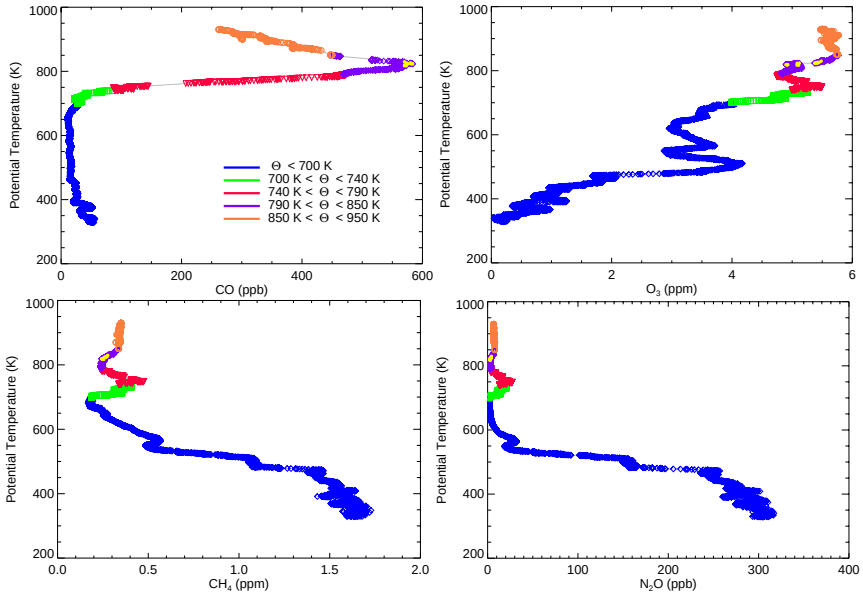

Figure 3.9: The vertical profile of CO (top left panel), ozone (top right panel), methane (bottom left panel), and N_2O (bottom right panel) from the SPIRALE measurements on 21 January 2003. The measurements are colour-coded according to altitude (see colour legend in top left panel). Air masses that are most strongly influenced by mesospheric air (CO ranging between 570 and 584 ppb) are marked by solid yellow circles. (Figure taken from Müller et al., 2007).

On 21 January 2003, balloon-borne measurements of a variety of species were taken with a very high vertical resolution by the SPIRALE experiment (Spectroscopie Infra-Rouge par Absorption de Laser Embarqué, Huret et al., 2006). Here the mixing ratios of CO, ozone, methane, and nitrous oxide are shown against potential temperature (Figure 3.9). An intrusion of mesospheric air and the signature of mixing between (stratospheric) mid-latitude air and mesospheric air within the polar vortex were clearly identified (Huret et al., 2006). The mesospheric intrusion is most obvious as a layer with strongly enhanced CO mixing ratios (Figure 3.9).

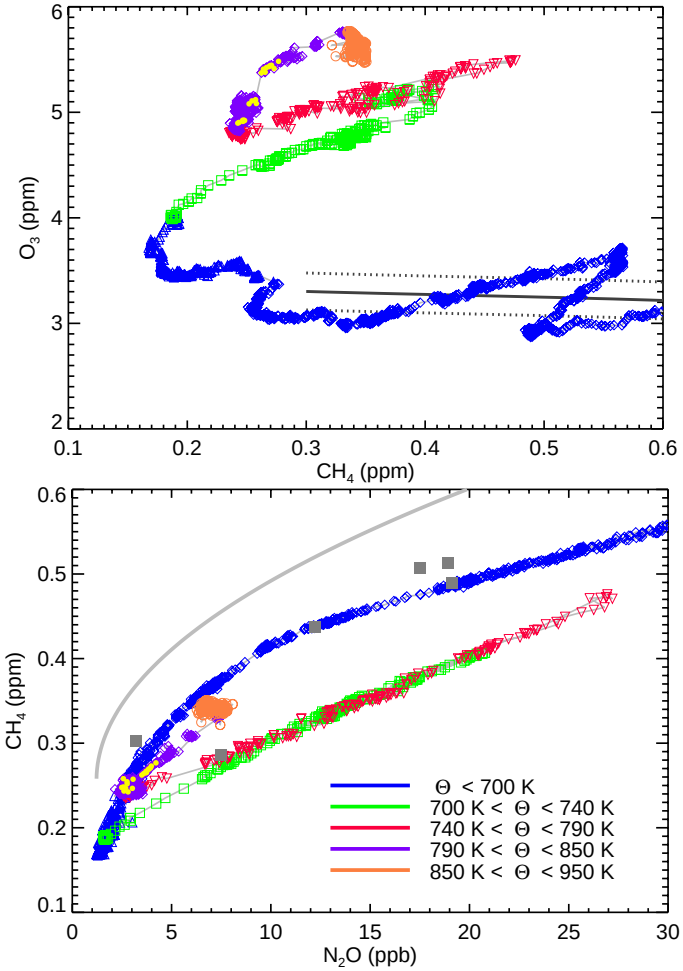

Figure 3.10: The ozone–methane (top panel) and the methane–N_2O relation (bottom panel) from the SPIRALE measurements on 21 January 2003. The measurements are colour-coded according to altitude as in Figure 3.9 (colour legend in bottom panel). Air masses that are most strongly influenced by mesospheric air (CO ranging between 570 and 584 ppb) are marked by solid yellow circles. Grey squares in the bottom panel show the BONBON measurements on 6 March 2003 that are not influenced by mesospheric air. The solid grey line in the bottom panel indicates the methane-N_2O relation for mid-latitudes reported by Michelsen et al. (1998) adjusted to 2003 conditions by increasing N_2O by 2.3% and CH_4 by 3.2%. The solid black line in the top panel shows an early vortex reference deduced from MkIV measurements on 16 December 2002 (Tilmes, 2004), dotted lines show the uncertainty of the reference. (Figure taken from Müller et al., 2007).

The high vertical resolution of SPIRALE allows a detailed analysis of the complexity of the mixing patterns. Below 700 K (blue symbols in Figures 3.9 and 3.10) the measurements are taken within the polar vortex (sometimes close to the vortex edge). The CH_4–N_2O relation measured by SPIRALE is a typical vortex relation, it agrees with earlier ATMOS measurements (Michelsen et al., 1998) of this relation in the polar vortex (as was shown by Huret et al., 2006) and with the BONBON measurements on 6 March 2003 that are not influenced by mesospheric air (grey squares in Figure 3.10, bottom panel). The polar CH_4–N_2O relation measured by SPIRALE is clearly distinct from a typical mid-latitude CH_4–N_2O relation (grey line in Figure 3.10, bottom panel), consistent with the arguments of Plumb (2007). Likewise, the ozone–methane relation below 700 K (blue symbols in Figure 3.10, top panel) agrees with an early vortex reference deduced from MkIV measurements on 16 December 2002 (Tilmes, 2004).

In the layer between 700 K and 740 K (green symbols in Figures 3.9 and 3.10), stratospheric vortex air is mixed with mid-latitude stratospheric air. CO mixing ratios in this layer are relatively low, below 100 ppb (Figure 3.9). Mixing of vortex and out-of-vortex air masses leads to mixing lines towards air with greater ozone and greater tracer mixing ratios, i.e. air of mid-latitude characteristics (Section 3.3, see also Müller et al., 2005). This effect is clearly noticeable in the SPIRALE measurements of the ozone–methane relation (Figure 3.10, top panel, green symbols). The effect of mixing is also noticeable in the CH_4–N_2O relation (Figure 3.10, top panel); extrapolating the approximately linear mixing line leads to a mid-latitude endpoint of $\sim$0.85 ppm CH_4 and 70 ppb N_2O.

Above 740 K, the mesospheric influence increases and CO mixing ratios exceed 100 ppb. The layer between 740 K and 790 K (red symbols) consists of a mixture of mesospheric air masses (characterised by large CO mixing ratios) with mid-latitude air (characterised by larger tracer values). Both the layers between 700–740 K and 740–790 K are strongly mixed, as can be seen from the CH_4–N_2O relation that is practically linear in both cases (Figure 3.10). However, the two mixing lines can be clearly distinguished, especially in the ozone–CH_4 relation (Figure 3.10, top panel). Note that one BONBON data point (that taken at 23.9 km, 598 K) is located on a mixing line, indicating that a mixed air mass was sampled here as well. A similar case of mixing between vortex air and out-of-vortex air masses leading to a linear CH_4–N_2O relation was reported by Rex et al. (1999) based on high-altitude aircraft measurements in the Arctic on 26 April 1997.

The largest CO mixing ratios occur between 790 K and 850 K (purple symbols), which indicates that this air mass is most strongly influenced by mesospheric air. The air masses at the top of the SPIRALE profile, above 850 K (orange symbols), show lower CO mixing ratios and therefore less mesospheric influence. Indeed the CH_4–N_2O relation of these air masses becomes similar to the undisturbed vortex relation (blue symbols) again.

In Figure 3.10, it can be seen that the mixing lines in the air mass below the mesospheric layer are much longer than those in the air mass above. A possible explanation is the fact that the air mass below the mesospheric layer was mixed with mid-latitude air. In contrast, the air mass above the mesospheric layer was mixed with vortex air with a different descent rate (Huret et al., 2006). Therefore, the mixing line in the air mass below the mesospheric layer 'aims' at an air mass farther away in tracer-tracer space.

Mesospheric air in the MIPAS-B measurements on 20 March 2003

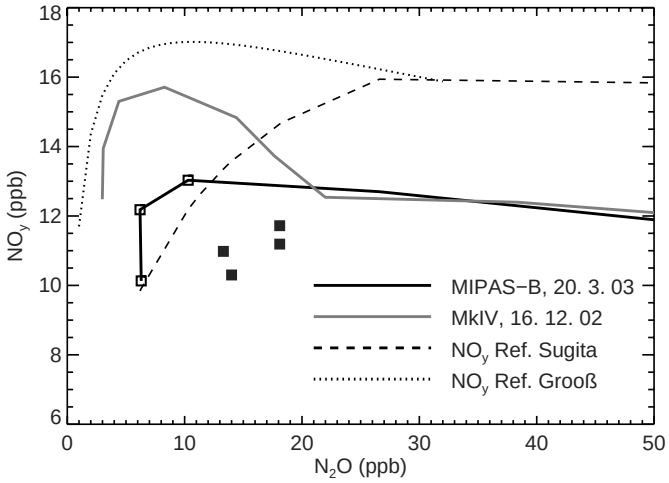

Figure 3.11: The relation of NO_y and N_2O (thick black line and squares) from the MIPAS-B measurements on 20 March 2003 in the polar vortex. Open squares indicate measurements (at 21-23 km) taken in mesospheric air according to Engel et al. (2006); here the samples between 24–27 km (solid squares) are identified as of mesospheric origin (see text); the thick black line shows the measurements below 24 km. Also shown are: NO_y–N_2O from the MkIV measurement on 16 December 2002 (thick grey line), the NO_y–N_2O reference for mid-latitude conditions based on atmospheric trace molecule spectroscopy (ATMOS) measurements reported by Sugita et al. (1998) (dashed black line), and the NO_y–N_2O reference (dotted line) deduced for winter 2002/2003 by Grooß et al. (2005). (Figure taken from Müller et al., 2007).

The MIPAS-B instrument (Friedl-Vallon et al., 2004) took measurements inside the polar vortex on 20 March 2003. In a layer between 21–23 km, substantially greater amounts of NO_y (by $\sim$30%) were found than predicted from a NO_y–N_2O reference for undisturbed winter conditions, according to the MIPAS dataset analysed by (Engel et al., 2006). Production of NO from N_2 in the upper atmosphere may indeed lead to enhancement of NO_y in the mesosphere and in the stratosphere (e.g., Strobel, 1971; Solomon et al., 1982; WMO, 2007). Therefore, Engel et al. (2006) attributed this enhanced NO_y to enhanced NO in mesospheric air and concluded that at $\sim$22 km MIPAS-B had sampled the descending layer of mesospheric air in the Arctic vortex in early 2003.

Here, reanalysed MIPAS-B data are considered that were produced with improved spectroscopic parameters (Rothman et al., 2005). (The vertical profiles of N_2O, CH_4, and ozone are shown in Müller et al. (2007)). The MIPAS NO_y values changed significantly (by up to 1 ppb) due to the improved spectroscopic parameters, so that it is not straightforward to compare these data with previously reported NO_y–N_2O reference relations. Compared to a NO_y–N_2O reference for mid-latitude conditions based on atmospheric trace molecule spectroscopy (ATMOS) measurements reported by Sugita et al. (1998) (dashed black line

in Figure 3.11), the NO_y in the 21–23 km layer (open squares in Figure 3.11) on 20 March 2003 is somewhat enhanced.

However, the NO_y measured by MIPAS-B on 20 March 2003 between 21–23 km is *not* enhanced compared to the NO_y–N_2O relation from the MkIV measurement on 16 December 2002 (thick grey line in Figure 3.11). At lower altitudes, below about 26 km (corresponding to 650 K, $N_2O = 15$ ppb) the MkIV measurements show signs of early denitrification (Grooß et al., 2005). Therefore, also a NO_y–N_2O reference is shown, derived to describe unperturbed conditions in winter 2002/2003 (Grooß et al., 2005, dotted line in Figure 3.11). This relation supports the interpretation that NO_y is not enhanced in the 21–23 km layer on 20 March 2003.

Strong enhancements of NO_x are intermittently observed caused by unusually strong energetic parcel precipitation or by solar proton events (e.g., Heath et al., 1977; Randall et al., 2005; López-Puertas et al., 2005; Jackman et al., 2006; WMO, 2007; Vogel et al., 2008). Such conditions did not prevail in Arctic winter 2002/2003. In contrast, findings based on MIPAS-Envisat measurements (Funke et al., 2005) suggest that in Arctic winter 2002/2003 rather inefficient NO_x downward transport occurred with negligible deposition of NO_x into the lower and middle stratosphere. Further, model studies (Vitt et al., 2000) predict that the enhancement of the NO_y budget in the stratosphere caused by thermospheric NO_x sources is rather moderate, about 3% and 8% in the northern and southern polar region, respectively. In the south polar night, the simulated enhancement at $\sim$30 km is 10%, although the enhancement strongly increases with altitude (Vitt et al., 2000).

In contrast to the measurements between 21-23 km, the MIPAS measurements at 24–27 km (solid squares) clearly deviate from all NO_y–N_2O relations shown in Figure 3.11. Further, in late March, the mesospheric air will be mixed with stratospheric air, so that the mesospherically influenced points are expected to lie on a 'mixing line'[1] between mesospheric and stratospheric air. Indeed, the location of the measurements at 24-27 km (solid squares in Figure 3.11) in the NO_y–N_2O scatterplot is consistent with the assumption that these points are influenced by mixing.

Although it is a difficult retrieval, CO mixing ratios can be deduced from MIPAS-B spectra (Figure 3.12). There is a clear peak in CO noticeable in the layer at 24–27 km, where the values exceed 100 ppb. This observation corroborates the interpretation that the layer at 24–27 km is influenced by mesospheric air.

The body of evidence discussed above, leads to the conclusion that the mesospheric layer was sampled by MIPAS-B on 20 March 2003 at 24–27 km altitude. This attribution agrees with the prediction by the KASIMA model of the location of the mesospheric layer in late March 2003 (Engel et al., 2006).

Balloon-borne observations of ozone-tracer relations in winter 2002/2003

The measurements of the ozone–tracer relation from the four balloon flights in Arctic winter 2002/2003 are shown in Figure 3.13. The measurements by the MkIV instrument (Toon

[1] Here, the concept of a mixing *line* is an idealisation; the mixing between mesospheric and stratospheric air will certainly not occur in one single event.

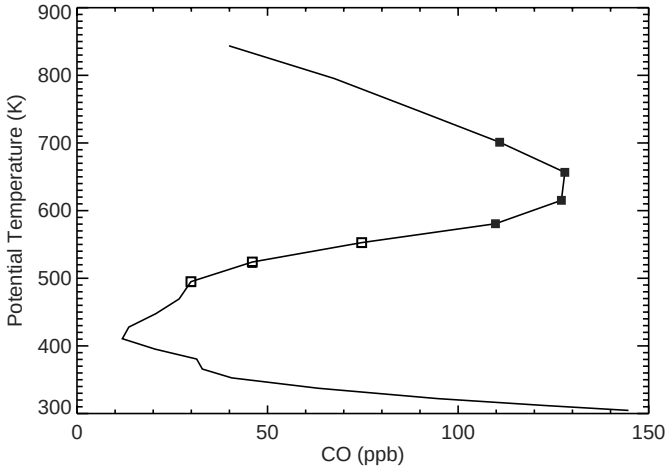

Figure 3.12: The vertical profile of the CO mixing ratio (against potential temperature) on 20 March 2003 inside the vortex measured by MIPAS-B. Solid squares (corresponding to 24-27 km) indicate measurements identified as being under mesospheric influence owing to the elevated CO mixing ratio. Open squares (corresponding to 21-23 km) indicate the measurements considered as mesospheric in an earlier publication (Engel et al., 2006). (Figure taken from Müller et al., 2007).

et al., 1999) on 16 December 2002 (open diamonds in Figure 3.13) show a rather typical "early vortex" relation (Tilmes et al., 2003a, 2004, see also Figure 2.4 and Section 3.1). At the top of the MkIV profile (above 750 K, not shown) maximum HF mixing ratios occur, SF_6 mixing ratios are 3.2–3.4 ppt, and the CO mixing ratio at the top altitude is 35 ppb; all these values are typical of upper stratospheric air.

The ozone–N_2O relation measured by SPIRALE on 21 January 2003 (Huret et al., 2006, thick grey line in Figure 3.13) agrees with the MkIV relation in parts of the profile, but also shows deviations towards greater ozone and greater tracer mixing ratios that are indicative of mixing of polar with mid-latitude air (e.g., Müller et al., 2005). Indeed, the enhancement of ozone at around 100 ppb N_2O, where O_3 exceeds 4 ppm, occurs at $\sim$500 K where SPIRALE sampled the vortex edge region (Huret et al., 2006). At greater altitudes, complex mixing patterns developed between mesospheric air and stratospheric air of vortex and mid-latitude origin (see discussion in Section 3.4.1).

The ozone–N_2O relation measured by BONBON on 6 March 2003 in the lower stratosphere (Engel et al., 2006) shows lower ozone mixing ratios than the MkIV relation due to halogen-induced chemical ozone destruction (e.g., Tilmes et al., 2003a). At greater altitudes, above 550 K (N_2O $\sim$3 ppb at 550 K), both ozone and N_2O mixing ratios in the BONBON measurements are larger compared to the MkIV measurements in December. This is consistent with increasing mixing of polar with mid-latitude air due to the start of weakening of the polar vortex at those altitudes.

The MIPAS measurements (Friedl-Vallon et al., 2004) on 20 March 2003 show a further decrease in ozone mixing ratios relative to N_2O, consistent with continuing chemical ozone

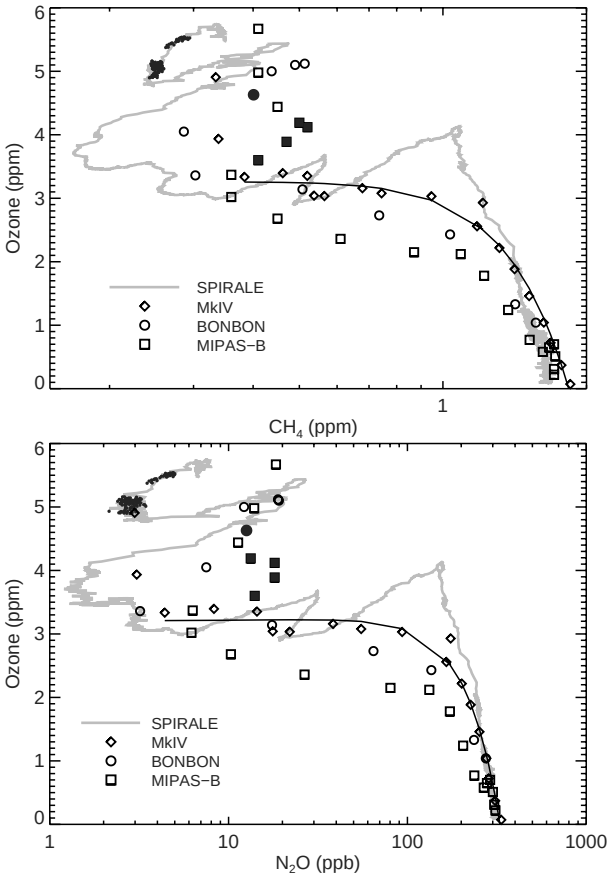

Figure 3.13: The ozone–methane (top panel) and the ozone–N_2O relation (bottom panel) from balloon measurements in the Arctic polar vortex on 20 March 2003 (from MIPAS-B, Wetzel et al., 2006, squares), on 6 March 2003 (from BONBON, Engel et al., 2006, circles), on 21 January 2003 (from SPIRALE, Huret et al., 2006, thick grey line), and on 16 December 2002 (from MkIV, Tilmes et al., 2003a, diamonds). Measurements in the mesospheric air mass in January (CO mixing ratios greater than 570 ppb) and in March 2003 are shown as filled symbols. Note the logarithmic scaling of the x-axis. The solid black lines show an empirical fit through the stratospheric measurements on 16 December 2002; top panel, the ozone–methane relation reported by Tilmes et al. (2003a) and, bottom panel, the empirical relation $\mu_{O_3} = 3.20 + 1.47 \cdot 10^{-3} \times \mu_{N_2O} - 2.80 \cdot 10^{-5} \times (\mu_{N_2O})^2 - 1.81 \cdot 10^{-8} \times (\mu_{N_2O})^3$ (where the ozone mixing ratio μ_{O_3} is in ppm and the N_2O mixing ratio μ_{N_2O} is in ppb; the uncertainty of the fit is 0.2 ppm). (Figure taken from Müller et al., 2007).

destruction. The measurements above about 550 K show a pattern very similar to that of the BONBON measurements in early March. The layer between 580-700 K (corresponding to 24-27 km) is considered to be influenced by mesospheric air owing to the enhanced CO mixing ratios (Figure 3.12). The ozone mixing ratios in this layer have decreased compared to early March.

In the measured ozone–N_2O relations, the mesospheric data points do not stand out in any of the three balloon profiles measured in the vortex in early 2003 (Figure 3.13). Therefore, additional information from measurements of other gases such as CO is necessary in order to identify mesospheric air-masses in the ozone–N_2O scatterplot (Figure 3.13). Ozone mixing ratios in these air masses range between 4.8–5.6 ppm on 21 January, 4.6 ppm on 6 March, and 3.6–4.2 ppm on 20 March. They are thus clearly greater than typical upper stratospheric or mesospheric ozone mixing ratios. This means that the ozone mixing ratios in the stratospheric air masses of mesospheric origin are considerably greater than typical mesospheric ozone mixing ratios ($\sim$2 ppm). It is likely that ozone mixing ratios in the air masses of mesospheric origin will have increased chemically during descent owing to the short lifetime of ozone in the mesosphere and in the upper stratosphere. Mesospheric air mixes moreover with surrounding air masses during descent (see Section 3.4.1). These points are important for assessing the impact of mesospheric intrusions on the accuracy of ozone loss estimates based on ozone–tracer relations.

None of the air masses where the lowest N_2O (and CH_4) mixing ratios were observed, neither in January (less than 2 ppb N_2O at altitudes of $\sim$700 K) nor in March 2003 (3–6 ppb N_2O at altitudes of $\sim$530–550 K), show mesospheric characteristics (Figures 3.9 and 3.13). This indicates that the mesospheric air must have been diluted with stratospheric air during descent. The measurements in March 2003 at $\sim$530–550 K, where N_2O mixing ratios range from 3–6 ppb, show ozone mixing ratios of 3–3.5 ppm consistent with the balloon measurements in December and January (Figure 3.13). Therefore, in contrast to the mesospheric layer, these air masses have likely remained largely unmixed and without substantial chemical change over the course of the winter. At an altitude of about 600 K, above the minimum N_2O values in March, disturbances of the weakening vortex occurred (e.g., Harvey et al., 2002; Manney et al., 2005; Steinhorst et al., 2005) resulting in mixing with air from outside the vortex, thereby causing higher N_2O mixing ratios.

3.4.2 Chemical Change of Ozone in Descending Mesospheric Air

In the mesosphere, ozone production is balanced by very efficient ozone loss cycles driven by HO_x radicals (Figure 1.3) resulting in low ozone mixing ratios. At lower altitudes, below about 45 km (2 hPa), these cycles rapidly lose their efficiency (e.g., Crutzen et al., 1995; Grooß et al., 1999, see also Section 1.1.2). Therefore, when mesospheric air descends, ozone mixing ratios will tend to increase (except when the decent occurs in complete darkness in polar night without any excursion to lower latitudes). And the increase, i.e. the adjustment to local photochemical equilibrium, will be fast owing to the short chemical lifetime of ozone in the mesosphere and upper stratosphere. When mesospheric air is enhanced

in NO_x, e.g., due to energetic particle precipitation (Funke et al., 2005; Randall et al., 2005, 2006; WMO, 2007) a reduction of ozone in the middle stratosphere might be expected due to NO_x-catalysed ozone loss cycles. However, even under such circumstances, effects of enhanced NO_x on ozone in the middle stratosphere are not always observed (Randall et al., 2006). In Arctic winter 2002/2003, rather inefficient NO_x downward transport with negligible deposition of NO_x in the lower and middle stratosphere occurred (Funke et al., 2005). However, significant ozone loss is noticeable for the unusually strong enhancements of NO_x in November/December 2003 and January 2004 (Randall et al., 2005; López-Puertas et al., 2005; WMO, 2007; Vogel et al., 2008), but even under such circumstances, upper stratospheric ozone mixing ratios (at 40 km) are greater than 5 ppm and thus clearly greater than mesospheric ozone mixing ratios.

The composition of the air in the mesospheric intrusion is not only determined by chemical change but also by mixing during the descent to the stratosphere. The development of the mesospheric layer started in November 2002 with the descent of mesospheric air that was later cut off by the subsidence of upper stratospheric air triggered by a minor warming that occurred in late December (Engel et al., 2006). It is remarkable that the mesospheric air was first observed on 21 January 2003 immediately after the first vortex split and then twice in March 2003 after the second vortex split in mid-February (e.g., Günther et al., 2008). This means that the signature of the mesospheric layer survived the perturbation of the two vortex splits, although the splits likely contributed to a further dilution of the mesospheric air. The CO mixing ratios observed in March 2003 are substantially lower than those observed in January 2003 (Müller et al., 2007, see also Figures 3.12 and 3.9) and the tracer values are clearly higher (Figure 3.13). Ozone mixing ratios in the mesospheric air are lower in March than in January (Figure 3.13). Thus, if one interprets the lower CO and greater tracer values in March as the result of mixing, the dilution of mesospheric air would reduce ozone mixing ratios in the mesospheric intrusion.

For a first rough estimate of the potential impact of intrusions of mesospheric air on polar stratospheric ozone–tracer relations, we assume that the air mass of the entire mesosphere between 1 and 0.01 hPa is 'flushed' into (and mixed with) the polar stratospheric air poleward of 60° between 100 and 10 hPa. The mass of this stratospheric polar air is about six times that of the air of the entire mesosphere. Assuming that the air in the entire mesosphere were deposited in the polar stratosphere and displaced an equivalent volume of stratospheric air, the polar stratospheric air would contain 17% of mesospheric air. Therefore, assuming an ozone mixing ratio of 2 ppm and a methane mixing ratio of 0.1 ppm for the mesospheric air and an ozone mixing ratio of 4 ppm and a methane mixing ratio of 1 ppm for the stratospheric air, stratospheric ozone mixing ratios would change by 9% and methane mixing ratios by 15%.

A mesospheric fraction of air of 17% as deduced from this rather crude estimate is a smaller value than that reported by Engel et al. (2006) for the layer of mesospheric air in the Arctic vortex in 2006, but is greater than the value deduced by Ray et al. (2002) for the Arctic polar vortex in winter 1999/2000. The latter report a fraction of mesospheric air in the vortex of 2–4%.

However, the assumption that ozone does not change chemically during descent is clearly not correct. Because ozone in the mesosphere and in the upper stratosphere has a short life-

time (less than ∼30 hours above 5 hPa or 1000 K outside the polar night, e.g., Sankey and Shepherd, 2003) ozone mixing ratios will change chemically during descent by adjusting rapidly towards local photochemical equilibrium. Since ozone mixing ratios increase with decreasing altitude in the upper stratosphere and in the mesosphere (above ∼5 hPa (1000 K), e.g., Grooß and Russell, 2005), ozone is expected to increase during the descent of mesospheric air, as long as the air parcel receives sufficient sunlight. The ozone mixing ratios should be "frozen in" at the photochemical equilibrium value in the region, where, during poleward and downward transport, the chemical lifetime of ozone becomes substantially longer than the transport timescales.

Ozone lifetimes exceeding a week occur at altitudes of about 10 hPa corresponding to climatological ozone mixing ratios in high latitudes in winter of about 5 ppm (e.g., Grooß and Russell, 2005). This crude estimate agrees with the ozone mixing ratios reported by Engel et al. (2006) for the first sampling of mesospheric air on 21 January 2003 by SPIRALE (see also Figure 3.13). The concept of a rapid chemical equilibrium that is suddenly "frozen in" in polar night is, of course, an oversimplification. In reality, a smoother transition between the two regimes will occur. Such a transition could be analysed (and the resulting ozone mixing ratios better quantified) by a comprehensive model study.

3.5 Calculation of Chemical Ozone Loss in the Arctic in March 2003 Based on ILAS-II Measurements

The method of deducing chemical ozone loss from ozone tracer–relations is discussed in detail in Section 3.1. Here, the method is employed to calculate ozone loss in Arctic winter 2002/2003 based on measurements of the ILAS-II (Improved Limb Atmospheric Spectrometer-II) instrument aboard ADEOS-II (Advanced Earth Observing Satellite-II) (Nakajima et al., 2006), the Halogen Occultation Experiment (HALOE) (Russell et al., 1993), and on MIPAS-B and MkIV balloon-borne measurements.

Comparing an "early vortex" reference from 16 December 2002 with the ozone–HF relation in February and April measured by HALOE shows the typical signature of chemical ozone loss in the Arctic (Tilmes et al., 2003a). In agreement with the deduced chemical ozone loss, strong chlorine activation was observed during this winter (Tilmes et al., 2003a). This picture is corroborated by the MIPAS-B measurements on 20 March 2003. The MIPAS-B ozone–N_2O relation confirms the earlier balloon measurements at altitudes above 550 K, and additionally shows lower ozone mixing ratios for comparable tracer values of the early winter reference function below 550 K (Figure 3.13).

Moreover, the ILAS-II instrument observed the Arctic winter 2002/2003 from 19 January to 19 April, 2003 (Nakajima et al., 2006). The ILAS-II measurements between January and March were obtained during the early turn-on operations during which no major problems occurred (Nakajima, 2006). Based on these measurements, chemical ozone loss can be estimated using tracer-tracer correlations.

The early winter reference is based on the balloon-borne measurements of the ozone–N_2O relationship by the MkIV instrument (Toon et al., 1999) on 16 December 2002. However, below 550 K ILAS-II N_2O mixing ratios are $\sim$40 ppb lower than MkIV observations according to the validation study by Ejiri et al. (2006). Similarly, ILAS-II N_2O values are $\sim$40 ppb smaller than N_2O mixing ratios deduced from HALOE HF measurements using an HF to N_2O relation based on MkIV measurements on 3 December 1999

$$\mu_{\mathrm{HF}} = 1.5484 - 4.9386 \cdot 10^{-3} \cdot \mu_{\mathrm{N_2O}} \tag{3.1}$$

(where μ_{HF} denotes the HF mixing ratio in ppb and $\mu_{\mathrm{N_2O}}$ the N_2O mixing ratio in ppb). Therefore, a N_2O offset of 40 ppb is assumed when deriving an early winter reference function from the MkIV data for the ILAS-II observations. In Figure 3.15 and Table 3.1, the ozone loss derived using ILAS-II observations is compared to the HALOE-based ozone loss reported by Tilmes et al. (2003a).

Here only ILAS-II measurements made inside the polar vortex are considered and grouped according to two regions of the vortex: the vortex core and the outer vortex (the area between vortex core and vortex edge). Both the edge of the vortex and the boundary of the vortex core are defined using the gradient of the potential vorticity constrained by wind velocities as a criterion (Tilmes et al., 2003b).

The ILAS-II observations during the early turn-on operations are relatively sparse (Tilmes et al., 2006c). Therefore, only one ILAS-II profile was observed within the outer vortex in

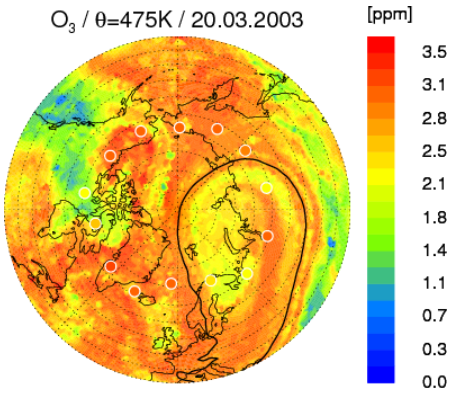

Figure 3.14: Model simulation with the Chemical Lagrangian Model of the Stratosphere (CLaMS) for 20 March 2003 on the 475 K potential temperature surface; this simulation is described in detail elsewhere (Grooß et al., 2005). The white circles show the corresponding ILAS-II measurements on 20 March 2003 adjusted to the synoptic time (12 UT) of the model results. The black line denotes the edge of the polar vortex according to the criterion of the maximum gradient in potential vorticity (Nash et al., 1996). (Figure taken from Müller et al., 2007).

January and one in the vortex core in February. Chemical ozone loss derived using these ILAS-II observations is 5-10 DU larger at 380–550 K and 4–8 DU smaller at 400–500 K than the value derived using HALOE measurements, but is still in agreement within the uncertainty of the results. Both ILAS-II and HALOE results show a similar increase of ozone loss values between January and February of 21–24 DU at 380–550 K and 18–22 DU at 400–500 K.

For March, only ILAS-II and MIPAS-B observations are available. The ILAS-II vortex-averaged ozone loss in March is less than the vortex-averaged ozone loss in February derived from HALOE observations. However, profiles in March show a much larger variability than in February (the standard deviation of ozone loss profiles is 16 DU for 380–550 K and 14 DU for 400–500 K within the polar vortex core). Individual profiles show a rather large chemical ozone loss (55 DU in 380–550 K and 35 DU in 400–500 K).

The strong variability noted here of both ozone loss and ozone mixing ratios within the vortex in late March 2003 is consistent with the results of a model simulation using the Chemical Lagrangian Model of the Stratosphere (CLaMS) of winter 2002/2003 (Grooß et al., 2005). Indeed, the simulated ozone values in March 2003 on the 475 K potential temperature surface in general agree rather well with the ILAS-II measurements (see white circles in Figure 3.14). An exception is the Canadian Arctic where ozone values measured by ILAS-II are higher than those obtained from observations. This problem arises in a region where an intrusion of low-latitude, ozone-poor air occurs pointing to problems in the initialisation of low-latitude ozone as a possible explanation for the apparent discrepancy.

Later, in April, a separation of air masses within the vortex is noticeable; a few profiles show large ozone loss values of more than 1.5 ppm at $\sim$440 K while most profiles show an

Table 3.1: Arctic column ozone loss in winter 2002/2003

Date	Experiment	Vortex Core	Outer Vortex	Maximum
380–550 K				
19–26. 1.	(HALOE)		23 ± 9 (14)	33 ± 8
21. 1.	(ILAS-II)			42 ± 6 [a]
15–25. 2.	(HALOE)	51 ± 9 (6)	26 ± 9 (12)	57 ± 10
25. 2.	(ILAS-II)			63 ± 10 [b]
20–22. 3.	(ILAS-II)	37 ± 11 (16)	41 ± 11 (16)	55 ± 5
11–19. 4.	(HALOE)	49 ± 10 (11)	40 ± 10 (12)	61 ± 10
9–19. 4.	(ILAS-II)	50 ± 10 (13)	48 ± 11 (12)	67 ± 11
400–500 K				
19–26. 1.	(HALOE)		21 ± 5 (13)	29 ± 6
21. 1.	(ILAS-II)			21 ± 5 [a]
15–25. 2.	(HALOE)	43 ± 6 (7)	24 ± 6 (11)	47 ± 6
25. 2.	(ILAS-II)			43 ± 6 [b]
20–22. 3.	(ILAS-II)	24 ± 6 (14)	26 ± 9 (6)	35 ± 6
11–19. 4.	(HALOE)	37 ± 6 (10)	32 ± 6 (9)	52 ± 6
9–19. 4.	(ILAS-II)	31 ± 6 (10)	33 ± 6 (8)	50 ± 6

Column ozone loss in Dobson units in winter 2002/2003 calculated from HALOE measurements using HF as the long-lived tracer (Tilmes et al., 2003a) and ILAS-II measurements using N_2O as the long-lived tracer. Also reported is the uncertainty of the ozone loss estimate caused by the uncertainty of the early vortex reference and, in brackets, the standard deviation of the computed vortex average loss values. Additionally, the maximum ozone loss of all observations within the respective period is shown.
[a] One single profile in the outer vortex
[b] One single profile in the vortex core

ozone loss of 0.5-1.0 ppm between ∼400–500 K. A few profiles that scatter above the early reference function are likely influenced by mid-latitude air masses during the start of the breakup of the polar vortex. ILAS-II and HALOE ozone loss profiles and calculated loss in column ozone agree very well for April 2003 (Table 3.1).

The chemical ozone loss in Arctic winter 2002/2003 deduced here from the ILAS-II measurements can be compared with ozone loss estimates for this winter reported in a number of previous studies. Singleton et al. (2005) found a maximum chemical loss of 1.2 ppm in mid-March at 425 K in approximate agreement with the ozone loss profiles reported here (Figure 3.15). The ozone loss deduced for the partial column between 400–500 K (56 ± 4 DU) using the Match technique (Streibel et al., 2006) is greater than the loss values reported here (Table 3.1). It is no surprise that chemical ozone loss estimates based on ozone–tracer relations in a winter where the Arctic vortex is strongly impacted by mixing are lower than

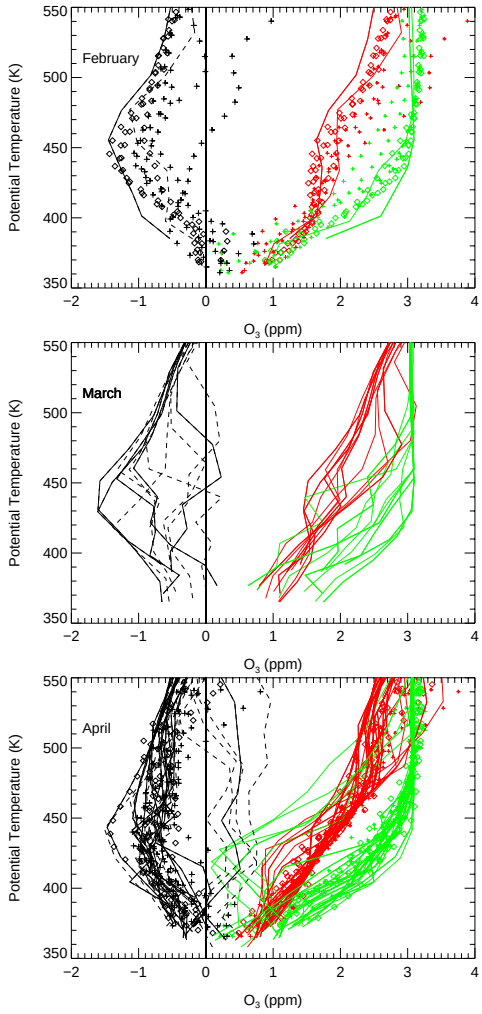

Figure 3.15: Vertical profiles of measured O_3 mixing ratios (red symbols), O_3 mixing ratios expected in the absence of chemical change ($\hat{O}_3$), (green symbols), and calculated O_3 loss profiles, (black symbols), for February (top panel) and March (middle panel) and April (bottom panel) in winter 2002/2003. $\hat{O}_3$ was deduced using HF as the long-lived tracer for HALOE measurements and using N_2O as the long-lived tracer for ILAS-II. HALOE profiles are located inside the vortex core (diamonds) and inside the outer vortex (plus signs) in February and April. ILAS-II profiles are located inside the vortex core (solid lines) and inside the outer vortex (dashed lines) between January and April 2003. (Figure taken from Müller et al., 2007).

estimates based on the Match technique. This is the case because mixing across the vortex edge will mask chemical ozone loss deduced from ozone–tracer relations (e.g., Müller et al., 2005) whereas Match is designed to exclude this effect. Further, Grooß et al. (2008) argued that the Match method might overestimate ozone loss at lower altitudes leading to an overestimation of the ozone loss in the total column. Whether these effects can quantitatively account for the observed discrepancy remains to be analysed. The column ozone loss based on the vortex average method in winter 2002/2003 (Christensen et al., 2005) does not agree with our results if an average over the entire vortex is considered. However, the ozone loss reported for the vortex core, within the error bars, is in agreement with the loss deduced here from ILAS-II measurements. Goutail et al. (2005) report a chemical loss in column ozone of $\sim 19 \pm 4\%$ by 20 March 2003. They estimate that the 23 DU loss for the partial column 380–550 K corresponds to a loss of $\sim 10\%$ in column ozone (Section 4 in Goutail et al., 2005) so that $19 \pm 4\%$ corresponds to a loss of $\sim 44 \pm 9$ DU for the partial column 380–550 K, a value that is in agreement with the chemical ozone loss reported here.

In summary, measurements of ozone and N_2O by the MkIV instrument on 16 December 2002 were combined with ILAS-II satellite measurements to deduce chemical ozone loss in the Arctic vortex in March and April 2003. The estimated ozone loss for April is in agreement with previous estimates based on HALOE measurements (Tilmes et al., 2003a). The average chemical ozone loss in the vortex core for the partial column 380–550 K is 37 ± 11 DU in March and 50 ± 10 DU in April 2003.

4 Epilogue

4.1 Summary

Since the pioneering papers by Proffitt et al. (1990) and Fahey et al. (1990), tracer-tracer relations have been used in numerous studies to identify physiochemical change in the stratospheric polar vortices. An issue neglected in earlier studies (e.g., Müller et al., 1996) is that it is necessary to assess the impact of mixing processes on tracer-tracer relationships in the polar vortex for a reliable quantification of physiochemical change. This neglect has attracted criticism. In particular, the use of ozone-tracer relations was criticised by the argument that mixing processes have the potential to affect ozone tracer relations in a way that leads to an overestimation of chemical ozone loss (Plumb et al., 2000). Specific processes considered were mixing among vortex air masses following differential descent in the vortex, mixing of stratospheric vortex air with a mesospheric intrusion, and mixing of vortex air with out-of-vortex air by mixing across the transport barrier at the vortex edge.

Here, it has been shown that differential descent within the vortex and the subsequent mixing among vortex air masses cannot have a significant impact on ozone-tracer relations (Section 3.3). Further, intrusions of mesospheric air into the stratosphere cannot affect ozone loss estimates if they do not reach the altitudes ($\sim$600 K) up to which the ozone-tracer relations are usually employed (e.g., Müller et al., 1996; Tilmes et al., 2004) or if the intrusions reach the lower stratosphere before the establishment of the early vortex reference relation, i.e., before late November or December in the northern hemisphere. Ozone mixing ratios in mesospheric air are rather low, less than $\sim$2 ppm, but because of the short chemical lifetime of ozone in the upper stratosphere and above, ozone mixing ratios of mesospheric air increase photochemically during downward transport (Salawitch et al., 2002). Indeed, observed ozone mixing ratios in air masses influenced by mesospheric air in the lower stratosphere in January and March 2003 are greater than those in the surrounding stratospheric air and clearly greater than those found in the 'early vortex' reference relation employed to deduce chemical ozone loss (Section 3.4). Thus, if mesospheric air masses were to reach the lower stratosphere and mix strongly enough so that they could no longer be identified, ozone mixing ratios in the lower stratosphere would increase so that the chemical ozone loss signal would be underestimated. Therefore, intrusions of mesospheric air are unlikely to have a significant impact on ozone loss estimates based on the ozone–tracer relation method and, if they were to have an effect, could only lead to an underestimate of chemical ozone loss.

Considering mixing between inside and outside vortex air, it is important to note that these two types of air masses are characterised by different ozone-tracer relationships, with the outside vortex relationships showing greater ozone mixing ratios (and a stronger variability) for the same values of the tracer than inside relationships (Sections 3.2 and 3.3, see also

Proffitt et al., 1993; Müller et al., 1999; Plumb, 2007). Consequently, mixing between air masses inside and outside the vortex should lead to points lying above the original ozone-tracer relation in the vortex (Figure 3.1), as is indeed observed (Figures 3.6 and 3.13, see also Rex et al., 2002; Jost et al., 2002). Therefore, mixing across the vortex edge, if it occurs during the period of chemical ozone loss, will lead to an *underestimate* of ozone loss.

The findings discussed above contrast with the conclusion of Plumb et al. (2000), who state that "estimates of ozone depletion inferred from ozone-tracer relations are likely to be overestimates". There are several reasons for this difference. First, as demonstrated in Section 3.2.1, but contrary to the interpretation by Plumb et al. (2000), there is no substantial quantitative difference between the reference relation put forward by Michelsen et al. (1998) and the 'early vortex relations' used for deducing chemical ozone loss from ozone-tracer relations (Tilmes et al., 2004).

Second, diffusivities for transport across the vortex edge in the conceptual model of Plumb et al. (2000) are very likely too high by more than an order of magnitude and it is assumed in this model that the same tracer-tracer relation prevails inside and outside the vortex; an assumption that is not valid for the ozone-tracer relation in the polar region (Section 3.3.1). Third, the conceptual model is formulated in terms of artificial, chemically inert tracers. The development of the relation of these inert tracers is driven primarily by a supply of air from high altitudes with very low mixing ratios of both species. However, even though air low in ozone exists in the mesosphere (Figure 2.2), ozone is quickly regenerated by gas phase photochemistry as these air parcels descend into the stratosphere (Section 3.4, see also Salawitch et al., 2002). Indeed, ozone mixing ratios ranging between 3.6 ppm and 5.6 ppm, and thus substantially higher than mesospheric ozone mixing ratios, have been measured in mesospheric air masses that intruded into the Arctic stratosphere in early 2003 (Section 3.4.1).

Drawing together all the pieces of information considered here, the following picture of the development of ozone-tracer relations in the polar vortex develops (Figure 3.1). In the incipient vortex, the vortex air mass is characterised by low ozone mixing ratios; the remainders of polar ozone destruction due to NO_x-driven chemical cycles in summer (e.g., Farman et al., 1985b) and autumn (Kawa et al., 2002; Tilmes et al., 2006b). Although the vortex air mass is separated to a certain extent from ozone-rich, mid-latitude air, the vortex is not yet completely isolated. Thus, through mixing, ozone values in the vortex increase during this period (Tilmes et al., 2003b, 2006c). When the vortex is well established, the transport barrier at the vortex edge effectively separates vortex air from mid-latitude air. Mixing within the vortex air mass produces a compact ozone-tracer relation in the vortex. This is the point in time when the reference relation for the ozone-tracer relation method should ideally be derived.

In cold winters, a beginning chemical ozone loss first becomes noticeable at greater altitudes ($\sim$500 K), typically in late January/early February in the Arctic (Tilmes et al., 2003b). Towards late winter, the ozone loss accelerates with strongly increasing solar illumination. Thus, in early spring, the signal of accumulated ozone loss is very pronounced in the ozone-tracer relation (Figure 3.1, bottom panel). Under such conditions, mixing across the vortex edge clearly leads to an underestimated ozone loss.

The development of ozone-tracer relations in the vortex could be observed nicely in Arc-

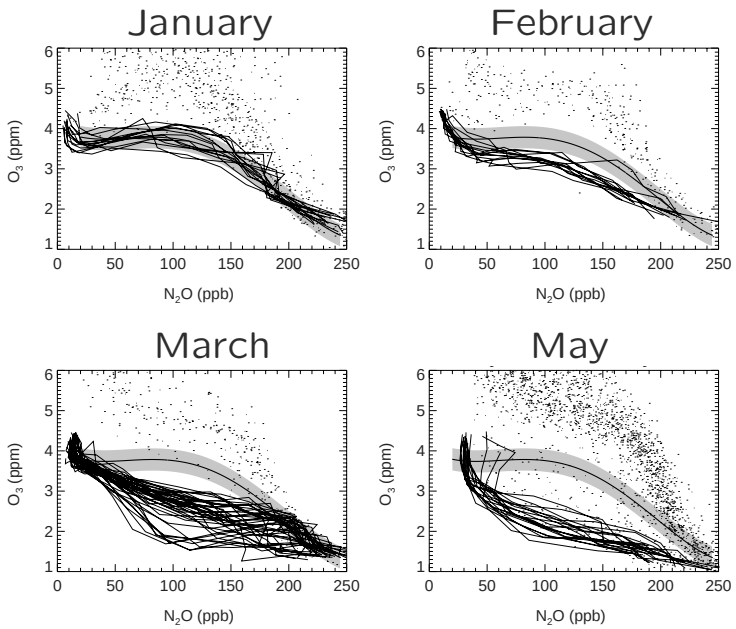

Figure 4.1: The development of the O_3/N_2O relation in the Arctic in winter 1996/1997 based on ILAS measurements (Tilmes et al., 2003b). Shown are four different time periods (1-15 January, 17-21 February , 21-31 March, 1-15 May 1997). Black lines indicate profiles measured inside the polar vortex core, defined using the Nash et al. (1996) potential vorticity criterion. Black dots indicate measurements outside the polar vortex. (Figure adapted from Müller et al., 2005).

tic winter 1996/1997 when measurements by the ILAS satellite experiment provided a good spatial and temporal coverage of the polar region (Figure 4.1). The establishment of a compact 'early vortex' relation in January that is distinct from the out-of-vortex measurements is clearly visible. In February, the beginning ozone depletion causes a moderate deviation of the ozone-tracer relation from the reference relation. In late March, the accumulated chemical ozone loss is obvious as a strong deviation from the reference. The loss was not uniform throughout the vortex in March, but in May, in the remaining vortex parts, a compact ozone-tracer relation indicates that that mixing in the vortex had, by that time, again homogenised the vortex air mass.

In the absence of chemical change, however, tracer-tracer relations do indeed remain compact and unaltered throughout the existence of the vortex (Figure 2.5). In this way it was shown that heterogeneous chemistry initiated by the action of cosmic rays (a mechanism put forward by Lu and Sanche, 2001a) cannot be a significant process in the polar vortex (Section 2.2.1, see also Müller, 2003).

Recently, the question of the behaviour of ozone-tracer relations in the results of model simulations has attracted interest (see Chapter 3 and references therein). It has been shown here that the representation of mixing in three-dimensional atmospheric models can have

a substantial impact on the development of the tracer relation in the model. Of particular importance is a realistic representation of transport barriers (such as the polar vortex edge) in the model. Rather compact ozone-tracer relations develop –in agreement with observations– in the vortex of the Lagrangian model CLaMS (McKenna et al., 2002b), where mixing is anisotropic and driven by the deformation of the flow (Section 3.2.2).

We conclude that in order to use ozone-tracer relations to deduce chemical ozone loss, it is crucial that a reliable 'early vortex' reference can be obtained and that vortex measurements are well separated from mid-latitude measurements. If these conditions are met, ozone-tracer relations constitute a reliable tool for the quantitative determination of chemical ozone loss in the polar vortex.

4.2 Outlook

By the middle of the 21st century, the halogen burden of the stratosphere will be significantly lower than today; it is expected to be similar to that present in 1980 before the onset of clearly noticeable ozone depletion (Figure 1.8). However, most chlorine and bromine source gases have long atmospheric lifetimes and will thus disappear from the atmosphere only slowly. As a consequence, concentrations of stratospheric halogens will remain elevated for decades to come (Figure 1.8). Therefore, polar ozone loss will remain an important environmental issue for the foreseeable future and methods allowing chemical ozone loss to be estimated, like the ozone-tracer relation method, will continue to be applied and improved.

However, the atmosphere in 2050 will not be the same as in 1980, mostly because of global change. It is expected that atmospheric concentrations of CH_4 and N_2O will be greater in 2050 than in 1980 and that stratospheric temperatures will be lower (WMO, 2007; Solomon et al., 2007b). The future development of stratospheric water vapour mixing ratios is more uncertain. Clearly, increasing atmospheric CH_4 will lead to an increase in stratospheric water vapour, but recent stratospheric water vapour trends are not understood well enough to make reliable predictions for the future (e.g., Röckmann et al., 2004; Randel et al., 2006; Riese et al., 2006; Solomon et al., 2007b, 2010). Further, there is a possible future anthropogenic impact beyond a continuing emission of greenhouse gases. A possible future hydrogen economy has a potential influence on stratospheric ozone (Feck et al., 2008) and, if implemented, concepts for cooling the Earth's climate by the artificial introduction of sulphate aerosol particles into the stratosphere (Crutzen, 2006; Rasch et al., 2008) will have important consequences for stratospheric ozone (Tilmes et al., 2008a, 2009).

Recent projections of climate change (Solomon et al., 2007b) are based on climate models that focus on tropospheric change and largely neglect stratospheric processes. Nonetheless, there are important coupling processes between the stratosphere and the troposphere. For example, the ozone hole in the southern hemisphere spring has affected the Antarctic surface climate (Gillett and Thompson, 2003; Thompson et al., 2005; Keeley et al., 2007). Conversely, nearly all climate models with a well-represented stratosphere indicate that the Brewer-Dobson circulation will accelerate because of climate change (Butchart et al., 2006), a change that would have a substantial impact on the stratosphere. Although one does not

expect the inclusion of stratospheric ozone-climate effects in coupled atmosphere-ocean climate models to drastically alter overall estimates of globally averaged surface warming, because of the possible dynamical responses in the troposphere to the stratospheric changes, projections of the evolution of polar climate could be substantially different (Baldwin et al., 2007). It is likely that the inclusion of an appropriate representation of stratospheric circulation and chemistry in climate models will be possible for prognostic studies that will be included in the next IPCC report. One aspect of such simulations will be as accurate as possible a representation of polar ozone loss, which will allow both the impact of stratospheric change on the troposphere to be addressed and the influence of changing atmospheric conditions on the recovery of the polar stratosphere from halogen-driven ozone loss. An accurate quantification of chemical polar ozone loss from observations will be an essential contribution to this research.

A Units of Measurement Used in this Book

In stratospheric chemistry, the most common way of expressing the abundance of a species in the gas phase is as the ratio of the number of moles of the species to the number of moles of air. Throughout this work, the abbreviations ppm (parts per million) and ppb (parts per billion) are used to denote molar mixing ratios. For an ideal gas, the molar mixing ratio is equivalent to the volume mixing ratio, so that the abbreviations ppmv and ppbv are also in frequent use. However, for non-ideal gases (e.g., CO_2), the molar mixing ratio is not equal to the volume mixing ratio and the difference between the two is in a range that can be resolved by modern gas chromatographs. When mass mixing ratios are used in the literature, the abbreviations ppmm and ppbm are commonly employed. Advection of an air parcel alone, even if the density changes through ascent or descent, does not change mixing ratios of trace species. Therefore, in a moving air parcel, in the absence of chemical change or mixing with different air parcels, mixing ratios are preserved.

The total thickness of the ozone layer is commonly measured in Dobson units (DU), one DU is defined as 2.687×10^{16} ozone molecules per square centimetre. The Dobson unit describes the thickness of a layer of pure ozone, would the total amount of ozone in the atmosphere be brought to standard conditions (surface pressure, zero degrees Celsius). For example, an ozone column of 300 DU brought down to the surface of the Earth would occupy a 3 mm thick layer.

To convert the mixing ratio μ_X of a species X to a concentration [X] in units of particles per cubic centimetre, the mixing ratio is multiplied by the density of air M in units of molecules per cubic centimetre

$$M = \frac{n}{V} \cdot \mathrm{N_A} \tag{A.1}$$

where n is number of moles, V is volume, and $\mathrm{N_A} = 6.0221 \cdot 10^{23}$ molecules mole^{-1} is the Avogadro constant. Then,

$$[\mathrm{X}] = \mu_X \cdot M \quad . \tag{A.2}$$

The ideal gas law describes the dependence of M on pressure p and temperature T. Combining the ideal gas law

$$\frac{p}{\mathrm{R} \cdot T} = \frac{n}{V} \tag{A.3}$$

where $\mathrm{R} = 8.314\,\mathrm{J\,K^{-1}\,mole^{-1}}$ is the gas constant, with equation A.1, one obtains

$$M = \frac{\mathrm{N_A}}{\mathrm{R}} \cdot \frac{p}{T} \tag{A.4}$$

and, when pressure and temperature are expressed in units of hPa and K, respectively, (as is common in the atmospheric sciences) a useful relation results for M in units of molecules per cubic centimetre

$$M = 7.243 \cdot 10^{18} \cdot \frac{p}{T} \quad . \tag{A.5}$$

The air density M can be converted to the mass density ρ in units of gram per cubic centimetre through the relation

$$\rho = M \cdot \frac{m_a}{\mathrm{N_A}} \tag{A.6}$$

where $m_a = 29$ g/mole is the molecular mass of dry air.

For ozone it is sometimes useful to express the concentration in DU per km rather than in molecules per cubic centimetre (see e.g., Figure 1.5). From the definition of the Dobson unit one obtains 1 DU/km $\approx 3.717 \cdot 10^{-12}$ molecules per cubic centimetre.

B Calculation of Column Ozone Loss

As discussed in Section 3.1, polar chemical ozone loss ΔO_3 in late winter and early spring can be quantified as the difference between the mixing ratio of the ozone proxy $\mu_{\hat{O}_3}$ and the corresponding observed ozone mixing ratio μ_{O_3}

$$\Delta O_3 = \mu_{\hat{O}_3} - \mu_{O_3} \tag{B.1}$$

Here, the ozone proxy $\mu_{\hat{O}_3}$ is calculated from the tracer mixing ratio measured in late winter/early spring using the early vortex reference function $\mathscr{F}$ (see also Section 3.1)

$$\mu_{\hat{O}_3} = \mathscr{F}(\text{tracer}) \tag{B.2}$$

The uncertainty of the ozone proxy $\mu_{\hat{O}_3}$ is determined by the uncertainty of the early winter reference function $\mathscr{F}$.

From the profile of local chemical ozone loss, the loss in column ozone (see Appendix A) can be calculated. (The description of the algorithm for the calculation of the chemical loss in column ozone below closely follows the presentation by Tilmes (2004)). The loss in column ozone is calculated as the difference between the column of measured ozone (Col_{O_3}) and the column of the corresponding proxy ozone ($\text{Col}_{\hat{O}_3}$).

$$\text{Col}_{O_{3\text{loss}}} = \text{Col}_{\hat{O}_3} - \text{Col}_{O_3} \tag{B.3}$$

Ozone loss in the stratosphere occurs mainly at altitudes between about 350 and 550 K potential temperature (see e.g., Figures 1.13 and 3.15). Therefore, the loss in this altitude range is a good estimate for the depletion in total column ozone.

The number density of ozone $[O_3]$ (and $[\hat{O}_3]$), in molecules/cm^3 is vertically integrated over a certain altitude range dz (between the geometric heights z_1 and z_2) to obtain column ozone $\text{Col}_{O_{3\text{loss}}}$ in units of molecules per cm^2.

$$\text{Col}_{O_{3\text{loss}}} = \int_{z_1}^{z_2} [\hat{O}_3] dz - \int_{z_1}^{z_2} [O_3] dz \tag{B.4}$$

The number densities $[O_3]$ (and $[\hat{O}_3]$) can be written as the ozone mixing ratio μ_{O_3} ($\mu_{\hat{O}_3}$) multiplied by the number density of air M in molecules/cm^3 (see Appendix A). Therefore, the column ozone can be calculated as follows:

$$\int_{z_1}^{z_2} [O_3] dz \;=\; \int_{z_1}^{z_2} \mu_{O_3}\, \text{M} dz. \tag{B.5}$$

The transformation to pressure coordinates is achieved by inserting the hydrostatic relation $dp =$

$-\rho g \cdot dz$:

$$\int_{z_1}^{z_2} [\mathrm{O_3}] dz \quad = \quad \int_{p_2}^{p_1} \frac{1}{g} \cdot \frac{M}{\rho} \, \mu_{\mathrm{O_3}} \, dp \tag{B.6}$$

where the acceleration of gravity $g = 9.81$ m/sec^{-2}, ρ is the mass density (in g/cm^3) and p is pressure (in hPa).
The ratio of the number density of air M and mass density ρ can be derived from Equation A.6:

$$\frac{M(p,T)}{\rho(p,T)} = \frac{\mathrm{N_A}}{\mathrm{m_a}} = \text{const.} \tag{B.7}$$

where $\mathrm{N_A} = 6.0221 \cdot 10^{23}$ molecules mole^{-1} is the Avogadro constant and $m_a = 29$ g/mole is the molecular mass of dry air. Because this ratio is constant, one can define the constant α

$$\alpha \quad = \quad \frac{1}{g} \cdot \frac{M}{\rho} = \frac{1}{g} \cdot \frac{\mathrm{N_A}}{m_a} \tag{B.8}$$

$$\alpha \quad = \quad \frac{1}{981} \cdot \frac{6.0221 \cdot 10^{23}}{29} \left[\frac{\text{molec} \cdot \text{sec}^2}{\text{cm} \cdot \text{g}} \right] \tag{B.9}$$

$$= \quad 2.117 \cdot 10^{19} \left[\frac{\text{molec} \cdot \text{sec}^2}{\text{cm} \cdot \text{g}} \right] \tag{B.10}$$

$$= \quad 2.117 \cdot 10^{22} \left[\frac{\text{molec}}{\text{hpa} \cdot \text{cm}^2} \right] \tag{B.11}$$

and Equation B.6 becomes

$$\mathrm{Col_{O_3}} = \alpha \cdot \int_{p_2}^{p_1} \mu_{\mathrm{O_3}} dp \quad . \tag{B.12}$$

The column ozone in a certain altitude range may be expressed in Dobson units (see appendix A)

$$\int_{z_1}^{z_2} [\mathrm{O_3}] dz \quad = \quad \frac{\alpha}{2.687 \cdot 10^{16}} \cdot \int_{p_2}^{p_1} \mu_{\mathrm{O_3}} dp \tag{B.13}$$

$$\int_{z_1}^{z_2} [\hat{\mathrm{O}}_3] dz \quad = \quad \frac{\alpha}{2.687 \cdot 10^{16}} \cdot \int_{p_2}^{p_1} \mu_{\hat{\mathrm{O}}_3} dp \quad . \tag{B.14}$$

The dominant uncertainty in calculating the column ozone loss in Dobson units is introduced through the first term on the right hand side of Equation B.3 ($\mathrm{Col_{\hat{O}_3}}$). The uncertainty of $\mathrm{Col_{\hat{O}_3}}$ is largely a consequence of the uncertainty of the early winter reference function $\mathscr{F}$.

Symbols and Abbreviations

Symbol	Description	unit, value
c_p	specific heat at constant pressure	$\mathrm{J{\cdot}K^{-1}{\cdot}mol^{-1}}$
$\mathscr{F}$	early vortex reference function	
g	acceleration due to gravity	$9.81\,\mathrm{m{\cdot}s^{-2}}$
M	density of air	particles per $\mathrm{cm^3}$
m_a	molecular mass of dry air	$0.028964\,\mathrm{kg{\cdot}mol^{-1}}$
N_A	Avogadro constant	$6.0221 \cdot 10^{23}\,\mathrm{mol^{-1}}$
PV	potential vorticity	PVU (1 PVU = $10^{-6}\mathrm{Km^2/(kg\,s)}$
R	universal gas constant	$8.314\,\mathrm{J\,K^{-1}\,mole^{-1}}$
z	geometric altitude	km
η	vertical component of absolute vorticity	PVU
θ	potential temperature	K
$\dot{\theta}$	vertical velocity in isentropic coordinates	$\mathrm{K{\cdot}d^{-1}}$
λ	wavelength	nm
μ	mixing ratio	
ρ	mass density	$\mathrm{kg/m^3}$
ϕ	latitude	°N
ϕ_{eq}	equivalent latitude	°N

Acronym	Description
AAOE	Airborne Antarctic Ozone Experiment
ACE-FTS	Atmospheric Chemistry Experiment – Fourier Transform Spectrometer
ADEOS	Advanced Earth Observing Satellite
ALIAS	Aircraft Laser Infrared Absorption Spectrometer
ATMOS	Atmospheric Trace Molecule Spectroscopy experiment
CCM	Chemistry climate model
CFCs	Chlorofluorocarbons
CFC-11	$CFCl_3$
CFC-12	CF_2Cl_2
CLaMS	Chemical Lagrangian Model of the Stratosphere
CMAM	Canadian Middle Atmosphere Model
CTM	Chemistry transport model
CRISTA	Cryogenic Infrared Spectrometers and Telescopes for the Atmosphere
DEA	Dissociative electron attachment
DFA	Detrended fluctuation analysis
DLR	Deutsches Zentrum für Luft- und Raumfahrt (German Aerospace Centre)
DU	Dobson units

Acronym	Description
EASOE	European Arctic Stratospheric Ozone Experiment
ECMWF	European Centre for Medium-range Weather Forecasts
EESC	Equivalent effective stratospheric chlorine
GBMS	Ground-Based Millimetre-wave Spectrometer
HALOE	Halogen Occultation Experiment
HCFCs	Hydrogenated chlorofluorocarbons
ICG	Institute of Chemistry and Dynamics of the Geosphere
ILAS	Improved Limb Atmospheric Spectrometer
IPCC	Intergovernmental Panel on Climate Change
IR	Infrared radiation
MIPAS	Michelson Interferometer for Passive Atmospheric Sounding
MIPAS-B	MIPAS-Balloon
MPG	Max-Planck-Gesellschaft (Max Planck Society)
NASA	National Aeronautics and Space Administration
NAT	Nitric acid trihydrate
NIWA	National Institute of Water and Atmospheric Research
NOZE	National Ozone Expedition
PSCs	Polar stratospheric clouds
PVUs	Potential vorticity units
ppb	parts per billion, 10^{-9}
ppm	parts per million, 10^{-6}
ppt	parts per trillion, 10^{-12}
SAOZ	Système d'Analyse par Observation Zénithale
SAGE	Stratospheric Aerosol and Gas Experiment
SAT	Sulphuric acid tetrahydrate
SBUV	Solar backscatter UV
SPIRALE	Spectroscopie Infra-Rouge par Absorption de Laser Embarqué
SROC	Special report on ozone and climate
STS	Supercooled ternary solutions
TEAP	Technology and Economic Assessment Panel
TRAC	Tracer-tracer correlation technique
TTL	Tropical tropopause layer
UARS	Upper Atmosphere Research Satellite
UNEP	United Nations Environmental Programme
UV	Ultraviolet radiation
WACCM3	Whole Atmosphere Community Climate Model
WMO	World Meteorological Organization

List of Figures

List of Tables

References

Allam, R. J., Groves, K. S., and Tuck, A. F.: Global OH distribution derived from general-circulation model fields of ozone and water-vapor, J. Geophys. Res., 86, 5303–5320, 1981.

Allen, M., Yung, Y. L., and Waters, J. W.: Vertical transport and photochemistry in the terrestrial mesosphere and lower thermosphere (50–120 km), J. Geophys. Res., 86(A5), 3617–3627, 1981.

Anderson, J. G., Toohey, D. W., and Brune, W. H.: Free Radicals Within the Antarctic Vortex: The Role of CFCs in Antarctic Ozone Loss, Science, 251, 39–46, 1991.

Baldwin, M. P., Dameris, M., and Shepherd, T. G.: How will the stratosphere affect climate change?, Science, 316(5831), 1576–1577, doi:10.1126/science.1144303, 2007.

Bates, D. R. and Nicolet, M.: The photochemistry of atmospheric water vapor, J. Geophys. Res., 55, 301–327, 1950.

Becker, G., Müller, R., McKenna, D. S., Rex, M., and Carslaw, K. S.: Ozone loss rates in the Arctic stratosphere in the winter 1991/92: Model calculations compared with Match results, Geophys. Res. Lett., 25(23), 4325–4328, 1998.

Becker, G., Müller, R., McKenna, D. S., Rex, M., Carslaw, K. S., and Oelhaf, H.: Ozone loss rates in the Arctic stratosphere in the winter 1994/1995: Model simulations underestimate results of the Match analysis, J. Geophys. Res., 105, 15 175–15 184, 2000.

Bjerknes, V.: Sur les relations entre l'ozone et les mouvements de la troposphère, Gerl. Beitr. Geophys., 24, 23, 1929.

Bodeker, G. E., Scott, J. C., Kreher, K., and McKenzie, R. L.: Global ozone trends in potential vorticity coordinates using TOMS and GOME intercompared against the Dobson network: 1978-1998, J. Geophys. Res., 106(D19), 23 029–23 042, 2001.

Bodeker, G. E., Shiona, H., and Eskes, H.: Indicators of Antarctic ozone depletion, Atmos. Chem. Phys., 5, 2603–2615, 2005.

Borrmann, S., Dye, J. E., Baumgardner, D., Wilson, J. C., Johnson, H. H., Brock, C. A., Loewenstein, M., Podolske, J. R., Ferry, G. V., and Barr, K. S.: In situ measurements of changes in stratospheric aerosol and in the N_2O-aerosol relationship inside and outside of the polar vortex, Geophys. Res. Lett., 20(22), 2559–2562, 1993.

Brandtjen, R., Klüpfel, T., Perner, D., and Knudsen, B. M.: Airborne measurements during the European Arctic Stratospheric Ozone Experiment: Observations of OClO, Geophys. Res. Lett., 21(13), 1363–1366, 1994.

Brasseur, G., Granier, C., and Walters, S.: Future changes in stratospheric ozone and the role of heterogeneous chemistry, Nature, 348, 626–628, 1990.

Brewer, A. W.: Evidence for a world circulation provided by the measurements of helium and water vapour distribution in the stratosphere, Q. J. R. Meteorol. Soc., 75, 351–363, 1949.

Brönnimann, S., Staehelin, J., Farmer, S. F. G., Svendby, T., and Svenøe, T.: Total ozone observations prior to the IGY. I: A history, Q. J. R. Meteorol. Soc., 129, 2797–2817, 2003.

Butchart, N., Scaife, A. A., Bourqui, M., de Grandpre, J., Hare, S. H. E., Kettleborough, J., Langematz, U., Manzini, E., Sassi, F., Shibata, K., Shindell, D., and Sigmond, M.: Simulations of anthropogenic change in the strength of the Brewer-Dobson circulation, Clim. Dyn., 27, 727–741, 2006.

Cabannes, J. and Dufay, J.: Mesure de l'altitude de la couche d'ozone dans l'atmosphère, Comp. Rend., 181, 302–304, 1925.

Cadle, R. D., Crutzen, P. J., and Ehhalt, D. H.: Heteorogeneous chemical reactions in the stratosphere, J. Geophys. Res., 80, 3381–3385, 1975.

Callis, L. and Natarajan, M.: The Antarctic ozone minimum: Relationship to odd nitrogen, odd chlorine, the final warming, and the 11-year solar cycle, J. Geophys. Res., 91, 10 771–10 780, 1986.

Carslaw, K. S., Peter, T., and Clegg, S. L.: Modeling the composition of liquid stratospheric aerosols, Rev. Geophys., 35, 125–154, 1997.

Carslaw, K. S., Wirth, M., Tsias, A., Luo, B. P., Dörnbrack, A., Leutbecher, M., Volkert, H., Renger, W., Bacmeister, J. T., Reimer, E., and Peter, T.: Increased Stratospheric Ozone Depletion Due to Mountain-Induced Atmospheric Waves, Nature, 391, 675–678, 1998.

Chan, K. R., Bowen, S. W., Bui, T. P., Scott, S. G., and Dean-Day, J.: Temperature and wind measurements and model atmospheres of the 1989 Airborne Arctic Stratospheric Expedition, Geophys. Res. Lett., 17(4), 341–344, 1990.

Chandra, S. and McPeters, R. D.: The solar-cycle variation of ozone in the stratosphere inferred from Nimbus-7 and NOAA-11 satellites, J. Geophys. Res., 99, 20 665–20 671, 1994.

Chapman, S.: A theory of upper atmospheric ozone, Mem. Roy. Soc., 3, 103–109, 1930.

Chapman, S.: The gases of the atmosphere, Q. J. R. Meteorol. Soc., 60, 127–142, 1934.

Chipperfield, M. P. and Pyle, J. A.: Model sensitivity studies of Arctic ozone depletion, J. Geophys. Res., 103, 28 389–28 403, 1998.

Christensen, T., Knudsen, B. M., Streibel, M., Anderson, S. B., Benesova, A., Braathen, G., Davies, J., De Backer, H., Dier, H., Dorokhov, V., Gerding, M., Gil, M., Henchoz, B., Kelder, H., Kivi, R., Kyrö, E., Litynska, Moore, D., Peters, G., Skrivankova, P., Stübi, R., Turunen, T., Vaughan, G., Viatte, P., Vik, A. F., von der Gathen, P., and Zaitcev, I.: Vortex-averaged Arctic ozone depletion in the winter 2002/2003, Atmos. Chem. Phys., 5, 131–138, 2005.

Chubachi, S.: Preliminary result of ozone observations at Syowa station from February 1982 to January 1983, Mem. Natl. Inst. Polar Res. Spec. Issue, 34, 13–19, 1984.

Cornu, A.: Observation de la limite ultra-violette du spectre solaire à diverses altitudes, C. R. Hebd. Seances Acad. Sci., 89, 808–814, 1879.

Cox, R. A., MacKenzie, A. R., Müller, R. H., Peter, T., and Crutzen, P. J.: Activation of stratospheric chlorine by reactions in liquid sulphuric acid, Geophys. Res. Lett., 21(13), 1439–1442, 1994.

Crutzen, P. J.: The influence of nitrogen oxides on the atmospheric ozone content, Q. J. R. Meteorol. Soc., 96, 320–325, 1970.

Crutzen, P. J.: Ozone production rates in oxygen-hydrogen-nitrogen oxide atmosphere, J. Geophys. Res., 76, 7311–7327, 1971.

Crutzen, P. J.: Estimates of possible future ozone reductions from continued use of fluro-chloromethanes (CF_2Cl_2, $CFCl_3$), Geophys. Res. Lett., 1, 205–208, 1974.

Crutzen, P. J.: Tropospheric ozone: An overview, in Tropospheric ozone, edited by I. S. A. Isaksen, pp. 3–32, D. Reidel Publishing Company, 1988.

Crutzen, P. J.: My Life with O_3, NO_x and other YZO_xs, p. 54, Swedish Academy of Sciences, 1995.

Crutzen, P. J.: My Life with O_3, NO_x and other YZO_x compounds, Angew. Chem. Intern. Ed., 35(16), 1747–1871, 1996.

Crutzen, P. J.: Albedo enhancements by stratospheric sulfur injections: a contribution to resolve a policy dilemma? An Editorial Essay, Clim. Change, 77, 211–219, 2006.

Crutzen, P. J. and Arnold, F.: Nitric acid cloud formation in the cold Antarctic stratosphere: A major cause for the springtime 'ozone hole', Nature, 342, 651–655, 1986.

Crutzen, P. J. and Brühl, C.: Catalysis by NO_x as the main cause of the spring to fall stratospheric ozone decline in the Northern Hemisphere, J. Phys. Chem. A, 105, 1579–1582, 2001.

Crutzen, P. J., Müller, R., Brühl, C., and Peter, T.: On the potential importance of the gas phase reaction $CH_3O_2 + ClO \rightarrow ClOO + CH_3O$ and the heterogeneous reaction $HOCl + HCl \rightarrow H_2O + Cl_2$ in "ozone hole" chemistry, Geophys. Res. Lett., 19(11), 1113–1116, doi:10.1029/92GL01172, 1992.

Crutzen, P. J., Grooß, J.-U., Brühl, C., Müller, R., and Russell III, J. M.: A Reevaluation of the ozone budget with HALOE UARS data: No evidence for the ozone deficit, Science, 268, 705–708, 1995.

Curtius, J., Weigel, R., Vössing, H. J., Wernli, H., Werner, A., Volk, C. M., Konopka, P., Krebsbach, M., Schiller, C., Roiger, A., Schlager, H., Dreiling, V., and Borrmann, S.: Observations of meteoric material and implications for aerosol nucleation in the winter Arctic lower stratosphere derived from in situ particle measurements, Atmos. Chem. Phys., 5, 3053–3069, 2005.

Dameris, M., Grewe, V., Ponater, M., Deckert, R., Eyring, V., Mager, F., Matthes, S., Schnadt, C., Stenke, A., Steil, B., Brühl, C., and Giorgetta, M. A.: Long-term changes and variability in a transient simulation with a chemistry-climate model employing realistic forcing, Atmos. Chem. Phys., 5, 2121–2145, 2005.

Daniel, J. S., Solomon, S., and Albritton, D. L.: On the evaluation of halocarbon radiative forcing and global warming potentials, J. Geophys. Res., 100, 1271–1285, 1996.

de Zafra, R. L. and Muscari, G.: CO as an important high-altitude tracer of dynamics in the polar stratosphere and mesosphere, J. Geophys. Res., 109, D06105, doi:10.1029/2003JD004099, 2004.

de Zafra, R. L., Jaramillo, M., Parrish, A., Solomon, P., Connor, B., and Barrett, J.: High concentrations of chlorine monoxide at low altitudes in the Antarctic spring stratosphere: diurnal variation, Nature, 328, 408–411, 1987.

DeMore, W. B., Sander, S. P., Golden, D. M., Hampson, R. F., Kurylo, M. J., Howard, C. J., Ravishankara, A. R., Kolb, C. E., and Molina, M. J.: Chemical kinetics and photochemical data for use in stratospheric modeling, JPL Publication 97-4, 1997.

Dobson, G. M. B.: The ozone in the Earth's upper atmosphere, Beitr. Phys. Atmos., 16, 76–85, 1930.

Dobson, G. M. B.: Forty years' research on atmospheric ozone at Oxford: a history, Appl. Opt., 7(3), 387–405, 1968.

Dobson, G. M. B. and Harrison, D. N.: Measurements of the amount of ozone in the Earth's atmosphere and its relation to other geophysical conditions, Proc. R. Soc. London A, 110(756), 660–693, 1926.

Dobson, G. M. B., Harrison, D. N., and Lawrence, J.: Measurements of the amount of ozone in the Earth's atmosphere and its relation to other geophysical conditions. Part III, Proc. R. Soc.

London A, 122, 456–486, 1929.

Dobson, G. M. B., Brewer, A. W., and Cwilong, B. M.: Meteorology of the lower stratosphere, Proc. R. Soc. London A, 185, 144–175, 1946.

Dotto, L. and Schiff, H.: The ozone war, Doubleday, New York, 1978.

Douglass, A. R., Schoeberl, M. R., Stolarski, R. S., Waters, J. W., Russell III, J. M., Roche, A. E., and Massie, S. T.: Interhemispheric differences in springtime production of HCl and $ClONO_2$ in the polar vortices, J. Geophys. Res., 100, 13 967–13 978, 1995.

Dütsch, H. U. and Staehelin, J.: Results of the new and old Umkehr algorithm compared with ozone soundings, J. Atmos. Terr. Phys., 54(5), 557–569, 1992.

Ehhalt, D. H., Röth, E. P., and Schmidt, U.: On the temporal variance of stratospheric trace gas concentrations, J. Atmos. Chem., 1, 27–51, 1983.

Ehhalt, D. H., Rohrer, F., Wahner, A., Prather, M. J., and Blake, D. R.: On the use of hydrocarbons for the determination of tropospheric OH concentrations, J. Geophys. Res., 103(D15), 18 981–18 998, doi:10.1029/98JD01106, 1998.

Ejiri, M. K., Terao, Y., Sugita, T., Nakajima, H., Yokota, T., Toon, G. C., Sen, B., Wetzel, G., Oelhaf, H., Urban, J., Murtagh, D., Irie, H., Saitoh, N., Tanaka, T., Kanzawa, H., Shiotani, M., Aoki, S., Hashida, G., Machida, T., Nakazawa, T., Kobayashi, H., and Sasano, Y.: Validation of the Improved Limb Atmospheric Spectrometer–II (ILAS-II) Version 1.4 nitrous oxide and methane profiles, J. Geophys. Res., 111(D22), D22S90, doi:10.1029/2005JD006449, 2006.

Elkins, J. W., Fahey, D. W., Gilligan, J. M., Dutton, G. S., Baring, T. J., Volk, C. M., Dunn, R. E., Myers, R. C., Montzka, S. A., Wamsley, P. R., Hayden, A. H., Butler, J. H., Thompson, T. M., Swanson, T. H., Dlugokencky, E. J., Novelli, P. C., Hurst, D. F., Lobert, J. M., Ciciora, S. J., McLaughlin, R. J., Thompson, T. L., Winkler, R. H., Fraser, P. J., Steele, L. P., and Lucarelli, M. P.: Airborne gas chromatograph for in situ measurements of long-lived species in the upper troposphere and lower stratosphere, Geophys. Res. Lett., 23(4), 347–350, doi:10.1029/96GL00244, 1996.

Engel, A., Schmidt, U., and McKenna, D. S.: Stratospheric trends of CFC-12 over the past two decades: Recent observational evidence of declining growth rates, Geophys. Res. Lett., 25(17), 3319–3322, doi:10.1029/98GL02520, 1998.

Engel, A., Möbius, T., Haase, H.-P., Bönisch, H.-P., Wetter, T., Schmidt, U., Levin, I., Reddmann, T., Oelhaf, H., Grunow, K., Huret, N., and Pirre, M.: Observation of mesospheric air inside the Arctic stratospheric polar vortex in early 2003, Atmos. Chem. Phys., 6, 267–282, 2006.

Eyring, V., Butchart, N., Waugh, D. W., Akiyoshi, H., Austin, J., Bekki, S., Bodeker, G. E., Boville, B. A., Brühl, C., Chipperfield, M. P., Cordero, E., Dameris, M., Deushi, M., Fioletov, V. E., Frith, S. M., Garcia, R. R., Gettelman, A., Giorgetta, M. A., Grewe, V., Jourdain, L., Kinnison, D. E., Mancini, E., Manzini, E., Marchand, M., Marsh, D. R., Nagashima, T., Nielsen, E., Newman, P. A., Pawson, S., Pitari, G., Plummer, D. A., Rozanov, E., Schraner, M., Shepherd, T. G., Shibata, K., Stolarski, R. S., Struthers, H., Tian, W., and Yoshiki, M.: Assessment of temperature, trace species and ozone in chemistry-climate simulations of the recent past, J. Geophys. Res., 111(D22), D22308, doi:10.1029/2006JD007327, 2006.

Eyring, V., Waugh, D. W., Bodeker, G. E., Cordero, E., Akiyoshi, H., Austin, J., Beagley, S. R., Boville, B. A., Braesicke, P., Brühl, C., Butchart, N., Chipperfield, M. P., Dameris, M., Deckert, R., Deushi, M., Frith, S. M., Garcia, R. R., Gettelman, A., Giorgetta, M. A., Kinnison, D. E., Mancini, E., Manzini, E., Marsh, D. R., Matthes, S., Nagashima, T., Newman, P. A., Nielsen, J. E.,

Pawson, S., Pitari, G., Plummer, D. A., Rozanov, E., Schraner, M., Scinocca, J. F., Semeniuk, K., Shepherd, T. G., Shibata, K., Steil, B., Stolarski, R. S., Tian, W., and Yoshiki, M.: Multimodel projections of stratospheric ozone in the 21st century, J. Geophys. Res., 112(D16), D16303, doi: 10.1029/2006JD008332, 2007.

Fabry, C. and Buisson, H.: Étude de l'extrémité ultra-violette du spectre solaire, J. Physique, 3, 197–226, 1921.

Fahey, D. W. and Ravishankara, A. R.: Summer in the stratosphere, Science, 285, 208–210, 1999.

Fahey, D. W., Kelly, K. K., Kawa, S. R., Tuck, A. F., Loewenstein, M., Chan, K. R., and Heid, L. E.: Observations of denitrification and dehydration in the winter polar stratosphere, Nature, 344, 321–324, 1990.

Fahey, D. W., Kawa, S. R., Woodbridge, E. L., Tin, P., Wilson, J. C., Jonsson, H. H., Dye, J. E., Baumgardner, D., Borrmann, S., and Toohey, D. W.: In situ measurements constraining the role of sulphate aerosols in mid-latitude ozone depletion, Nature, 363, 509–514, 1993.

Fahey, D. W., Gao, R. S., Carslaw, K. S., Kettleborough, J., Popp, P. J., Northway, M. J., Holecek, J. C., Ciciora, S. C., McLaughlin, R. J., Thompson, T. L., Winkler, R. H., Baumgardner, D. G., Gandrud, B., Wennberg, P. O., Dhaniyala, S., McKinley, K., Peter, T., Salawitch, R. J., Bui, T. P., Elkins, J. W., Webster, C. R., Atlas, E. L., Jost, H., Wilson, J. C., Herman, R. L., Kleinböhl, A., and von König, M.: The detection of large HNO_3-containing particles in the winter Arctic stratosphere, Science, 291, 1026–1031, 2001.

Farman, J. C.: Measurements of total ozone using Dobson spectrometers: Some comments on their history, Planet. Space Sci., 37(12), 1601–1604, 1989.

Farman, J. C., Gardiner, B. G., and Shanklin, J. D.: Large losses of total ozone in Antarctica reveal seasonal ClO_x/NO_x interaction, Nature, 315, 207–210, 1985a.

Farman, J. C., Murgatroyd, R. J., Silnickas, A. M., and Thrush, B. A.: Ozone photochemistry in the Antarctic stratosphere in summer, Q. J. R. Meteorol. Soc., 111, 1013–1025, 1985b.

Farman, J. C., O'Neill, A., and Swinbank, R.: The dynamics of the Arctic polar vortex during the EASOE campaign, Geophys. Res. Lett., 21, 1195–1198, 1994.

Farmer, C. B., Toon, G. C., Schaper, P. W., Blavier, J.-F., and Lowes, L. L.: Stratospheric trace gases in the spring 1986 Antarctic atmosphere, Nature, 329, 126–130, 1987.

Feck, T., Grooß, J.-U., and Riese, M.: Sensitivity of Arctic ozone loss to stratospheric H_2O, Geophys. Res. Lett., 35, L01803, doi:10.1029/2007GL031334, 2008.

Fisher, M., O'Neill, A., and Sutton, R.: Rapid descent of mesospheric air into the stratospheric polar vortex, Geophys. Res. Lett., 20, 1267–1270, 1993.

Fortuin, J. P. F. and Kelder, H.: An ozone climatology based on ozonesonde and satellite measurements, J. Geophys. Res., 103, 31 709–31 734, 1998.

Friedl-Vallon, F., Maucher, G., Kleinert, A., Lengel, A., Keim, C., Oelhaf, H., Fischer, H., Seefeldner, M., and Trieschmann, O.: Design and characterization of the balloon-borne Michelson Interferometer for Passive Atmospheric Sounding (MIPAS-B2), Appl. Opt., 43, 3335–3355, 2004.

Fueglistaler, S., Buss, S., Luo, B. P., Wernli, H., Flentke, H., Hostetler, C., Poole, L. R., Carslaw, K. S., and Peter, T.: Detailed modeling of mountain wave PSCs, Atmos. Chem. Phys., 3, 697–712, 2003.

Funke, B., López-Puertas, M., Gil-López, S., von Clarmann, T., Stiller, G. P., Fischer, H., and Kellmann, S.: Downward transport of upper atmospheric NO_x into the polar stratosphere and

lower mesosphere during the Antarctic 2003 and Arctic 2002/2003 winters, J. Geophys. Res., 110, D24308, doi:10.1029/2005JD006463, 2005.

Funke, B., López-Puertas, M., Gil-López, S., von Clarmann, T., Stiller, G., Glatthor, N., Milz, M., Höpfner, M., Kellmann, S., Linden, A., Kiefer, M. Mengistu Tsidu, G., Grabowski, U., Steck, T., Fischer, H., and Wang, D. Y.: Carbon monoxide measurements from MIPAS on ENVISAT, Geophysical Research Abstracts, 8, 10 642, 2006.

Garcia, R. R. and Solomon, S.: The effect of breaking gravity waves on the dynamics and chemical composition of the mesosphere and lower thermosphere, J. Geophys. Res., 90, 3850–3868, 1985.

Garcia, R. R., Marsh, D. R., Kinnison, D. E., Boville, B. A., and Sassi, F.: Simulation of secular trends in the middle atmosphere, 1950–2003, J. Geophys. Res., 112, D09301, doi: 10.1029/2006JD007485, 2007.

Gernandt, H.: The vertical ozone distribution above the GDR research base, Antarctica in 1985, Geophys. Res. Lett., 14(1), 84–86, 1987.

Gernandt, H., Plessing, P., Feister, U., Peters, G., and Pisch, H.: A preliminary result of the ozone observation at GDR-research base (70.77°S, 11.85°E) from May to December 1985, Mem. Nat. Inst. Polar Res. Spec. Issue, 48, 256–271, 1987.

Gillett, N. P. and Thompson, D. W. J.: Simulation of Recent Southern Hemisphere Climate Change, Sciene, 302(5643), 273–275, doi:10.1126/science.1087440, 2003.

Götz, F. W. P.: Zum Strahlungsklima des Spitzbergensommers, Gerl. Beitr. Geophys., 31, 119–154, 1931.

Götz, F. W. P. and Dobson, G. M. B.: Observations of the height of the ozone in the upper atmosphere, Proc. R. Soc. London A, 120, 251–259, 1928.

Götz, F. W. P., Dobson, G. M. B., and Meetham, A. R.: Vertical distribution of ozone in the atmosphere, Nature, 132, 281, 1933.

Goutail, F., Pommereau, J.-P., Lefèvre, F., Roozendael, M. V., Andersen, S. B., Kåstad-Høiskar, B.-A., Dorokhov, V., Kyrö, E., Chipperfield, M. P., and Feng, W.: Early unusual ozone loss during the Arctic winter 2002/2003 compared to other winters, Atmos. Chem. Phys., 5, 665–677, 2005.

Greenblatt, J. B., Jost, H.-J., Loewenstein, M., Podolske, J. R., Bui, T. P., Hurst, D. F., Elkins, J. W., Herman, R. L., Webster, C. R., Schauffler, S. M., Atlas, E. L., Newman, P. A., Lait, L. L., Müller, M., Engel, A., and Schmidt, U.: Defining the polar vortex edge from an N_2O:potential temperature correlation, J. Geophys. Res., 107, 8268, doi:10.1029/2001JD000575, 2002.

Grooß, J.-U. and Russell, J. M.: Technical note: A stratospheric climatology for O_3, H_2O, CH_4, NO_x, HCl and HF derived from HALOE measurements, Atmos. Chem. Phys., 5, 2797–2807, 2005.

Grooß, J.-U., Müller, R., Becker, G., McKenna, D. S., and Crutzen, P. J.: The upper stratospheric ozone budget: An update of calculations based on HALOE data, J. Atmos. Chem., 34, 171–183, 1999.

Grooß, J.-U., Günther, G., Müller, R., Konopka, P., Bausch, S., Schlager, H., Voigt, C., Volk, C. M., and Toon, G. C.: Simulation of denitrification and ozone loss for the Arctic winter 2002/2003, Atmos. Chem. Phys., 5, 1437–1448, 2005.

Grooß, J.-U., Müller, R., Konopka, P., Steinhorst, H.-M., Engel, A., Möbius, T., and Volk, C. M.: The impact of transport across the polar vortex edge on Match ozone loss estimates, Atmos. Chem. Phys., 8, 565–578, 2008.

Groves, K. S. and Tuck, A. F.: Simultaneous effects of CO_2 and chlorofluoromethanes on strato-

spheric ozone, Nature, 280, 127–129, doi:10.1038/280127a0, 1979.

Groves, K. S., Mattingly, S. R., and Tuck, A. F.: Increased atmospheric carbon dioxide and stratospheric ozone, Nature, 273, 711–715, doi:10.1038/273711a0, 1978.

Günther, G., Müller, R., von Hobe, M., Stroh, F., Konopka, P., and Volk, C. M.: Quantification of transport across the boundary of the lower stratospheric vortex during Arctic winter 2002/2003, Atmos. Chem. Phys., 8(13), 3655–3670, 2008.

Gushchin, G. P.: History of development of the ozonometric network in Russia, Izv. A. N. Fiz. Atmos. Ok., 31(1), 6, (English translation, Atmos. Ocean. Phys., June 1995), 1995.

Haagen-Smit, A. H.: Chemistry and physiology of the Los Angeles photochemical smog, Ind. Eng. Chem., 44(6), 1342–1346, 1952.

Haigh, J. D. and Pyle, J. A.: A two-dimensional calculation including atmospheric carbon dioxide and stratospheric ozone, Nature, 279, 222–224, doi:10.1038/279222a0, 1979.

Hampson, J.: Photochemical behaviour of the ozone layer, Tech. rep., Canadian Armament Research and Development Establishment, CARDE technical note 1627, 1964.

Hanson, D. R. and Ravishankara, A. R.: The reaction probabilities of $ClONO_2$ and N_2O_5 on 40 to 75% sulfuric acid solutions, J. Geophys. Res., 96, 17 307–17 314, 1991.

Hanson, D. R., Ravishankara, A. R., and Solomon, S.: Heterogeneous reactions in sulfuric acid aerosols: A framework for model calculations, J. Geophys. Res., 99, 3615–3629, 1994.

Harris, N., Hudson, R., and Phillips, C., eds.: Assessment of Trends in the Vertical Distribution of Ozone, SPARC Report No. 1, WMO, 1998.

Harris, N. R. P., Farman, J. C., and Fahey, D. W.: Comment on "Effects of cosmic rays on atmospheric chlorofluorocarbon dissociation and ozone depletion", Phys. Rev. Lett., 89, 219801, 2002a.

Harris, N. R. P., Rex, M., Goutail, F., Knudsen, B. M., Manney, G. L., Müller, R., and von der Gathen, P.: Comparison of empirically derived ozone loss rates in the Arctic vortex, J. Geophys. Res., 107(D20), 8264, doi:10.1029/2001JD000482, 2002b.

Hartley, W. N.: On the absorption spectrum of ozone, J. Chem. Soc., 39, 57–60, 1881.

Harvey, V. L., Pierce, R. B., Fairlie, T. D., and Hitchman, M. H.: A climatology of stratospheric polar vortices and anticyclones, J. Geophys. Res., 107(D20), 4442, doi:10.1029/2001JD001471, 2002.

Hays, P. B. and Olivero, J. J.: Carbon dioxide and monoxide above the troposphere, Planet. Space Sci., 18(12), 1729–1733, 1970.

Heath, D. F., Krueger, A. J., and Crutzen, P. J.: Solar Proton Event: Influence on Stratospheric Ozone, Science, 197(4306), 886–889, doi:10.1126/science.197.4306.886, 1977.

Hegglin, M. I. and Shepherd, T. G.: O_3-N_2O correlations from the Atmospheric Chemistry Experiment: Revisiting a diagnostic of transport and chemistry in the stratosphere, J. Geophys. Res., D19301, doi:10.1029/2006JD008281, 2007.

Hoffmann, L., Kaufmann, M., Spang, R., Müller, R., Volk, C. M., and Riese, M.: Envisat MIPAS measurements of CFC-11: Retrieval, validation, and climatology, Atmos. Chem. Phys., 8, 3671–3688, 2008.

Hofmann, D. J. and Solomon, S.: Ozone destruction through heterogeneous chemistry following the eruption of El Chichón, J. Geophys. Res., 94(D4), 5029–5041, 1989.

Hofmann, D. J., Harder, J. W., Rolf, S. R., and Rosen, J. M.: Balloonborne observations of the temporal development and vertical structure of the Antarctic ozone hole in 1986, Nature, 326, 59–62, 1987.

Hofmann, D. J., Deshler, T. L., Aimedieu, P., Matthews, W. A., Johnston, P. V., Kondo, Y., Byrne, W. R. S. G. J., and Benbrook, J. R.: Stratospheric clouds and ozone depletion in the Arctic during January 1989, Nature, 340, 117–121, 1989.

Holton, J. R.: An advective model for two-dimensional transport of stratospheric trace species, J. Geophys. Res., 86(C12), 11 989–11 994, 1981.

Holton, J. R., Haynes, P., McIntyre, M. E., Douglass, A. R., Rood, R. B., and Pfister, L.: Stratosphere-troposphere exchange, Rev. Geophys., 33, 403–439, 1995.

Hoor, P., Fischer, H., Lange, L., Lelieveld, J., and Brunner, D.: Seasonal variations of a mixing layer in the lowermost stratosphere as identified by the CO-O_3 correlation from in situ measurements, J. Geophys. Res., 107(D5), 4044, doi:10.1029/2000JD000289, 2002.

Hoppel, K., Bevilacqua, R., Allen, D., Nedoluha, G., and Randall, C.: POAM III Observations of the anomalous 2002 Antarctic ozone hole, Geophys. Res. Lett., 30(7), 1394, doi:10.1029/2002GL016899, 2003.

Huck, P. E., Tilmes, S., Bodeker, G. E., Randel, W. J., McDonald, A. J., and Nakajima, H.: An improved measure of ozone depletion in the Antarctic stratosphere, J. Geophys. Res., 112, D1110, doi:10.1029/2006JD007860, 2007.

Huret, N., Pirre, M., Hauchecorne, A., Robert, C., and Catoire, V.: On the vertical structure of the stratosphere at midlatitudes during the first stage of the polar vortex formation and in the polar region in the presence of a large mesospheric descent, J. Geophys. Res., D06111, doi:10.1029/2005JD0067102, 2006.

IPCC/TEAP: Special Report on Safeguarding the Ozone Layer and the Global Climate System: Issues Related to Hydrofluorocarbons and Perfluorocarbons, Cambridge University Press, Cambridge, United Kingdom, and New York, NY, USA, edited by B. Metz, L. Kuijpers, S. Solomon, S. O. Andersen, O. Davidson, J. Pons, D. de Jager, T. Kestin, M. Manning and L. Meyer, 2005.

Iwasaka, Y. and Kondoh, K.: Depletion of Antarctic ozone: Height of ozone loss region and its temporal changes, Geophys. Res. Lett., 14(1), 87–90, 1987.

Jackman, C. H., Deland, M. T., Labow, G. J., Fleming, E. L., and López-Puertas, M.: Satellite measurements of middle atmospheric impacts by solar proton events in solar cycle 23, Space Sci. Rev., 125(1-4), 381–391, 2006.

Jánosi, I. M. and Müller, R.: Empirical mode decomposition and correlation properties of long daily ozone records, Phys. Rev. E, 71, 056 126, 2005.

Johnston, H.: Reduction of stratospheric ozone by nitrogen oxide catalysts from supersonic transport exhaust, Science, 173, 517–522, 1971.

Jones, A. E. and Shanklin, J. D.: Continued decline of total ozone over Halley, Antarctica, since 1985, Nature, 376, 409–411, 1995.

Jost, H.-J., Loewenstein, M., Greenblatt, J. G., Podolske, J. R., Bui, T. P., Hurst, D. F., Elkins, J. W., Herman, R. L., Webster, C. R., Schauffler, S. M., Atlas, E. L., Newman, P. A., Lait, L., and Wofsy, S. C.: Mixing events revealed by anomalous tracer relationships in the Arctic vortex during winter 1999/2000, J. Geophys. Res., 107, 4795, doi:10.1029/2002JD002380, 2002.

Jung, T. and Leutbecher, M.: Performance of the ECMWF forecasting system in the Arctic during

winter, Q. J. R. Meteorol. Soc., 133, 1327–1340, doi:10.1002/qj.99, 2007.

Kahlbaum, G. W. A. and Thon, E., eds.: Justus von Liebig und Christian Friedrich Schönbein. Briefwechsel 1853–1868, Johann Ambrosius Barth, 1900.

Kawa, S. R., Bevilacqua, R. M., Margitan, J. J., Douglass, A. R., Schoeberl, M. R., Hoppel, K. W., and Sen, B.: Interaction between dynamics and chemistry of ozone in the setup phase of the Northern Hemisphere polar vortex, J. Geophys. Res., 107, 8310, doi:10.1029/2001JD001527, [printed *108*(D5), 2003], 2002.

Keeley, S. P. E., Gillett, N. P., Thompson, D. W. J., Solomon, S., and Forster, P. M.: Is Antarctic climate most sensitive to ozone depletion in the middle or lower stratosphere?, Geophys. Res. Lett., 34, L22812, doi:10.1029/2007GL031238, 2007.

Kelly, K. K., Tuck, A. F., Murphy, D. M., Proffitt, M. H., Fahey, D. W., Jones, R. L., McKenna, D. S., Loewenstein, M., Podolske, J. R., Strahan, S. E., Ferry and K. R. Chan and J. F. Vedder, G. V., Gregory, G. L., Hypes, W. D., McCormick, M. P., Browell, E. V., and Heidt, L. E.: Dehydration in the lower Antarctic stratosphere during late winter and early spring, 1987, J. Geophys. Res., 94, 11 317–11 357, 1989.

Khosrawi, F., Müller, R., Irie, H., Engel, A., Toon, G. C., Sen, B., Aoki, S., Nakazawa, T., Traub, W. A., Jucks, K. W., Johnson, D. G., Oelhaf, H., Wetzel, G., Sugita, T., Kanzawa, H., Yokota, T., Nakajima, H., and Sasano, Y.: Validation of CFC-12 measurements from the Improved Limb Atmospheric Spectrometer (ILAS) with the Version 6.0 retrieval algorithm, J. Geophys. Res., 109, D06311, doi:10.1029/2003JD004325, 2004a.

Khosrawi, F., Müller, R., Proffitt, M., and Nakajima, H.: Monthly averaged ozone and nitrous oxide from the Improved Limb Atmospheric Spectrometer (ILAS) in the Northern and Southern Hemisphere polar regions, J. Geophys. Res., 109, D10301, doi:10.1029/2003JD004365, 2004b.

Khosrawi, F., Müller, R., Proffitt, M. H., and Nakajima, H.: Monthly averages of nitrous oxide and ozone for the Northern and Southern Hemisphere high latitudes: A "1-year climatology" derived from ILAS/ILAS-II observations, J. Geophys. Res., 111, D11S11, doi:10.1029/2005JD006384, 2006.

Kiendler, A., Matejcik, S., Skalny, J. D., Stamatovic, and Mark, T. D.: Dissociative electron attachment to CF_2Cl_2 using a high-resolution crossed-beams technique, J. Phys. B, 29, 6217–6225, 1996.

Kiss, P., Müller, R., and Jánosi, I. M.: Long-range correlations of extrapolar total ozone are determined by the global atmospheric circulation, Nonlin. Processes Geophys., 14, 435–442, 2007.

Konopka, P., Grooß, J.-U., Bausch, S., Müller, R., McKenna, D. S., Morgenstern, O., and Orsolini, Y.: Dynamics and chemistry of vortex remnants in late Arctic spring 1997 and 2000: Simulations with the Chemical Lagrangian Model of the Stratosphere (CLaMS), Atmos. Chem. Phys., 3, 839–849, 2003.

Konopka, P., Steinhorst, H.-M., Grooß, J.-U., Günther, G., Müller, R., Elkins, J. W., Jost, H.-J., Richard, E., Schmidt, U., Toon, G., and McKenna, D. S.: Mixing and Ozone Loss in the 1999-2000 Arctic Vortex: Simulations with the 3-dimensional Chemical Lagrangian Model of the Stratosphere (CLaMS), J. Geophys. Res., 109, D02315, doi:10.1029/2003JD003792, 2004.

Konopka, P., Grooß, J.-U., Hoppel, K. W., Steinhorst, H.-M., and Müller, R.: Mixing and chemical ozone loss during and after the Antarctic polar vortex major warming in September 2002, J. Atmos. Sci., 62(3), 848–859, 2005a.

Konopka, P., Günther, G., McKenna, D. S., Müller, R., Offermann, D., Spang, R., and Riese, M.: How homogeneous and isotropic is stratospheric mixing? Comparison of CRISTA-1 observations with transport studies based on the Chemical Lagrangian Model of the Stratosphere (CLaMS), Q. J. R. Meteorol. Soc., 131(606), 565–579, doi:10.1256/qj.04.47, 2005b.

Konopka, P., Engel, A., Funke, B., Müller, R., Grooß, J.-U., Günther, G., Wetter, T., Stiller, G., von Clarmann, T., Glatthor, N., Oelhaf, H., Wetzel, G., López-Puertas, M., Pirre, M., Huret, N., and Riese, M.: Ozone loss driven by nitrogen oxides and triggered by stratospheric warmings may outweigh the effect of halogens, J. Geophys. Res., 112, D05105, doi:10.1029/2006JD007064, 2007a.

Konopka, P., Günther, G., Müller, R., dos Santos, F. H. S., Schiller, C., Ravegnani, F., Ulanovsky, A., Schlager, H., Volk, C. M., Viciani, S., Pan, L. L., McKenna, D.-S., and Riese, M.: Contribution of mixing to upward transport across the tropical tropopause layer (TTL), Atmos. Chem. Phys., 7, 3285–3308, 2007b.

Koppmann, R., Johnen, F. J., Plass-Dülmer, C., and Rudolph, J.: Distribution of methylchloride, dichloromethane, trichloroethene and tetrachloroethene over the North and South Atlantic, J. Geophys. Res., 98, 20 517–20 526, 1993.

Kouker, W., Beck, A., Fischer, H., and Petzoldt, K.: Downward transport in the upper stratosphere during the minor warming in February 1979, J. Geophys. Res., 100(D6), 11 069–11 084, 1995.

Krämer, M., Müller, R. I., Bovensmann, H., Burrows, J., Brinkmann, J., Röth, E. P., Grooß, J. U., Müller, R. O., Woyke, T. H., Ruhnke, R., Günther, G., Hendricks, J., Lippert, E., Carslaw, K. S., Peter, T., Zieger, A., Brühl, C. H., Steil, B., Lehmann, R., and McKenna, D. S.: Intercomparison of stratospheric chemistry models under polar vortex conditions, J. Atmos. Chem., 45, 51–77, doi:10.1023/A:1024056026432, 2003.

Kreher, K., Keys, J. G., Johnston, P. V., Platt, U., and Liu, X.: Ground-based measurements of OClO and HCl in austral spring 1993 at Arrival Heights, Antarctica, Geophys. Res. Lett., 23(12), 1545–1548, 1996.

Lambert, P., Déjardin, G., and Chalonge, D.: Sur l'extrémité ultraviolette du spectre solaire et la couche d'ozone de la haute atmosphère, Comp. Rend. Hebd. Acad. Sci., 183, 800–801, 1926.

Lefèvre, F., Bertaux, J.-L., Clancy, R. T., Encrenaz, T., Fast, K., Forget, F., Lebonnois, S., Montmessin, F., and Perrier, S.: Heterogeneous chemistry in the atmosphere of Mars, Nature, pp. 971–975, doi:doi:10.1038/nature07116, 2008.

Lemmen, C., Dameris, M., Müller, R., and Riese, M.: Chemical ozone loss in a chemistry-climate model from 1960 to 1999, Geophys. Res. Lett., 33(15), L15820, doi:10.1029/2006GL026939, 2006a.

Lemmen, C., Müller, R., Konopka, P., and Dameris, M.: Critique of the tracer-tracer correlation technique and its potential to analyse polar ozone loss in chemistry-climate models, J. Geophys. Res., 111(D18), D18307, doi:10.1029/2006JD007298, 2006b.

Lender: Das atmosphärische Ozon, nach Messungen in Marienbad, Kissingen, Mentone, Meran und Wiesbaden, Separat-Abdruck aus Göschen's „Deutscher Klinik" No. 19, G. Reimer, Berlin, 1872.

Lender: Atmosphärisches Ozon, II. Theil, Separat-Abdruck aus Göschen's „Deutscher Klinik", G. Reimer, Berlin, 1873.

Lipson, J. B., Elrond, M. J., Beiderhase, T. W., Molina, L. T., and Molina, M. J.: Temperature dependence of the rate constant and branching ratio for the OH + ClO reaction, J. Chem. Soc.,

Faraday Trans., 93, 2665–2673, 1997.

Loewenstein, M., Podolske, J. R., and Chan, K. R.: N_2O as a dynamical tracer in the Arctic vortex, Geophys. Res. Lett., 17(4), 477–480, 1990.

Loewenstein, M., Jost, H., Grose, J., Eilers, J., Lynch, D., Jensen, S., and Marmie, J.: Argus: A new instrument for the measurement of the stratospheric dynamical tracers, N_2O and CH_4, Spectrochimica Acta Part A-Molecular and Biomolecular Spectroscopy, 58(11), 2329–2345, 2002.

London, J. and Liu, S.: Long-term tropospheric and lower stratospheric ozone variations from ozonesonde observations, J. Atmos. Terr. Phys., 54(5), 599–625, 1992.

López-Puertas, M., Funke, B., Gil-López, S., von Clarmann, T., Stiller, G. P., Höpfner, M., Kellmann, S., Fischer, H., and Jackman, C. H.: Observation of NO_x enhancement and ozone depletion in the Northern and Southern hemispheres after the October–November 2003 Solar Proton Events, J. Geophys. Res., 110, doi:10.1029/2005JA01105, 2005.

Lu, Q.-B.: Correlation between cosmic rays and ozone depletion, Phys. Rev. Lett., 102, 118501, 2009.

Lu, Q.-B.: Cosmic-ray-driven electron-induced reactions of halogenated molecules adsorbed on ice surfaces: Implications for atmospheric ozone depletion and global climate change, Phys. Rep., 487(5), 141–167, 2010.

Lu, Q.-B. and Madey, T. E.: Negative-Ion Enhancements in Electron-Stimulated Desorption of CF_2Cl_2 Coadsorbed with Nonpolar and Polar Gases on Ru(0001), Phys. Rev. Lett., 82(20), 4122–4125, doi:10.1103/PhysRevLett.82.4122, 1999.

Lu, Q.-B. and Sanche, L.: Effects of cosmic rays on atmospheric chloroflurocarbon dissociation and ozone depletion, Phys. Rev. Lett., 87, 078501, 2001a.

Lu, Q.-B. and Sanche, L.: Large enhancements in dissociative electron attachement to HCl adsorbed on H_2O ice via transfer of presolvated electrons, J. Chem. Phys., 115, 5711–5713, 2001b.

Lu, Q.-B. and Sanche, L.: Comment on "Effects of cosmic rays on atmospheric chlorofluorocarbon dissociation and ozone depletion" - Reply, Phys. Rev. Lett., 89, 219802, 2002a.

Lu, Q.-B. and Sanche, L.: Comment on "Effects of cosmic rays on atmospheric chlorofluorocarbon dissociation and ozone depletion" - Reply, Phys. Rev. Lett., 89, 219804, 2002b.

Lu, Q.-B., Baskin, J. S., and Zewail, A. H.: The presolvated electron in water: Can it be scavenged at long range?, J. Phys. Chem. B, 108(29), 10 509–10 514, 2004.

Mahlman, J. D., Levy II, H., and Moxim, W. J.: Three-dimensional simulations of stratospheric N_2O: Predictions for other trace constituents, J. Geophys. Res., 91, 2687–2707, 1986.

Manney, G. L., Michelsen, H. A., Santee, M. L., Gunson, M. R., Irion, F. W., Roche, A. E., and Livesey, N. J.: Polar vortex dynamcis during spring and fall diagnosed using trace gas observations from the Atmospheric Trace Molecule Spectroscopy instument, J. Geophys. Res., 104, 18 841–18 866, 1999.

Manney, G. L., Krüger, K., Sabutis, J. L., Amina Sena, S., and Pawson, S.: The remarkable 2003-2004 winter and other recent warm winters in the Arctic stratosphere in the late 1990s, J. Geophys. Res., 110, D04107, doi:10.1029/2004JD005367, 2005.

Manney, G. L., Santee, M. L., Livesey, N. J., Froidevaux, L., Read, W. G., Pumphrey, H. C., Waters, J. W., and Pawson, S.: EOS Microwave Limb Sounder observations of the Antarctic polar vortex breakup in 2004, Geophys. Res. Lett., 32(12), L12811, 2005.

Manney, G. L., Santee, M. L., Froidevaux, L., Hoppel, K., Livesey, N. J., and Waters, J. W.: EOS

MLS observations of ozone loss in the 2004-2005 Arctic winter, Geophys. Res. Lett., 33, L04802, doi:10.1029/2005GL024494, 2006.

Manney, G. L., Daffer, W. H., Zawodny, J. M., Bernath, P. F., Hoppel, K. W., Walker, K. A., Knosp, B. W., Boone, C., Remsberg, E. E., Santee, M. L., Harvey, V. L., Pawson, S., Jackson, D. R., Deaver, L., McElroy, C. T., McLinden, C. A., Drummond, J. R., Pumphrey, . H. C., Lambert, A., Schwartz, M. J., Froidevaux, L., McLeod, S., Takacs, L. L., Suarez, M. J., Trepte, C. R., Cuddy, D. C., Livesey, N. J., Harwood, R. S., , and Waters, J. W.: Solar occultation satellite data and derived meteorological products: Sampling issues and comparisons with Aura Microwave Limb Sounder, J. Geophys. Res., 112, D24S50, doi:10.1029/2007JD008709, 2007.

McElroy, M. B., Salawitch, R. J., Wofsy, S. C., and Logan, J. A.: Antarctic ozone: Reductions due to synergistic interactions of chlorine and bromine, Nature, 321, 759–762, 1986.

McKenna, D. S., Jones, R. L., Poole, L. R., Solomon, S., Fahey, D. W., Kelly, K. K., Proffitt, M. H., Brune, W. H., Loewenstein, M., and Chan, K. R.: Calculations of ozone destruction during the 1988/89 Arctic winter, Geophys. Res. Lett., 17(17), 553–556, doi:10.1029/90GL00048, 1990.

McKenna, D. S., Grooß, J.-U., Günther, G., Konopka, P., Müller, R., Carver, G., and Sasano, Y.: A new Chemical Lagrangian Model of the Stratosphere (CLaMS): 2. Formulation of chemistry scheme and initialization, J. Geophys. Res., 107(D15), 4256, doi:10.1029/2000JD000113, 2002a.

McKenna, D. S., Konopka, P., Grooß, J.-U., Günther, G., Müller, R., Spang, R., Offermann, D., and Orsolini, Y.: A new Chemical Lagrangian Model of the Stratosphere (CLaMS): 1. Formulation of advection and mixing, J. Geophys. Res., 107(D16), 4309, doi:10.1029/2000JD000114, 2002b.

Michelsen, H. A., Manney, G. L., Gunson, M. R., and Zander, R.: Correlations of stratospheric abundances of NO_y, O_3, N_2O, and CH_4 derived from ATMOS measurements, J. Geophys. Res., 103, 28 347–28 359, 1998.

Miller, A. J., Flynn, L. E., Hollandsworth, S. M., DeLuisi, J. J., Petropavlovskikh, I. V., Tiao, G. C., Reinsel, G. C., Wuebbles, D. J., Kerr, J., Nagatani, R. M., Bishop, L., and Jackman, C. H.: Information content of Umkehr and solar backscattered ultraviolet (SBUV) 2 satellite data for ozone trends and solar responses in the stratosphere, J. Geophys. Res., 102, 19 257–19 263, 1997.

Molina, L. T. and Molina, M. J.: Production of Cl_2O_2 from the selfreaction of the ClO radical, J. Phys. Chem., 91, 433–436, 1987.

Molina, M. J. and Rowland, F. S.: Stratospheric sink for chlorofluoromethanes : chlorine atom catalysed destruction of ozone, Nature, 249, 810–812, 1974.

Müller, R.: The performance of classical versus modern finite-volume advection schemes for atmospheric modelling in a one-dimensional test-bed, Mon. Wea. Rev., 120, 1407–1415, 1992.

Müller, R.: Impact of cosmic rays on stratospheric chlorine chemistry and ozone depletion, Phys. Rev. Lett., 91, 058502, 2003.

Müller, R.: Comment on: "Resonant dissociative electron transfer of the presolvated electron to CCl_4 in liquid: Direct observation and lifetime of the $CCl_4^{\star-}$ transition state" [JCP 128, 041102 (2008)], J. Chem. Phys., 129, 027101, 2008.

Müller, R.: A brief history of stratospheric ozone research, Meteorol. Z., 18, 3–24, doi: 10.1127/0941-2948/2009/353, 2009.

Müller, R. and Crutzen, P. J.: A possible role of galactic cosmic rays in chlorine activation during polar night, J. Geophys. Res., 98, 20 483–20 490, 1993.

Müller, R. and Grooß, J.-U.: Does cosmic-ray-induced heterogeneous chemistry influence strato-

spheric polar ozone loss?, Phys. Rev. Lett., 103, 228501, 2009.

Müller, R. and Tilmes, S.: Comment on "Middle atmospheric O_3, CO, N_2O, HNO_3, and temperature profiles during the warm Arctic winter 2001–2002" by Giovanni Muscari et al., J. Geophys. Res., 113, D18303, doi:10.1029/2007JD009709, 2008.

Müller, R., Crutzen, P. J., Oelhaf, H., Adrian, G. P., v. Clarmann, T., Wegner, A., Schmidt, U., and Lary, D.: Chlorine chemistry and the potential for ozone depletion in the Arctic stratosphere in the winter of 1991/92, Geophys. Res. Lett., 21, 1427–1430, 1994.

Müller, R., Crutzen, P. J., Grooß, J.-U., Brühl, C., Russell III, J. M., and Tuck, A. F.: Chlorine activation and ozone depletion in the Arctic vortex: Observations by the Halogen Occultation Experiment on the Upper Atmosphere Research Satellite, J. Geophys. Res., 101, 12 531–12 554, 1996.

Müller, R., Crutzen, P. J., Grooß, J.-U., Brühl, C., Russell III, J. M., Gernandt, H., McKenna, D. S., and Tuck, A. F.: Severe chemical ozone loss in the Arctic during the winter of 1995-96, Nature, 389, 709–712, 1997.

Müller, R., Grooß, J.-U., McKenna, D. S., Crutzen, P. J., Brühl, C., Russell, J. M., Gordley, L. L., Burrows, J. P., and Tuck, A. F.: Chemical ozone loss in the Arctic vortex in the winter 1995-1996: HALOE measurements in conjunction with other observations, Ann. Geophys., 17, 101–114, 1999.

Müller, R., Schmidt, U., Engel, A., McKenna, D. S., and Proffitt, M. H.: The O_3–N_2O relationship from balloon-borne observations as a measure of Arctic ozone loss in 1991/92, Q. J. R. Meteorol. Soc., 127, 1389–1412, 2001.

Müller, R., Tilmes, S., Grooß, J.-U., McKenna, D. S., Müller, M., Schmidt, U., Toon, G. C., Stachnik, R. A., Margitan, J. J., Elkins, J. W., Arvelius, J., and Russell III, J. M.: Chlorine activation and chemical ozone loss deduced from HALOE and balloon measurements in the Arctic during the winter of 1999-2000, J. Geophys. Res., 107, 8302, doi:10.1029/2001JD001423, [printed *108*(D5), 2003], 2002.

Müller, R., Tilmes, S., Konopka, P., Grooß, J.-U., and Jost, H.-J.: Impact of mixing and chemical change on ozone-tracer relations in the polar vortex, Atmos. Chem. Phys., 5, 3139–3151, 2005.

Müller, R., Tilmes, S., Grooß, J.-U., Engel, A., Oelhaf, H., Wetzel, G., Huret, N., Pirre, M., Catoire, V., Toon, G., and Nakajima, H.: Impact of mesospheric intrusions on ozone–tracer relations in the stratospheric polar vortex, J. Geophys. Res., 112, D23307, doi:10.1029/2006JD008315, 2007.

Müller, R., Grooß, J.-U., Lemmen, C., Heinze, D., Dameris, M., and Bodeker, G.: Simple measures of ozone depletion in the polar stratosphere, Atmos. Chem. Phys., 8(2), 251–264, 2008.

Muscari, G. and de Zafra, R. L.: Reply to comment by Rolf Müller and Simone Tilmes on "Middle atmospheric O_3, CO, N_2O, HNO_3, and temperature profiles during the warm Arctic winter 2001–2002", J. Geophys. Res., in press, 2008.

Muscari, G., Santee, M. L., and de Zafra, R. L.: Intercomparison of stratospheric HNO_3 measurements over Antarctica: Ground-based millimeter-wave versus UARS/MLS Version 5 retrievals, J. Geophys. Res., 107(D24), 4809, doi:10.1029/2002JD002546, 2002.

Muscari, G., di Sarra, A. G., de Zafra, R. L., Lucci, F., Baordo, F., Angelini, F., and Fiocco, G.: Middle atmospheric O_3, CO, N_2O, HNO_3, and temperature profiles during the warm Arctic winter 2001–2002, J. Geophys. Res., D14304, doi:10.1029/2006JD007849, 2007.

Nakajima, H.: Preface to special section on ILAS-II: The Improved Limb Atmospheric

Spectrometer–II, J. Geophys. Res., 111, D20S90, doi:10.1029/2006JD007412, 2006.

Nakajima, H., Sugita, T., Yokota, T., Ishigaki, T., Mogi, Y., Araki, N., Waragai, K., Kimura, N., Iwazawa, T., Kuze, A., Tanii, J., Kawasaki, H., Horikawa, M., Togami, T., Uemura, N., Kobayashi, H., and Sasano, Y.: Characteristics and performance of the Improved Limb Atmospheric Spectrometer-II (ILAS-II) on board the ADEOS-II satellite, J. Geophys. Res., 111, D11S01, doi:10.1029/2005JD006334, 2006.

Nakayama, N., Wilson, S. C., Stadelmann, L. E., Lee, H.-L. D., Cable, C. A., and Arumainayagam, C. R.: Low-Energy Electron-Induced Chemistry of CF_2Cl_2: Implications for the Ozone Hole?, J. Phys. Chem. B, 108, 7950–7954, doi:10.1021/jp031319j, 2004.

Nash, E. R., Newman, P. A., Rosenfield, J. E., and Schoeberl, M. R.: An objective determination of the polar vortex using Ertel's potential vorticity, J. Geophys. Res., 101, 9471–9478, 1996.

New York Times, 27 June: The highest balloon ascension ever made, The New York Times, 1909.

Newchurch, M. J., Yang, E. S., Cunnold, D. M., Reinsel, G. C., Zawodny, J. M., and Russell, J. M.: Evidence for slowdown in stratospheric ozone loss: First stage of ozone recovery, J. Geophys. Res., 108, 4507, doi:10.1029/2003JD003471, 2003.

Newman, P. A., Gleason, F., McPeters, R., and Stolarski, R.: Anomalously low ozone over the Arctic, Geophys. Res. Lett., 24, 2689–2692, doi:10.1029/97GL52381, 1997.

Newman, P. A., Nash, E. R., Kawa, S. R., Montzka, S. A., and Schauffler, S. M.: When will the Antarctic ozone hole recover?, Geophys. Res. Lett., 33, L12814, doi:10.1029/2005GL025232, 2006.

Newman, P. A., Daniel, J. S., Waugh, D. W., and Nash, E. R.: A new formulation of equivalent effective stratospheric chlorine (EESC), Atmos. Chem. Phys., 7(17), 4537–4552, 2007.

Oelhaf, H., v. Clarmann, T., Fischer, H., Friedl-Vallon, F., Fritzsche, C., Linden, A., Piesch, C., Seefeldner, M., and Völker, W.: Stratospheric $ClONO_2$ and HNO_3 profiles inside the Arctic vortex from MIPAS-B limb emission spectra obtained during EASOE, Geophys. Res. Lett., 21, 1263–1266, doi:10.1029/93GL01303, 1994.

Ordway III, F. I., Dahm, W. K., Dannenberg, K., Haeussermann, W., Reisig, G., Stuhlinger, E., von Tiesenhausen, G., and Willhite, I.: A memoir: From Peenemünde to USA: A classic case of technology transfer, Acta Astron., 60(1), 24–47, 2007.

Osterman, G. B., Salawitch, R. J., Sen, B., Toon, G. C., Stachnik, R. A., Pickett, H. M., Margitan, J. J., and Peterson, D. B.: Balloon-borne measurements of stratospheric radicals and their precursors: Implications for the production and loss of ozone, Geophys. Res. Lett., 24, 1107–1110, doi:10.1029/97GL00921, 1997.

Paetzold, H. K. and Regener, E.: Ozon in der Erdatmosphäre, in Handbuch der Physik, edited by S. Flügge, vol. XLVIII, pp. 370–426, Springer, 1957.

Pan, L. L., Konopka, P., and Browell, E. V.: Observations and Model Simulations of Mixing near the Extratropical Tropopause, J. Geophys. Res., 111(D05106), doi:10.1029/2005JD006480, 2006.

Park, M., Randel, W. J., Emmons, L. K., Bernath, P. F., Walker, K. A., and Boone, C. D.: Chemical isolation in the Asian monsoon anticyclone observed in Atmospheric Chemistry Experiment (ACE-FTS) data, Atmos. Chem. Phys., 8(3), 757–764, 2008.

Patra, P. K. and Santhanam, M. S.: Comment on "Effects of cosmic rays on atmospheric chlorofluorocarbon dissociation and ozone depletion", Phys. Rev. Lett., 89, 219803, 2002.

Peter, T.: Microphysics and heterogeneous chemistry of polar stratospheric clouds, Ann. Rev. Phys.

Chem., 48, 785–822, 1997.

Peter, T., Müller, R., Drdla, K., Petzoldt, K., and Reimer, E.: A micro-physical box model for EASOE: preliminary results for the January/February 1990 PSC event over Kiruna, Ber. Bunsenges. Phys. Chem., 96(3), 362–367, 1992.

Plumb, R. A.: Stratospheric transport, J. Meteorol. Soc. Jpn., 80(4B), 793–809, 2002.

Plumb, R. A.: Tracer interrelationships in the stratosphere, Rev. Geophys., 45, RG4005, doi: 10.1029/2005RG000179, 2007.

Plumb, R. A. and Ko, M. K. W.: Interrelationships between mixing ratios of long-lived stratospheric constituents, J. Geophys. Res., 97, 10 145–10 156, 1992.

Plumb, R. A., Waugh, D. W., and Chipperfield, M. P.: The effect of mixing on tracer relationships in the polar vortices, J. Geophys. Res., 105, 10 047–10 062, 2000.

Pope, F. D., Hansen, J. C., Bayes, K. D., Friedl, R. R., and Sander, S. P.: Ultraviolet Absorption Spectrum of Chlorine Peroxide, ClOOCl, J. Phys. Chem. A, 111(20), 4322–4332, doi: 10.1021/jp067660w, 2007.

Prather, M. J.: More rapid ozone depletion through the reaction of HOCl with HCl on polar stratospheric clouds, Nature, 355, 534–537, 1992.

Proffitt, M. H. and McLaughlin, R. J.: Fast-response dual-beam UV absorption ozone photometer suitable for use on stratospheric balloons, Rev. Sci. Instr., 54, 1719–1728, 1983.

Proffitt, M. H., Fahey, D. W., Kelly, K. K., and Tuck, A. F.: High latitude ozone loss outside the Antarctic ozone hole, Nature, 342, 233–237, 1989.

Proffitt, M. H., Margitan, J. J., Kelly, K. K., Loewenstein, M., Podolske, J. R., and Chan, K. R.: Ozone loss in the Arctic polar vortex inferred from high altitude aircraft measurements, Nature, 347, 31–36, 1990.

Proffitt, M. H., Solomon, S., and Loewenstein, M.: Comparison of 2-D model simulations of ozone and nitrous oxide at high latitudes with stratospheric measurements, J. Geophys. Res., 97, 939–944, 1992.

Proffitt, M. H., Aikin, K., Margitan, J. J., Loewenstein, M., Podolske, J. R., Weaver, A., Chan, K. R., Fast, H., and Elkins, J. W.: Ozone loss inside the northern polar vortex during the 1991-1992 winter, Science, 261, 1150–1154, 1993.

Proffitt, M. H., Aikin, K., Tuck, A. F., Margitan, J. J., Webster, C. R., Toon, G. C., and Elkins, J. W.: Seasonally averaged ozone and nitrous oxide in the northern hemisphere lower stratosphere, J. Geophys. Res., 108, 4110, doi:10.1029/2002JD002657, 2003.

Randall, C. E., Harvey, V. L., Manney, G. L., Orsolini, Y., Codrescu, M., Sioris, C., Brohede, S., Haley, C. S., Gordley, L. L., Zawodny, J. M., and Russell, J. M.: Stratospheric effects of energetic particle precipitation in 2003-2004, Geophys. Res. Lett., 32(5), L05802, doi: 10.1029/2004GL022003, 2005.

Randall, C. E., Harvey, V. L., Singleton, C. S., Bernath, P. F., Boone, C. D., and Kozyra, J. U.: Enhanced NO_x in 2006 linked to strong upper stratospheric Arctic vortex, Geophys. Res. Lett., L18811, doi:10.1029/2006GL027160, 2006.

Randel, W. J., Wu, F., Vömel, H., Nedoluha, G. E., and Forster, P.: Decreases in stratospheric water vapor after 2001: Links to changes in the tropical tropopause and the Brewer-Dobson circulation, J. Geophys. Res., 111, D12312, doi:10.1029/2005JD006744, 2006.

Randel, W. J., Shine, K. P., Austin, J., Barnett, J., Claud, C., Gillett, N. P., Keckhut, P., Langematz,

U., Lin, R., Long, C., Mears, C., Miller, A., Nash, J., Seidel, D. J., Thompson, D. W. J., Wu, F., and Yoden, S.: An update of observed stratospheric temperature trends, J. Geophys. Res., 114, D02107, doi:10.1029/2008JD010421, 2009.

Rasch, P. J., Crutzen, P. J., and Coleman, D. B.: Exploring the geoengineering of climate using stratospheric sulfate aerosols: The role of particle size, Geophys. Res. Lett., 35, L02809, doi: 10.1029/2007GL032179, 2008.

Ray, E. A., Moore, F. L., Elkins, J. W., Hurst, D. F., Romashkin, P. A., Dutton, G. S., and Fahey, D. W.: Descent and mixing in the 1999-2000 northern polar vortex inferred from in situ tracer measurements, J. Geophys. Res., 107, 8285, doi:10.1029/2001JD000961, 2002.

Regener, E.: Über das „photochemische“ Klima der Erde, Naturwissenschaften, 33(6), 163–166, 1946.

Regener, E. and Regener, V. H.: Aufnahmen des ultravioletten Sonnenspektums in der Stratosphäre und vertikale Ozonverteilung, Phys. Z., 35, 788–793, 1934.

Rex, M., Harris, N. R. P., von der Gathen, P., Lehmann, R., Braathen, G. O., Reimer, E., Beck, A., Chipperfield, M., Alfier, R., Allaart, M., O'Connor, F., Dier, H., Dorokhov, V., Fast, H., Gil, M., Kyrö, E., Litynska, Z., Mikkelsen, I. S., Molyneux, M., Nakane, H., Notholt, J., Rummukainen, M., Viatte, P., and Wenger, J.: Prolonged stratospheric ozone loss in the 1995/96 Arctic winter, Nature, 389, 835–838, doi:10.1038/39849, 1997.

Rex, M., von der Gathen, P., Harris, N. R. P., Lucic, D., Knudsen, B. M., Braathen, G. O., Reid, S. J., De Backer, H., Claude, H., Fabian, R., Fast, H., Gil, M., Kyrö, E., Mikkelsen, I. S., Rummukainen, M., Smit, H. G., Stähelin, J., Varotsos, C., and Zaitcev, I.: In situ measurements of stratospheric ozone depletion rates in the Arctic winter 1991/92: A Lagrangian approach, J. Geophys. Res., 103, 5843–5853, 1998.

Rex, M., Salawitch, R. J., Toon, G. C., Sen, B., Margitan, J. J., Osterman, G. B., Blavier, J.-F., Gao, R. S., Donnelly, S., Keim, E., Neumann, J., Fahey, D., Webster, C. R., Scott, D. C., Herman, R. L., May, R. D., Moyer, E. J., Gunson, M. R., Irion, F. W., Chang, A. Y., Rinsland, C. P., and Bui, T. P.: Subsidence, mixing and denitrification of Arctic polar vortex air measured during POLARIS, J. Geophys. Res., 104, 26 611–26 623, 1999.

Rex, M., Salawitch, R. J., Harris, N. R. P., von der Gathen, P., Schulz, G. O. B. A., Deckelman, H., Chipperfield, M., Sinnhuber, B.-M., Reimer, E., Alfier, R., Bevilacqua, R., Hoppel, K., Fromm, M., Lumpe, J., Küllmann, H., Kleinböhl, A., von König, H. B. M., Künzi, K., Toohey, D., Vömel, H., Richard, E., Aiken, K., Jost, H., Greenblatt, J. B., Loewenstein, M., Podolske, J. R., Webster, C. R., Flesch, G. J., Scott, D. C., Herman, R. L., Elkins, J. W., Ray, E. A., Moore, F. L., Hurst, D. F., Romanshkin, P., Toon, G. C., Sen, B., Margitan, J. J., Wennberg, P., Neuber, R., Allart, M., Bojkov, B. R., Claude, H., Davies, J., Davies, W., De Backer, H., Dier, H., Dorokhov, V., Fast, H., Kondo, Y., Kyrö, E., Litynska, Z., Mikkelsen, I. S., Molyneux, M. J., Moran, E., Nagai, T., Nakane, H., Parrondo, C., Ravegnani, F., Viatte, P. S. P., and Yushkov, V.: Chemical depletion of Arctic ozone in winter 1999/2000, J. Geophys. Res., 107, 8276, doi:10.1029/2001JD000533, 2002.

Rex, M., Salawitch, R. J., Santee, M. L., Waters, J. W., Hoppel, K., and Bevilacqua, R.: On the unexplained stratospheric ozone losses during cold Arctic Januaries, Geophys. Res. Lett., 30(1), 1010, doi:10.1029/2002GL016008, 2003.

Rex, M., Salawitch, R. J., von der Gathen, P., Harris, N. R. P., Chipperfield, M. P., and Naujokat, B.: Arctic ozone loss and climate change, Geophys. Res. Lett., 31, L04116, doi:

10.1029/2003GL018844, 2004.

Rex, M., Salawitch, R. J., Deckelmann, H., von der Gathen, P., Harris, N. R. P., Chipperfield, M. P., Naujokat, B., Reimer, E., Allaart, M., Andersen, S. B., Bevilacqua, R., Braathen, G. O., Claude, H., Davies, J., De Backer, H., Dier, H., Dorokov, V., Fast, H., Gerding, M., Godin-Beekmann, S., Hoppel, K., Johnson, B., Kyrö, E., Litynska, Z., Moore, D., Nakane, H., Parrondo, M. C., Risley Jr., A. D., Skrivankova, P., Stübi, R., Viatte, P., Yushkov, V., and Zerefos, C.: Arctic winter 2005: Implications for stratospheric ozone loss and climate change, Geophys. Res. Lett., 33, L23808, doi:10.1029/2006GL026731, 2006.

Richard, E. C., Aikin, K. C., Andrews, A. E., Daube, B. C., Gerbig, C., Wofsy, S. C., Romashkin, P. A., Hurst, D. F., Ray, E. A., Moore, F. L., Elkins, J. W., Deshler, T., and Toon, G. C.: Severe chemical ozone loss in the Arctic polar vortex during winter 1999-2000 inferred from in-situ airborne measurements, Geophys. Res. Lett., 28(11), 2197–2000, 2001.

Richard, E. C., Tuck, A. F., Aikin, K. C., Kelly, K. K., Herman, R. L., Troy, R. F., Hovde, S. J., Rosenlof, K. H., Thompson, T. L., and Ray, E. A.: High-resolution airborne profiles of CH_4, O_3, and water vapor near tropical Central America in late January to early February 2004, J. Geophys. Res., 111, D13304, doi:10.1029/2005JD006513, 2006.

Riese, M., Tie, X., Brasseur, G., and Offermann, D.: Three-dimensional simulation of stratospheric trace gas distributions measured by CRISTA, J. Geophys. Res., 104, 16 419–16 435, 1999.

Riese, M., Manney, G. L., Oberheide, J., Tie, X., Spang, R., and Küll, V.: Stratospheric transport by planetary wave mixing as observed during CRISTA-2, J. Geophys. Res., 107, 8179, doi: 101029/2001JD000629, 2002.

Riese, M., Grooß, J.-U., Feck, T., and Rohs, S.: Long-term changes of hydrogen-containing species in the stratosphere, J. Atmos. Solar Terr. Phys., 68(17), 1973–1979, 2006.

Rinsland, C. P., Salawitch, R. J., Gunson, M. R., Solomon, S., Zander, R., Mahieu, E., Newchurch, A. G. M. J., Irion, F. W., and Chang, A. Y.: Polar stratospheric descent of NO_y and CO and Arctic denitrification during winter 1992-1993, J. Geophys. Res., 104(D1), 1847–1861, 1999.

Roach, W. T.: Aircraft observations in the lower sub-Arctic stratosphere in winter, Meteorol. Res. Comm. Pap., 121, 1–7, available at: National Meteorological Library, Meteorological Office, Bracknell, UK, 1962.

Robinson, A. D., Millard, G. A., Danis, F., Guirlet, M., Harris, N. R. P., Lee, A. M., McIntyre, J. D., Pyle, J. A., Arvelius, J., Dagnesjo, S., Kirkwood, S., Nilsson, H., Toohey, D. W., Deshler, T., Goutail, F., Pommerau, J.-P., Elkins, J. W., Moore, F., Ray, E., Schmidt, U., Engel, A., and Müller, M.: Ozone loss derived from balloon-borne tracer measurements in the 1999/2000 Arctic winter, Atmos. Chem. Phys., 5, 1423–1436, 2005.

Roche, A. E., Nightingale, R. W., Kumer, J. B., Mergenthaler, J. L., Jackman, C. H., and Fleming, E. L.: Distribution and seasonal variation of CFCs in the stratosphere: Comparison of satellite global data and a 2-D model, Adv. Space Res., 21(10), 1383–1391, 1998.

Röckmann, T., Grooß, J.-U., and Müller, R.: The impact of anthropogenic chlorine emissions, stratospheric ozone change and chemical feedbacks on stratospheric water, Atmos. Chem. Phys., 4, 693–699, 2004.

Rodriguez, J. M., Ko, M. K. W., and N. D, S.: Antarctic chlorine chemistry – possible global implication, Geophys. Res. Lett., 15(3), 257–260, 1988.

Rodriguez, J. M., Ko, M. K. W., and N. D, S.: Role of heterogeneous conversion of N_2O_5 on sulphate

aerosols in global ozone losses, Nature, 352, 134–137, doi:10.1038/352134a0, 1991.

Rood, R. B.: Numerical advection algorithms and their role in atmospheric transport and chemistry models, Rev. Geophys., 25(1), 71–100, 1987.

Ross, D. E., Pyle, J. A., Harris, N. R. P., McIntyre, J. D., Millard, G. A., Robinson, A. D., and Busen, R.: Investigation of Arctic ozone depletion sampled over midlatitudes during the Egrett campaign of spring/summer 2000, Atmos. Chem. Phys., 4, 1407–1417, 2004.

Rothman, L. S., Jacquemart, D., Barbe, A., Benner, D. C., Birk, M., Brown, L. R., Carleer, M. R., Chackerian, C., Chance, K., Coudert, L. H., Dana, V., Devi, V. M., Flaud, J. M., Gamache, R. R., Goldman, A., Hartmann, J. M., Jucks, K. W., Maki, A. G., Mandin, J. Y., Massie, S. T., Orphal, J., Perrin, A., Rinsland, C. P., Smith, M. A. H., Tennyson, J., Tolchenov, R. N., Toth, R. A., Vander Auwera, J., Varanasi, P., and Wagner, G.: The HITRAN 2004 molecular spectroscopic database, J. Quant. Spectr. Radiat. Transfer, 96(2), 139–204, 2005.

Russell, J. M., Gordley, L. L., Park, J. H., Drayson, S. R., Tuck, A. F., Harries, J. E., Cicerone, R. J., Crutzen, P. J., and Frederick, J. E.: The Halogen Occultation Experiment, J. Geophys. Res., 98, 10 777–10 797, 1993.

Ryu, S., Chang, J., Kwon, H., and Kim, S. K.: Dynamics of solvated electron transfer in thin ice film leading to a large enhancement in photodissociation of $CFCl_3$, J. Amer. Chem. Soc., 128(11), 3500–3501, 2006.

Salawitch, R. J., McElroy, M. B., Yatteau, J. H., Wofsy, S. C., Schoeberl, M. R., Lait, L. R., Newman, P. A., Chan, K. R., Loewenstein, M., Podolske, J. R., Strahan, S. E., and Proffitt, M. H.: Loss of ozone in the Arctic vortex for the winter of 1989, Geophys. Res. Lett., 17, 561–564, doi: 10.1029/90GL00184, 1990.

Salawitch, R. J., Margitan, J. J., Sen, B., Toon, G. C., Osterman, G. B., Rex, M., Elkins, J. W., Ray, E. A., Moore, F. L., Hurst, D. F., Romashkin, P. A., Bevilacqua, R. M., Hoppel, K., Richard, E. C., and Bui, T. P.: Chemical loss of ozone during the Arctic winter of 1999-2000: an analysis based on balloon-borne observations, J. Geophys. Res., 107(D20), 8269, doi:10.1029/2001JD000620, 2002.

Sander, S. P., Friedl, R. R., Golden, D. M., Kurylo, M. J., Huie, R. E., Orkin, V. L., Moortgat, G. K., Ravishankara, A. R., Kolb, C. E., Molina, M. J., and Finlayson-Pitts, B. J.: Evaluation number 14, Chemical kinetics and photochemical data for use in atmospheric studies, NASA Panel for Data Evaluation, JPL Publication 02-25, Jet Propulsion Laboratory, California Insitute of Technology, Pasadena, California, 2003.

Sander, S. P., Friedl, R. R., Golden, D. M., Kurylo, M. J., Moortgat, G. K., Keller-Rudek, H., Wine, P. H., Ravishankara, A. R., Kolb, C. E., Molina, M. J., Finlayson-Pitts, B. J., Huie, R. E., and Orkin, V. L.: Chemical kinetics and photochemical data for use in atmospheric studies, JPL Publication 06-2, 2006.

Sankey, D. and Shepherd, T. G.: Correlations of long-lived chemical species in a middle atmosphere general circulation model, J. Geophys. Res., 108(D16), 4494, doi:10.1029/2002JD002799, 2003.

Santee, M. L., MacKenzie, I. A., Manney, G. L., Chipperfield, M. P., Bernath, P. F., Walker, K. A., Boone, C. D., Froidevaux, L., Livesey, N. J., and Waters, J. W.: A study of stratospheric chlorine partitioning based on new satellite measurements and modeling, J. Geophys. Res., 113, D12307, doi:10.1029/2007JD009057, 2008.

Sasano, Y., Suzuki, M., Yokota, T., and Kanzawa, H.: Improved Limb Atmospheric Spectrometer (ILAS) for stratospheric ozone layer measurements by solar occultation technique, Geophys. Res.

Lett., 26, 197–200, doi:10.1029/1998GL900276, 1999.

Schiller, C., Wahner, A., Platt, U., Dorn, H. P., Callies, J., and Ehhalt, D.: Near UV atmospheric absorption measurements of column abundances during Airborne Arctic Stratospheric Expedition, January–February 1989 2. OClO observations, Geophys. Res. Lett., 17(4), 501–504, 1990.

Schmidt, U., Bauer, R., Engel, A., Borchers, R., and Lee, J.: The variation of available chlorine Cl_y in the Arctic polar vortex during EASOE, Geophys. Res. Lett., 21, 1215–1218, doi: 10.1029/93GL01053, 1994.

Schulz, A., Rex, M., Steger, J., Harris, N. R. P., Braathen, G. O., Reimer, E., Alfier, R., Beck, A., Alpers, M., Cisneros, J., Claude, H., De Backer, H., Dier, H., Dorokhov, V., Fast, H., Godin, S., Hansen, G., Kanzawa, H., Kois, B., Kondo, Y., Kosmidis, E., Kyrö, E., Litynska, Z., Molyneux, M. J., Murphy, G., Nakane, H., Parrondo, C., Ravegnani, F., Varotsos, C., Vialle, C., Viatte, P., Yushkov, V., Zerefos, C., and von der Gathen, P.: Match observations in the Arctic winter 1996/97: High stratospheric ozone loss rates correlate with low temperatures deep inside the polar vortex, Geophys. Res. Lett., 27, 205–208, doi:10.1029/1999GL010811, 2000.

Shepherd, T. G.: Large-Scale Atmospheric Dynamics for Atmospheric Chemists, Chem. Rev., 103(12), 4509–4532, doi:10.1021/cr020511z, 2003.

Shi, Q., Jayne, J. T., Kolb, C. E., Worsnop, D. R., and Davidovits, P.: Kinetic model for reaction of $ClONO_2$ with H_2O and HCl and HOCl with HCl in sulfuric acid solutions, J. Geophys. Res., 106, 24 259–24 274, doi:10.1029/2000JD000181, 2001.

Singleton, C. G., Randell, C. E., Chipperfield, M., Davies, S., Feng, W., Bevilacqua, R. M., Hoppel, K. W., Fromm, M. D., Manney, G. L., and Harvey, V. L.: 2002–2003 Arctic ozone loss deduced from POAM III satellite observations and the SLIMCAT chemical transport model, Atmos. Chem. Phys., 5, 597–609, 2005.

Solomon, S.: Stratospheric ozone depletion: A review of concepts and history, Rev. Geophys., 37(3), 275–316, doi:10.1029/1999RG900008, 1999.

Solomon, S.: The hole truth, Nature, 427, 289–291, doi:10.1038/427289a, 2004.

Solomon, S. and Garcia, R. R.: On the distributions of long-lived tracers and chlorine species in the middle atmosphere, J. Geophys. Res., 89(D7), 11 633–11 644, 1984.

Solomon, S., Crutzen, P. J., and Roble, R. G.: Photochemical Coupling Between the Thermosphere and the Lower Atmosphere 1. Odd Nitrogen From 50 to 120 km, J. Geophys. Res., 87, 7206–7220, 1982.

Solomon, S., Garcia, R. R., Olivero, J. J., Bevilacqua, R. M., Schwartz, P. R., Clancy, R. T., and Muhleman, D. O.: Photochemistry and transport of carbon monoxide in the middle atmosphere, J. Atmos. Sci., 42(10), 1072–1083, 1985.

Solomon, S., Garcia, R. R., Rowland, F. S., and Wuebbles, D. J.: On the depletion of Antarctic ozone, Nature, 321, 755–758, 1986.

Solomon, S., Mount, G. H., Sanders, R. W., and Schmeltekopf, A. L.: Visible spectroscopy at McMurdo Station, Antarctica 2. Observations of OClO, J. Geophys. Res., 92, 8329–8338, 1987.

Solomon, S., Portmann, R. W., Sasaki, T., Hofmann, D. J., and Thompson, D. W. J.: Four decades of ozonesonde measurements over Antarctica, J. Geophys. Res., 110(D21), D21311, doi: 10.1029/2005JD005917, 2005.

Solomon, S., Portmann, R. W., and Thompson, D. W. J.: Contrasts between Antarctic and Arctic ozone depletion, Proc. Natl. Acad. Sci., 104(2), 445–449, 2007a.

Solomon, S., Qin, D., Manning, M., Marquis, M., Averyt, K., Tignor, M. M. B., Miller, H. L., and Chen, Z., eds.: Climate Change 2007: The Physical Science Basis. Contribution of Working Group I to the Fourth Assessment Report of the Intergovernmental Panel on Climate Change, Cambridge University Press, Cambridge, UK, and New York, NY, USA, 2007b.

Solomon, S., Rosenlof, K., Portmann, R., Daniel, J., Davis, S., Sanford, T., and Plattner, G.-K.: Contributions of stratospheric water vapor to decadal changes in the rate of global warming, Science, 327, 1219–1222, doi:10.1126/science.1182488, 2010.

Sonnemann, G.: Ozon: Natürliche Schwankungen und anthropogene Einflüsse, Akademie Verlag, 1992.

Staehelin, J., Kegel, R., and Harris, N. R. P.: Trend analysis of the homogenized total ozone series of Arosa (Switzerland), 1926-1996, J. Geophys. Res., 103, 5827–5841, 1998.

Steinbrecht, W., Claude, H., Schönenborn, F., McDermid, I. S., Leblanc, T., Godin, S., Song, T., Swart, D. P. J., Meijer, Y. J., Bodeker, G. E., Connor, B. J., Kämpfer, N., Hocke, K., Calisesi, Y., Schneider, N., de la Nöe, J., Parrish, A. D., Boyd, I. S., Brühl, C., Steil, B., Giorgetta, M. A., Manzini, E., Thomason, L. W., Zawodny, J. M., McCormick, M., Russell, J. M., Bhartia, P. K., Stolarski, R. S., and Hollandsworth-Frith, S. M.: Long-term evolution of upper stratospheric ozone at selected stations of the Network for the Detection of Stratospheric Change (NDSC), J. Geophys. Res., 111, D10308, doi:10.1029/2005JD006454, 2006.

Steinhorst, H.-M., Konopka, P., Günther, G., and Müller, R.: How permeable is the edge of the Arctic vortex — Model studies of the winter 1999-2000, J. Geophys. Res., 110, D06105, doi: 10.1029/2004JD005268, 2005.

Stolarski, R. S. and Cicerone, R. J.: Stratospheric chlorine: A possible sink of ozone, Canad. J. Chem., 52, 1610–1615, 1974.

Stolarski, R. S., Krueger, A. J., Schoeberl, M. R., McPeters, R. D., Newman, P. A., and Alpert, J. C.: Nimbus 7 satellite measurements of the springtime Antarctic ozone decrease, Nature, 322, 808–811, 1986.

Streibel, M., Rex, M., von der Gathen, P., Lehmann, R., Harris, N. R. P., Braathen, G. O., Reimer, E., Deckelmann, H., Chipperfield, M., Millard, G., Allaart, M., Andersen, S. B., Claude, H., Davies, J., De Backer, H., Dier, H., Dorokov, V., Fast, H., Gerding, M., Kyrö, E., Litynska, Z., Moore, D., Moran, E., Nagai, T., Nakane, H., Parrondo, C., Skrivankova, P., Stübi, R., Vaughan, G., Viatte, P., and Yushkov, V.: Chemical ozone loss in the Arctic winter 2002/2003 determined with Match, Atmos. Chem. Phys., 6, 2783–2792, 2006.

Strobel, D. F.: Diurnal Variation of Nitric Oxide in the Upper Atmosphere, J. Geophys. Res., 76(10), 2441–2452, 1971.

Sugita, T., Kondo, Y., Nakajima, H., Schmidt, U., Engel, A., Oelhaf, H., Wetzel, G., Koike, M., and Newman, P. A.: Denitrification observed inside the Arctic vortex in February 1995, J. Geophys. Res., 103(D13), 16 221–16 233, 1998.

Thompson, D. W. J., Baldwin, M. P., and Solomon, S.: Stratosphere-troposphere coupling in the Southern hemisphere, J. Atmos. Sci., 62(3), 708–715, 2005.

Thuburn, J. and McIntyre, M. E.: Numerical advection schemes, cross-isentropic random walks, and correlations between chemical species, J. Geophys. Res., 102(D6), 6775–6797, 1997.

Tilmes, S.: Chemical ozone loss in the Arctic polar stratosphere, Tech. rep., Institute of Chemistry and Dynamics of the Geosphere, Forschungszentrum Jülich, Germany, 2004.

Tilmes, S., Müller, R., Grooß, J.-U., Höpfner, M., Toon, G. C., and Russell, J. M.: Very early chlorine activation and ozone loss in the Arctic winter 2002–2003, Geophys. Res. Lett., 30(23), 2201, doi:10.1029/2003GL018079, 2003a.

Tilmes, S., Müller, R., Grooß, J.-U., McKenna, D. S., Russell, J. M., and Sasano, Y.: Calculation of chemical ozone loss in the Arctic winter 1996-1997 using ozone-tracer correlations: Comparison of Improved Limb Atmospheric Spectrometer (ILAS) and Halogen Occultation Experiment (HALOE) results, J. Geophys. Res., 108, 4045, doi:10.1029/2002JD002213, 2003b.

Tilmes, S., Müller, R., Grooß, J.-U., and Russell, J. M.: Ozone loss and chlorine activation in the Arctic winters 1991–2003 derived with the tracer-tracer correlations, Atmos. Chem. Phys., 4(8), 2181–2213, 2004.

Tilmes, S., Müller, R., Engel, A., Rex, M., and Russell III, J.: Chemical ozone loss in the Arctic and Antarctic stratosphere between 1992 and 2005, Geophys. Res. Lett., 33, L20812, doi: 10.1029/2006GL026925, 2006a.

Tilmes, S., Müller, R., Grooß, J.-U., Nakajima, H., and Sasano, Y.: Development of tracer relations and chemical ozone loss during the setup phase of the polar vortex, J. Geophys. Res., 111, D24S90, doi:10.1029/2005JD006726, 2006b.

Tilmes, S., Müller, R., Grooß, J.-U., Spang, R., Sugita, T., Nakajima, H., and Sasano, Y.: Chemical ozone loss and related processes in the Antarctic winter 2003 based on Improved Limb Atmospheric Spectrometer (ILAS)–II observations, J. Geophys. Res., 111, D11S12, doi: 10.1029/2005JD06260, 2006c.

Tilmes, S., Kinnison, D., Müller, R., Sassi, F., Marsh, D., Boville, B., and Garcia, R.: Evaluation of heterogeneous processes in the polar lower stratosphere in the Whole Atmosphere Community Climate Model, J. Geophys. Res., 112, D24301, doi:10.1029/2006JD008334, 2007.

Tilmes, S., Müller, R., and Salawitch, R. J.: The sensitivity of polar ozone depletion to proposed geoengineering schemes, Science, 320, 1201–1204, doi:10.1126/science.1153966, 2008a.

Tilmes, S., Müller, R., Salawitch, R. J., Schmidt, U., Webster, C. R., Oelhaf, H., Russell III, J. M., and Camy-Peyret, C. C.: Chemical ozone loss in the Arctic winter 1991–1992, Atmos. Chem. Phys., 8, 1897–1910, 2008b.

Tilmes, S., Garcia, R. R., Kinnison, D. E., Gettelman, A., and Rasch, P. J.: Impact of geoengineered aerosols on the troposphere and stratosphere, J. Geophys. Res., 114, D12305, doi: 10.1029/2008JD011420, 2009.

Tolbert, M. A., Rossi, M. J., and Golden, D. M.: Heterogeneous Interactions of Chlorine Nitrate, Hydrogen Chloride, and Nitric Acid with Sulfuric Acid Surfaces at Stratospheric Temperatures, Geophys. Res. Lett., 15(8), 847–850, 1988.

Toon, G. C., Blavier, J.-F., Sen, B., Margitan, J. J., Webster, C. R., May, R. D., Fahey, D., Gao, R., Del Negro, L., Proffitt, M., Elkins, J. W., Romashkin, P. A., Hurst, D. F., Oltmans, S., Atlas, E., Schauffler, S., Flocke, F., Bui, T. P., Stimpfle, R. M., Bonne, G. P., Voss, P. B., and Cohen, R. C.: Comparison of MkIV balloon and ER-2 aircraft measurements of atmospheric trace gases, J. Geophys. Res., 104, 26 779–26 790, 1999.

Toon, O. B., Hamill, P., Turco, R. P., and Pinto, J.: Condensation of HNO_3 and HCl in winter polar stratospheres, Geophys. Res. Lett., 13, 1284–1287, 1986.

Tuck, A. F.: Changes to the ozone layer, Phys. Bulletin, 29, 168–171, 1978.

Tuck, A. F.: Synoptic and chemical evolution of the Antarctic vortex in late winter and early spring,

1987, J. Geophys. Res., 94, 11 687–11 737, 1989.

Tuck, A. F., Watson, R. T., Condon, E. P., Margitan, J. J., and Toon, O. B.: The planning and execution of ER-2 and DC-8 aircraft flights over Antarctica, August and September 1987, J. Geophys. Res., 94, 11 181–11 222, 1989.

Tuck, A. F., Davies, T., Hovde, S. J., Noguer-Alba, M., Fahey, D. W., Kawa, S. R., Kelly, K. K., Murphy, D. M., Proffitt, M. H., Margitan, J. J., Loewenstein, M., Podolske, J. R., Strahan, S. E., and Chan, K. R.: Polar stratospheric cloud processed air and potential vorticity in the northern hemisphere lower stratosphere at mid-latitudes during winter, J. Geophys. Res., 97, 7883–7904, 1992.

Tuck, A. F., Hovde, S. J., Kelly, K. K., Mahoney, M. J., Proffitt, M. H., Richard, E. C., and Thompson, T. L.: Exchange between the upper tropical troposphere and the lower stratosphere studied with aircraft observations, J. Geophys. Res., 108(D23), 4734, doi:10.1029/2003JD003399, 2003.

Tung, K. K.: On the two-dimensional transport of stratospheric trace gases in isentropic coordinates, J. Atmos. Sci., 39, 2330–2355, 1982.

Tung, K. K., Ko, M. K. W., Rodriguez, J., and Sze, N. D.: Are Antarctic ozone variations manifestations of dynamics or chemistry?, Nature, 333, 811–814, 1986.

Ulanovskii, A. E., Luk'yanov, A. N., Yushkov, V. A., Sitnikov, N. M., Volk, M., Ivanova, E. V., and Ravegnani, F.: Estimation of the chemical loss of ozone in the Antarctic stratosphere in the 1999 winter-spring season from direct measurements and simulations, Izv. Atmos. Ocean. Phys., 40(6), 695–703, 2004.

Velazco, V., Wood, S. W., Sinnhuber, M., Kramer, I., Jones, N. B., Kasai, Y., Notholt, J., Warneke, T., Blumenstock, T., Hase, F., Murcray, F. J., and Schrems, O.: Annual variation of stratomesospheric carbon monoxide measured by ground-based Fourier transform infrared spectrometry, Atmos. Chem. Phys., 7, 1305–1312, 2007.

Vitt, F. M., Cravens, T. E., and Jackman, C. H.: A two-dimensional model of thermospheric nitric oxide sources and their contributions to the middle atmospheric chemical balance, J. Atmos. Solar Terr. Phys., 62, 653–667, 2000.

Vogel, B., Müller, R., Deshler, T., Grooß, J.-U., Karhu, J., McKenna, D. S., Müller, M., Toohey, D., Toon, G. C., and Stroh, F.: Vertical profiles of activated ClO and ozone loss in the Arctic vortex in January and March 2000: In situ observations and model simulations, J. Geophys. Res., 108(D22), 8334, doi:10.1029/2002JD002564, 2003.

Vogel, B., Konopka, P., Grooß, J.-U., Müller, R., Funke, B., López-Puertas, M., Reddmann, T., Stiller, G., von Clarmann, T., and Riese, M.: Model simulations of stratospheric ozone loss caused by enhanced mesospheric NO_x during Arctic Winter 2003/2004, Atmos. Chem. Phys., 8(17), 5279–5293, 2008.

Voigt, C., Schreiner, J., Kohlmann, A., Zink, P., Mauersberger, K., Larsen, N., Deshler, T., Kröger, C., Rosen, J., Adriani, A., Cairo, F., Donfrancesco, G. D., Viterbini, M., Ovarlez, J., Ovarlez, H., David, C., and Dörnbrack, A.: Nitric acid trihydrate (NAT) in polar stratospheric clouds, Science, 290, 1756–1758, 2000.

von der Gathen, P., Rex, M., Harris, N. R. P., Lucic, D., Knudsen, B. M., Braathen, G. O., De Backer, H., Fabian, R., Fast, H., Gil, M., Kyrö, E., Mikkelsen, I. S., Rummukainen, M., Stähelin, J., and Varotsos, C.: Observational evidence for chemical ozone depletion over the Arctic in winter 1991-92, Nature, 375, 131–13, 1995.

von Hobe, M.: Revisiting Ozone Depletion, Science, 318, 1878–1879, 2007.

von Hobe, M., Ulanovsky, A., Volk, C. M., Grooß, J.-U., Tilmes, S., Konopka, P., Günther, G., Werner, A., Spelten, N., Shur, G., Yushkov, V., Ravegnani, F., Schiller, C., Müller, R., and Stroh, F.: Severe ozone depletion in the cold Arctic winter 2004-05, Geophys. Res. Lett., 33, L17815, doi:10.1029/2006GL026945, 2006.

von Hobe, M., Salawitch, R. J., Canty, T., Keller-Rudek, H., Moortgat, G. K., Grooß, J.-U., Müller, R., and Stroh, F.: Understanding the kinetics of the ClO dimer cycle, Atmos. Chem. Phys., 7, 3055–3069, 2007.

von Hobe, M., Stroh, F., Beckers, H., Benter, T., and Willner, H.: The UV/Vis absorption spectrum of matrix-isolated dichlorine peroxide, ClOOCl, Phys. Chem. Chem. Phys., 11, 1571–1580, doi: 10.1039/b814373k, 2009.

Vyushin, D., Fioletov, V. E., and Shepherd, T. G.: Impact of long-range correlations on trend detection in total ozone, J. Geophys. Res., 112, D14307, doi:10.1029/2006JD008168, 2007.

Wagner, T., Leue, C., Pfeilsticker, K., and Platt, U.: Monitoring of the stratospheric chlorine activation by Global Ozone Monitoring Experiment (GOME) OClO measurements in the austral and boreal winters 1995 through 1999, J. Geophys. Res., 106(D5), 4971–4986, 2001.

Wang, C.-R., Drew, K., Luo, T., Lu, M.-J., and Lu, Q.-B.: Resonant dissociative electron transfer of the presolvated electron to CCl_4 in liquid: Direct observation and lifetime of the CCl_4^{*-} transition state, J. Chem. Phys., 128, 041102, 2008.

Waters, J. W., Froidevaux, L., Read, W. G., Manney, G. L., Elson, L. S., Flower, D. A., Jarnot, R. F., and Harwood, R. S.: Stratospheric ClO and ozone from the Microwave Limb Sounder on the Upper Atmosphere Research Satellite, Nature, 362, 597–602, 1993.

Waugh, D. W. and Randel, W. J.: Climatology of Arctic and Antarctic polar vortices using elliptical diagnostics, J. Atmos. Sci., 56, 1594–1613, 1999.

Waugh, D. W., Plumb, R. A., Elkins, J. W., Fahey, D. W., Boering, K. A., Dutton, G. S., Volk, C. M., Keim, E., Gao, R.-S., Daube, B. C., Wofsy, S. C., Loewenstein, M., Podolske, J. R., Chan, K. R., Proffitt, M. H., Kelly, K. K., Newman, P. A., and Lait, L. R.: Mixing of polar vortex air into middle latitudes as revealed by tracer-tracer scatterplots, J. Geophys. Res., 102, 13 119–13 134, 1997.

Webster, C. R., May, R., Toohey, D., Avallone, L., Anderson, J., Newman, P., Lait, L., Schoeberl, M., Elkins, J., and Chan, K.: Hydrochloric acid loss and chlorine chemistry on polar stratospheric cloud particles in the Arctic winter, Science, 261, 1130–1134, 1993.

Webster, C. R., May, R. D., Trimble, C. A., Chave, R. G., and Kendall, J.: Aircraft laser infrared absorption spectrometer (ALIAS) for in situ atmospheric measurements of HCl, N_2O, CH_4, NO_2, and HNO_3, Appl. Opt., 33, 454–472, 1994.

Wells, B.: The hole truth, Nature, 390, 438, 1997.

Wetzel, G., Oelhaf, H., Friedl-Vallon, F., Kleinert, A., Lengel, A., Maucher, G., Nordmeyer, H., Ruhnke, R., Nakajima, H., Sasano, Y., Sugita, T., and Yokota, T.: Intercomparison and validation of ILAS-II version 1.4 target parameters with MIPAS-B measurements, J. Geophys. Res., 111, D11S06, doi:10.1029/2005JD006287, 2006.

WMO: Scientific assessment of ozone depletion: 1985, Report No. 16, Geneva, Switzerland, 1986.

WMO: Scientific assessment of ozone depletion: 1989, Report No. 20, Geneva, Switzerland, 1990.

WMO: Scientific assessment of ozone depletion: 1994, Report No. 37, Geneva, Switzerland, 1995.

WMO: Scientific assessment of ozone depletion: 1998, Global Ozone Research and Monitoring Project–Report No. 44, Geneva, Switzerland, 1999.

WMO: Scientific assessment of ozone depletion: 2002, Global Ozone Research and Monitoring Project–Report No. 47, Geneva, Switzerland, 2003.

WMO: Scientific assessment of ozone depletion: 2006, Global Ozone Research and Monitoring Project–Report No. 50, Geneva, Switzerland, 2007.

Wolff, E. W. and Mulvaney, R.: Reactions on sulphuric acid aerosol and on polar stratospheric clouds in the Antarctic stratosphere, Geophys. Res. Lett., 18(6), 1007–1010, 1991.

Woyke, T., Müller, R., Stroh, F., McKenna, D. S., Engel, A., Margitan, J. J., Rex, M., and Carslaw, K. S.: A test of our understanding of the ozone chemistry in the Arctic polar vortex based on in-situ measurements of ClO, BrO, and O_3 in the 1994/95 winter, J. Geophys. Res., 104, 18 755–18 768, 1999.

Acknowledgements

It would not have been possible to complete this "Habilitationsschrift" without the continuous support of Martin Riese and Ralf Koppmann; my sincerest thanks go to them both.

My work on tracer-tracer correlations started years ago at the Max Planck Institute of Chemistry in Mainz. I would like to thank Jens-Uwe Grooß and Paul Crutzen for many discussions and their support during that time. Later, at Forschungszentrum Jülich, Danny McKenna and again Jens-Uwe Grooß were the colleagues with whom I collaborated most closely on this subject. Finally, particular thanks are due to Simone Tilmes and Carsten Lemmen. In their PhD theses and during the follow-up postdoc periods at Forschungszentrum Jülich they made extremely important contributions to my work on tracer-tracer correlations as is most evident in a number of co-authored papers.

Further, I had very helpful discussions on the results presented here and on the papers that the present publication is based on with a large number of colleagues. I would like to thank thank Andreas Engel, Bernd Funke, Hans-Jürg Jost, Paul Konopka, Hermann Oehlhaf, Mike Proffitt, Jim M. Russell, David Sankey, Ted S. Shepherd, Susan Solomon, Gabi Stiller, Bärbel Vogel, and Gerald Wetzel for fruitful discussions and for helpful comments. I also thank Susan Solomon for a through review of this work and for many helpful comments.

This study is based on a variety of in situ and remote sensing data without which this work would not have been possible. I thank J. W. Elkins for the ACATS N_2O measurements, E. Richard for the ozone photometer data, G. C. Toon for a variety of MkIV data, C. R. Webster for the ALIAS N_2O measurements, M. Loewenstein and H.-J. Jost for the ARGUS N_2O data, N. Huret and V. Catoire for the SPIRALE measurements of ozone, CO, N_2O, and CH_4 in early 2003, H. Oehlhaf and G. Wetzel for the MIPAS-B ozone, CO, N_2O, and CH_4 in early 2003, U. Schmidt and A. Engel for the balloon data of long-lived tracers from the EASOE campaign in Arctic winter 1991-1992 and from the Euplex campaign in early 2003, J. Shanklin for the total ozone measurements from Halley Station, Antarctica, and H. Gernandt for the ozone sonde measurements from Georg Forster Station, Antarctica in 1985. Moreover, I gratefully acknowledge J. M. Russell III and the HALOE team for providing a high quality data set of ozone and long-lived tracers (HALOE v19 data) and all members of the science team of the Improved Limb Atmospheric Spectrometer (ILAS-II) led by Y. Sasano and H. Nakajima for the ILAS-II version 1.4 data. ILAS-II was developed by the Ministry of the Environment, Japan, and was on board the ADEOS-II satellite launched by the Japan Aerospace Exploration Agency. ILAS-II data were processed at the ILAS-II Data Handling Facility, National Institute for Environmental Studies (NIES).

The cosmic ray intensities employed in Section 2.2.3 were obtained from the space physics data system of the University of New Hampshire supported by National Science Foundation Grant ATM-0339527 (http://ulysses.sr.unh.edu/NeutronMonitor/neutron_mon.html); the 10.7 cm solar flux was obtained from the UK Solar System Data Centre (http://www.ukssdc.ac.uk/wdcc1/wdc_menu.html).

Last but not least, I thank J. Carter-Sigglow for revising the grammar and style of the manuscript.

1. **Einsatz von multispektralen Satellitenbilddaten in der Wasserhaushalts- und Stoffstrommodellierung – dargestellt am Beispiel des Rureinzugsgebietes**
   von C. Montzka (2008), XX, 238 Seiten
   ISBN: 978-3-89336-508-1

2. **Ozone Production in the Atmosphere Simulation Chamber SAPHIR**
   by C. A. Richter (2008), XIV, 147 pages
   ISBN: 978-3-89336-513-5

3. **Entwicklung neuer Schutz- und Kontaktierungsschichten für Hochtemperatur-Brennstoffzellen**
   von T. Kiefer (2008), 138 Seiten
   ISBN: 978-3-89336-514-2

4. **Optimierung der Reflektivität keramischer Wärmedämmschichten aus Yttrium-teilstabilisiertem Zirkoniumdioxid für den Einsatz auf metallischen Komponenten in Gasturbinen**
   von A. Stuke (2008), X, 201 Seiten
   ISBN: 978-3-89336-515-9

5. **Lichtstreuende Oberflächen, Schichten und Schichtsysteme zur Verbesserung der Lichteinkopplung in Silizium-Dünnschichtsolarzellen**
   von M. Berginski (2008), XV, 171 Seiten
   ISBN: 978-3-89336-516-6

6. **Politikszenarien für den Klimaschutz IV – Szenarien bis 2030**
   hrsg.von P. Markewitz, F. Chr. Matthes (2008), 376 Seiten
   ISBN 978-3-89336-518-0

7. **Untersuchungen zum Verschmutzungsverhalten rheinischer Braunkohlen in Kohledampferzeugern**
   von A. Schlüter (2008), 164 Seiten
   ISBN 978-3-89336-524-1

8. **Inorganic Microporous Membranes for Gas Separation in Fossil Fuel Power Plants**
   by G. van der Donk (2008), VI, 120 pages
   ISBN: 978-3-89336-525-8

9. **Sinterung von Zirkoniumdioxid-Elektrolyten im Mehrlagenverbund der oxidkeramischen Brennstoffzelle (SOFC)**
   von R. Mücke (2008), VI, 165 Seiten
   ISBN: 978-3-89336-529-6

10. **Safety Considerations on Liquid Hydrogen**
    by K. Verfondern (2008), VIII, 167 pages
    ISBN: 978-3-89336-530-2

11. **Kerosinreformierung für Luftfahrtanwendungen**
von R. C. Samsun (2008), VII, 218 Seiten
ISBN: 978-3-89336-531-9

12. **Der 4. Deutsche Wasserstoff Congress 2008 – Tagungsband**
hrsg. von D. Stolten, B. Emonts, Th. Grube (2008), 269 Seiten
ISBN: 978-3-89336-533-3

13. **Organic matter in Late Devonian sediments as an indicator for environmental changes**
by M. Kloppisch (2008), XII, 188 pages
ISBN: 978-3-89336-534-0

14. **Entschwefelung von Mitteldestillaten für die Anwendung in mobilen Brennstoffzellen-Systemen**
von J. Latz (2008), XII, 215 Seiten
ISBN: 978-3-89336-535-7

15. **RED-IMPACT**
Impact of Partitioning, Transmutation and Waste Reduction Technologies on the Final Nuclear Waste Disposal
SYNTHESIS REPORT
ed. by W. von Lensa, R. Nabbi, M. Rossbach (2008), 178 pages
ISBN 978-3-89336-538-8

16. **Ferritic Steel Interconnectors and their Interactions with Ni Base Anodes in Solid Oxide Fuel Cells (SOFC)**
by J. H. Froitzheim (2008), 169 pages
ISBN: 978-3-89336-540-1

17. **Integrated Modelling of Nutrients in Selected River Basins of Turkey**
Results of a bilateral German-Turkish Research Project
project coord. M. Karpuzcu, F. Wendland (2008), XVI, 183 pages
ISBN: 978-3-89336-541-8

18. **Isotopengeochemische Studien zur klimatischen Ausprägung der Jüngeren Dryas in terrestrischen Archiven Eurasiens**
von J. Parplies (2008), XI, 155 Seiten, Anh.
ISBN: 978-3-89336-542-5

19. **Untersuchungen zur Klimavariabilität auf dem Tibetischen Plateau - Ein Beitrag auf der Basis stabiler Kohlenstoff- und Sauerstoffisotope in Jahrringen von Bäumen waldgrenznaher Standorte**
von J. Griessinger (2008), XIII, 172 Seiten
ISBN: 978-3-89336-544-9

20. **Neutron-Irradiation + Helium Hardening & Embrittlement Modeling of 9%Cr-Steels in an Engineering Perspective (HELENA)**
by R. Chaouadi (2008), VIII, 139 pages
ISBN: 978-3-89336-545-6

21. **in Bearbeitung**

22. **Verbundvorhaben APAWAGS (AOEV und Wassergenerierung) – Teilprojekt: Brennstoffreformierung – Schlussbericht**
von R. Peters, R. C. Samsun, J. Pasel, Z. Porš, D. Stolten (2008), VI, 106 Seiten
ISBN: 978-3-89336-547-0

23. **FREEVAL**
Evaluation of a Fire Radiative Power Product derived from Meteosat 8/9 and Identification of Operational User Needs
Final Report
project coord. M. Schultz, M. Wooster (2008), 139 pages
ISBN: 978-3-89336-549-4

24. **Untersuchungen zum Alkaliverhalten unter Oxycoal-Bedingungen**
von C. Weber (2008), VII, 143, XII Seiten
ISBN: 978-3-89336-551-7

25. **Grundlegende Untersuchungen zur Freisetzung von Spurstoffen, Heißgaschemie, Korrosionsbeständigkeit keramischer Werkstoffe und Alkalirückhaltung in der Druckkohlenstaubfeuerung**
von M. Müller (2008), 207 Seiten
ISBN: 978-3-89336-552-4

26. **Analytik von ozoninduzierten phenolischen Sekundärmetaboliten in *Nicotiana tabacum* L. cv Bel W3 mittels LC-MS**
von I. Koch (2008), III, V, 153 Seiten
ISBN 978-3-89336-553-1

27. **IEF-3 Report 2009. Grundlagenforschung für die Anwendung**
(2009), ca. 230 Seiten
ISBN: 978-3-89336-554-8

28. **Influence of Composition and Processing in the Oxidation Behavior of MCrAlY-Coatings for TBC Applications**
by J. Toscano (2009), 168 pages
ISBN: 978-3-89336-556-2

29. **Modellgestützte Analyse signifikanter Phosphorbelastungen in hessischen Oberflächengewässern aus diffusen und punktuellen Quellen**
von B. Tetzlaff (2009), 149 Seiten
ISBN: 978-3-89336-557-9

30. **Nickelreaktivlot / Oxidkeramik – Fügungen als elektrisch isolierende Dichtungskonzepte für Hochtemperatur-Brennstoffzellen-Stacks**
von S. Zügner (2009), 136 Seiten
ISBN: 978-3-89336-558-6

31. **Langzeitbeobachtung der Dosisbelastung der Bevölkerung in radioaktiv kontaminierten Gebieten Weißrusslands – Korma-Studie**
von H. Dederichs, J. Pillath, B. Heuel-Fabianek, P. Hill, R. Lennartz (2009), Getr. Pag.
ISBN: 978-3-89336-532-3

32. **Herstellung von Hochtemperatur-Brennstoffzellen über physikalische Gasphasenabscheidung**
von N. Jordán Escalona (2009), 148 Seiten
ISBN: 978-3-89336-532-3

33. **Real-time Digital Control of Plasma Position and Shape on the TEXTOR Tokamak**
by M. Mitri (2009), IV, 128 pages
ISBN: 978-3-89336-567-8

34. **Freisetzung und Einbindung von Alkalimetallverbindungen in kohlebefeuerten Kombikraftwerken**
von M. Müller (2009), 155 Seiten
ISBN: 978-3-89336-568-5

35. **Kosten von Brennstoffzellensystemen auf Massenbasis in Abhängigkeit von der Absatzmenge**
von J. Werhahn (2009), 242 Seiten
ISBN: 978-3-89336-569-2

36. **Einfluss von Reoxidationszyklen auf die Betriebsfestigkeit von anodengestützten Festoxid-Brennstoffzellen**
von M. Ettler (2009), 138 Seiten
ISBN: 978-3-89336-570-8

37. **Großflächige Plasmaabscheidung von mikrokristallinem Silizium für mikromorphe Dünnschichtsolarmodule**
von T. Kilper (2009), XVII, 154 Seiten
ISBN: 978-3-89336-572-2

38. **Generalized detailed balance theory of solar cells**
by T. Kirchartz (2009), IV, 198 pages
ISBN: 978-3-89336-573-9

39. **The Influence of the Dynamic Ergodic Divertor on the Radial Electric Field at the Tokamak TEXTOR**
von J. W. Coenen (2009), xii, 122, XXVI pages
ISBN: 978-3-89336-574-6

40. **Sicherheitstechnik im Wandel Nuklearer Systeme**
von K. Nünighoff (2009), viii, 215 Seiten
ISBN: 978-3-89336-578-4

41. **Pulvermetallurgie hochporöser NiTi-Legierungen für Implanat- und Dämpfungsanwendungen**
von M. Köhl (2009), XVII, 199 Seiten
ISBN: 978-3-89336-580-7

42. **Einfluss der Bondcoatzusammensetzung und Herstellungsparameter auf die Lebensdauer von Wärmedämmschichten bei zyklischer Temperaturbelastung**
von M. Subanovic (2009), 188, VI Seiten
ISBN: 978-3-89336-582-1

43. **Oxygen Permeation and Thermo-Chemical Stability of Oxygen Permeation Membrane Materials for the Oxyfuel Process**
by A. J. Ellett (2009), 176 pages
ISBN: 978-3-89336-581-4

44. **Korrosion von polykristallinem Aluminiumoxid (PCA) durch Metalljodidschmelzen sowie deren Benetzungseigenschaften**
von S. C. Fischer (2009), 148 Seiten
ISBN: 978-3-89336-584-5

45. **IEF-3 Report 2009. Basic Research for Applications**
(2009), 217 Seiten
ISBN: 978-3-89336-585-2

46. **Verbundvorhaben ELBASYS (Elektrische Basissysteme in einem CFK-Rumpf) - Teilprojekt: Brennstoffzellenabgase zur Tankinertisierung - Schlussbericht**
von R. Peters, J. Latz, J. Pasel, R. C. Samsun, D. Stolten
(2009), xi, 202 Seiten
ISBN: 978-3-89336-587-6

47. **Aging of ^{14}C-labeled Atrazine Residues in Soil: Location, Characterization and Biological Accessibility**
by N. D. Jablonowski (2009), IX, 104 pages
ISBN: 978-3-89336-588-3

48. **Entwicklung eines energetischen Sanierungsmodells für den europäischen Wohngebäudesektor unter dem Aspekt der Erstellung von Szenarien für Energie- und CO_2 - Einsparpotenziale bis 2030**
von P. Hansen (2009), XXII, 281 Seiten
ISBN: 978-3-89336-590-6

49. **Reduktion der Chromfreisetzung aus metallischen Interkonnektoren für Hochtemperaturbrennstofzellen durch Schutzschichtsysteme**
von R. Trebbels (2009), iii, 135 Seiten
ISBN: 978-3-89336-591-3

50. **Bruchmechanische Untersuchung von Metall / Keramik-Verbundsystemen für die Anwendung in der Hochtemperaturbrennstoffzelle**
von B. Kuhn (2009), 118 Seiten
ISBN: 978-3-89336-592-0

51. **Wasserstoff-Emissionen und ihre Auswirkungen auf den arktischen Ozonverlust**
Risikoanalyse einer globalen Wasserstoffwirtschaft
von T. Feck (2009), 180 Seiten
ISBN: 978-3-89336-593-7

52. **Development of a new Online Method for Compound Specific Measurements of Organic Aerosols**
by T. Hohaus (2009), 156 pages
ISBN: 978-3-89336-596-8

53. **Entwicklung einer FPGA basierten Ansteuerungselektronik für Justageeinheiten im Michelson Interferometer**
von H. Nöldgen (2009), 121 Seiten
ISBN: 978-3-89336-599-9

54. **Observation – and model – based study of the extratropical UT/LS**
by A. Kunz (2010), xii, 120, xii pages
ISBN: 978-3-89336-603-3

55. **Herstellung polykristalliner Szintillatoren für die Positronen-Emissions-Tomographie (PET)**
von S. K. Karim (2010), VIII, 154 Seiten
ISBN: 978-3-89336-610-1

56. **Kombination eines Gebäudekondensators mit H2-Rekombinatorelementen in Leichwasserreaktoren**
von S. Kelm (2010), vii, 119 Seiten
ISBN: 978-3-89336-611-8

57. **Plant Leaf Motion Estimation Using A 5D Affine Optical Flow Model**
by T. Schuchert (2010), X, 143 pages
ISBN: 978-3-89336-613-2

58. **Tracer-tracer relations as a tool for research on polar ozone loss**
by R. Müller (2010), 116 pages
ISBN: 978-3-89336-614-9

Energie & Umwelt / Energy & Environment
Band / Volume 58
ISBN 978-3-89336-614-9

JÜLICH
FORSCHUNGSZENTRUM